

Smart Materials for Adaptive Building Façades

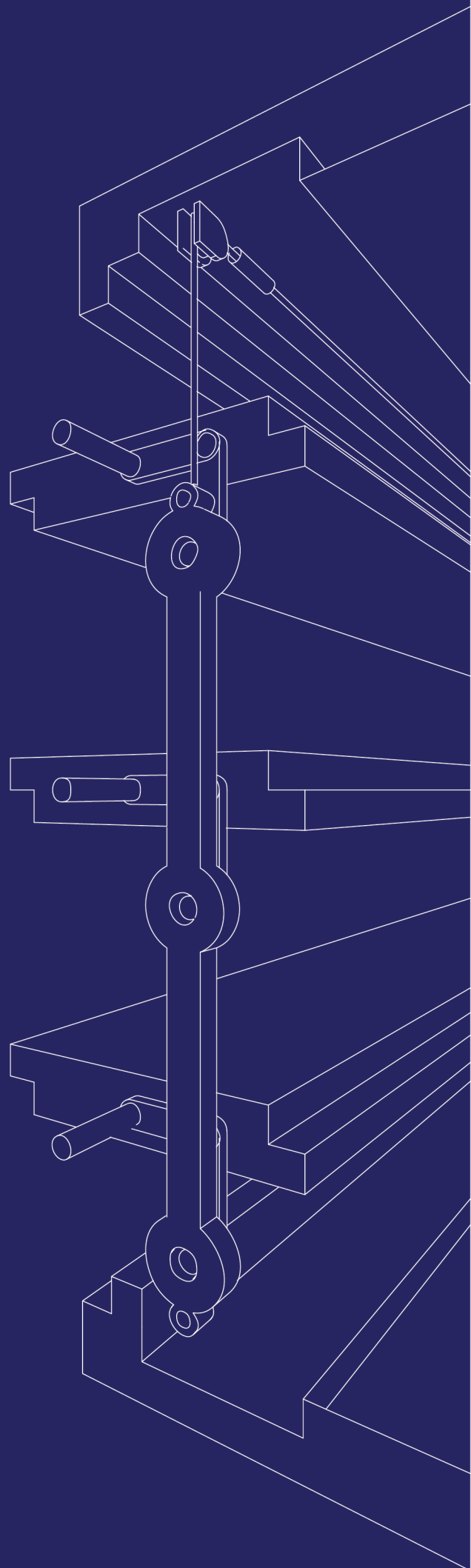
Improving Indoor Climate and
Building Performance through
Material Intelligence

E.M.I. Adam

MSc Architecture, Urbanism and Building Science
Building Technology
Delft University of Technology

In collaboration with Arup

2026



Smart Materials for Adaptive Building Façades

Improving Indoor Climate and Building Performance through Material Intelligence

By

E.M.I Adam

Author details: E.M.I. (Ella) Adam

Student number: 5284228

Thesis committee:	Ir. E.R. van den Ham	TU Delft, first supervisor
	Dr. Ing. M. Bilow	TU Delft, second supervisor
	Ir. J.A. Kuijper	TU Delft, delegate
Company Supervisors:	Ir. M.S. Di Maggio	Daily supervisor Arup

Master: MSc Architecture, Urbanism and Building Science
Track Building Technology
Delft University of Technology

Abstract

The built environment is responsible for a large share of global energy consumption. Where façades play a crucial role in regulating the interaction between indoor and outdoor conditions. While adaptive façades can improve indoor climate performance, many existing systems rely on motors, sensors and complex control systems. This research investigates how smart materials can be integrated into adaptive building façades to improve indoor climate performance and reduce energy demand.

The study follows a mixed-method approach consisting of a literature review, material evaluation, design development, physical prototyping and building performance simulations. First, different categories of smart materials were analysed and evaluated for façade integration. Shape Memory Alloys were selected for further development. This because of their temperature-responsive behaviour, reversible actuation, relatively high actuation force and suitability for passive façade applications.

The selected SMA was translated into a passive adaptive natural ventilation component. The design uses the linear contraction of an SMA wire to activate a Scotch yoke mechanism. Which rotates a set of lamellas to open and close the ventilation component. Experimental testing confirmed that the SMA wire can generate sufficient force and contraction to actuate the mechanism. The design was evaluated through building performance simulations in DesignBuilder and EnergyPlus. Using both a reference room and the Hartje Noord case study in Amsterdam.

The simulation results show that adaptive natural ventilation can reduce overheating when cooler outdoor air is available, especially during the evening, night and early morning. However, passive ventilation alone was not sufficient to maintain thermal comfort during peak summer conditions. The most promising result was found in the hybrid scenario. Where adaptive ventilation was combined with active cooling. In this case, the summer cooling demand was reduced by approximately 68% compared to the reference scenario.

The research demonstrates that SMA-driven adaptive ventilation can contribute to lower-energy building performance as part of a hybrid climate strategy. The proposed component should be considered a proof-of-concept, as further testing is needed regarding durability, airtightness, acoustic performance, draught risk and real-world façade integration.

Acknowledgement

During my graduation process, Joran, my delegate, once told me to look at my thesis as going grocery shopping. Before entering the supermarket, I should make a shopping list, collect the right ingredients, and use them to prepare my final recipe.

Of course, I entered the supermarket with great enthusiasm (*voor korte duur*), but without a proper shopping list. Before I knew it, my shopping cart was completely full, and I could no longer see the forest for the trees. Luckily, there were several people who helped me find my way through the aisles and eventually reach the checkout.

First of all, I would like to thank Eric, for always pointing me back in the right direction and reminding me of my shopping list. Without his guidance, I would probably still be wandering around the supermarket.

I would also like to thank Marcel, for helping me get the shopping cart moving from a mechanical point of view. His creative and spatial way of thinking was very valuable throughout the process.

Furthermore, I would like to thank Willem, who helped me find the way towards the eggs, or in this case, the solution in DesignBuilder. As always, they were not located where I expected them to be.

I would also like to thank Maria Sara and my colleagues at Arup for the inspiring conversations, the support, and for making me feel welcome from the beginning. And of course, for the many latte macchiatos, even though I do not actually drink coffee.

A special thank you goes to my dear parents, Ankie and Jos, and my sister Julie. Thank you for your endless support and for always allowing me to make my own choices. I sometimes describe your way of raising me as *liefdevolle verwaarlozing*.

I would also like to thank my friends and housemates. You are the ingredients I need in my life!

Last, but most important, I would like to thank Ger. Somewhere along the way, without even looking for you, I found in you the ingredients that matter most to me: *avontuurlijk, lief en koppig*.

Looking back, Joran may have been right after all. Next time I will try to make a shopping list first. For now, however, I am quite done with grocery shopping and mostly looking forward to going home.

Finally: *'t leven bestaat uit pieken en dalen, je weet nooit wanneer het omhoog of naar beneden gaat.*

Table of Contents

Abstract	4
Acknowledgement	5
Table of Contents	6
List of Figures	10
List of Tables	13
Nomenclatures	14
Abbreviations	14
Symbols	15
1. Introduction	1
Background	1
Motivation	1
Research Gap	2
Relevance	2
Research Questions	2
Research Objective	3
Scope	3
Thesis Structure	3
2. Methodology	5
Research Framework	5
Smart Material Investigation	5
Ventilation System Design	6
Performance Evaluation	6
PART I	7
3. Adaptive Building Façades	8
3.1 Static versus Responsive Façades	9
3.2 Active versus Passive Responsive Façades	9
3.3 Conclusion	10
4. Smart Materials	11
4.1 Definition of Smart Materials	11

4.2	Thermo-Responsive Materials	13
4.3	Light-Responsive Materials	17
4.4	Moisture-Responsive Materials	19
4.5	Electromagnetic Responsive Materials	22
4.6	Mechanical Stress Responsive Materials	24
4.7	Chemically Responsive Materials	25
4.8	Conclusion	26
5.	From Smart Materials to Façade Integration	27
5.1	Façade Functions Relevant to Indoor climate	27
5.1.1	Thermal Comfort	27
5.1.2	Visual Comfort	27
5.1.3	Indoor Air Quality	27
5.2	Linking Smart Materials Responses to Façade Functions	28
5.2.1	Thermo-Responsive Materials	28
5.2.2	Light-Responsive Materials	29
5.2.3	Moisture-Responsive	30
5.2.4	Electromagnetic Responsive Materials	31
5.2.5	Other Main Categories	31
5.3	Selection Criteria for Smart Materials for Façade Integration	32
5.4	Conclusion	33
6.	Material Deep Dive	34
6.1	Shape Memory Alloys (SMAs)	34
6.1.1	Martensitic Transformation	34
6.1.2	Temperature Threshold	34
6.1.3	Actuation Force	35
6.1.4	Metal Fatigue	35
6.1.5	Advantages & Limitations	36
6.2	Thermo-bimetals	36
6.2.1	Temperature Response Range	37
6.2.2	Actuation Force & Displacement	37
6.2.3	Advantages & Limitations	37
6.3	Hygro-morphic Materials	37
6.3.1	Hygroscopic Expansion	38
6.3.2	Relative Humidity Response Range	38
6.3.3	Actuation Magnitude	39
6.3.4	Advantages & Limitations	39
6.4	Evaluation of Selected Smart Materials	40
6.5	Conclusion	40

PART II	41
7. Design structure	42
7.1 Smart material as Design Input	43
7.2 Passive System strategy	43
7.2.1 Façade system selection	43
7.2.2 Climate Relevance of Adaptive Ventilation	44
7.2.3 Natural Ventilation	44
7.2.4 Ventilation Principles	44
7.3 Design Criteria	45
7.4 Conclusion	46
8. Adaptive Ventilation Component Design	47
8.1 Required Operating Logic	47
8.2 Component Dimensioning	48
8.3 SMA Actuation	49
8.3.1 Experimental Testing of the SMA wire	49
8.3.2 Phase Transition behaviour	51
8.3.3 Translation to Practical Operating Temperatures	52
8.4 Actuation Mechanism	53
8.4.1 Exploration of Mechanisms	53
8.4.2 Evaluation of Mechanisms	54
8.5 Geometry and Component Design	55
8.5.1 System Overview	55
8.5.2 Lamella Design	56
8.5.3 Mechanism Geometry	57
8.5.4 SMA Wire Routing and Acting Forces	59
8.5.5 Manual Override Mechanism	63
8.6 Final Component Design	64
8.7 Design Criteria Evaluation	70
8.8 Conclusion	71
9. Building Performance Simulations	72
9.1 Aim and Scope of the Simulations	72
9.2 Methodology	72
9.2.1 Simulation Software	72
9.2.2 Climate and Location	72
9.2.3 General Ventilation and Control Logic	73
9.2.4 Performance Indicators	74
9.3 Reference Room	75

9.3.1	Model Geometry	75
9.3.2	Boundary Conditions	76
9.3.3	Simulation Scenarios	77
9.4	Case Study Setup	78
9.4.1	Case Study Description	78
9.4.2	Boundary Conditions	79
9.4.3	Adaptive Ventilation Configuration	80
9.4.4	Simulation Scenarios	80
9.5	Conclusion	82
10.	Simulation Results	83
10.1	Setpoint Sensitivity Analysis	83
10.2	Reference Room	84
10.2.1	Scenario Comparison	84
10.2.2	High Air Change Rates Peaks	88
10.2.3	Detailed Summer Week	90
10.2.4	Winter Period Check	95
10.3	Case Study	96
10.3.1	Model Verification with Vabi Results	96
10.3.2	Scenario comparison	97
10.3.3	High Air Change Rate Peaks in CS2	99
10.3.4	Cooling Demand	101
10.3.5	Detailed Summer Week	102
10.3.6	Ventilation and System Operation	104
10.3.7	Case Study Summary	105
10.4	Conclusion	106
11.	Discussion	107
12.	Conclusion	110
	Recommendations	111
13.	Reflection	112
	References	114
	Appendix A	118
	Appendix B	119
	Appendix C	122
	Appendix D	123
	Appendix E	125

List of Figures

Figure 2.1 Methodological framework of the research process.	5
Figure 3.1 Façade function based on occupants' comfort.	8
Figure 3.2 Examples of active responsive façades.	9
Figure 4.1 Smart materials components.	11
Figure 4.2 Main categories.	12
Figure 4.3 Family tree of smart materials discussed in this research.	11
Figure 4.4 Technology Readiness Levels (TRL) scale.	13
Figure 4.5 Example of thermochromic material.	13
Figure 4.6 Detailed illustration of thermoelectric module.	14
Figure 4.7 Flexibility changes of phase change composite elastomers before and after phase change.	15
Figure 4.8 Thermally induced shape memory effect of Shape Memory Polymers (SMPs).	15
Figure 4.9 Shape memory effect with SMAs.	16
Figure 4.10 Shape memory alloys (e.g., Nitinol) that exhibit thermally induced shape memory effects.	16
Figure 4.11 Comparative material matrix of thermo-responsive materials.	17
Figure 4.12 Schematic illustration of photochromic glazing.	18
Figure 4.13 Schematic representation of photoluminescence, which forms the fundamental mechanism behind luminescent solar concentrator (LSC) materials.	19
Figure 4.14 A self-cleaning glass system based on titanium oxide (TiO ₂).	19
Figure 4.15 Comparative material matrix of light-responsive materials.	20
Figure 4.16 Reversible moisture-driven closing (wet conditions) and opening (dry conditions) of spruce cones.	20
Figure 4.17 Principle of the response of hygro-morphic composites based on active and passive layer.	21
Figure 4.18 Examples of hygroscopic bio-based insulation material: peat (left), moss (right).	22
Figure 4.19 Comparative material matrix of moisture-responsive materials.	22
Figure 4.20 Electrochromic glass.	23
Figure 4.21 Deformation of a soft magnetoactive actuator under a magnetic field.	23
Figure 4.22 Comparative material matrix of electromagnetic-responsive materials.	24
Figure 4.23 Optical microscopy images of a mechano-chromic film under increasing strain.	24
Figure 4.24 Comparative material matrix of mechanical stress responsive materials.	25
Figure 4.25 Chemochromic material example.	26
Figure 4.26 Swelling/de-swelling of drug-loaded hydrogel matrix, resulting from the change in ambient pH.	26
Figure 4.27 Comparative material matrix of chemically responsive materials.	27
Figure 5.1 Schematic mapping of thermo-responsive material responses to façade functions.	29
Figure 5.2 Schematic mapping of light-responsive material responses to façade functions.	30
Figure 5.3 Boathouses in Nordmøre, Norway, enhancing natural ventilation in dry weather.	30
Figure 5.4 Schematic mapping of moisture-responsive material responses to façade functions.	31
Figure 5.5 Schematic mapping of electromagnetic responsive material responses to façade functions.	32
Figure 5.6 Design criteria for smart materials.	33
Figure 6.1 SMA wire in bending.	36
Figure 6.2 Cross-section of a tree trunk showing growth rings and wood grain directions, highlighting tangential, radial, and longitudinal orientations.	39
Figure 7.1 Design structure of Part II.	43
Figure 7.2 Natural ventilation strategies.	46

Figure 8.1 Operating principles of passive ventilation system.	49
Figure 8.2 Dimensions for ventilation component in front view.	49
Figure 8.3 Progress images of experimental testing of SMA wire.	50
Figure 8.4 Stress–strain response of the SMA wire during tensile loading up to 4% elongation.	50
Figure 8.5 Force-temperature response of SMA wire.	51
Figure 8.6 Phase temperatures of SMA wire in practice.	53
Figure 8.7 Actuation mechanisms for lamella rotation.	55
Figure 8.8 Mechanism overview of the SMA-driven ventilation component, responding to outside conditions.	57
Figure 8.9 Key dimensions of lamella in cross-section.	58
Figure 8.10 Crank arm and pin attached to the lamella rotation axis.	58
Figure 8.11 Influence of lever arm length on force and SMA contraction.	59
Figure 8.12 Design of the yoke.	60
Figure 8.13 Potential strategies to protect the SMA wire from direct airflow.	60
Figure 8.14 Force-displacement behaviour of SMA wire.	61
Figure 8.15 Force balance of the SMA-driven mechanism during heating and cooling responding to outdoor conditions.	62
Figure 8.16 SMA-driven mechanism showing all active forces in both open and closed positions, with one side responding to outdoor and the other to indoor temperature.	63
Figure 8.17 Manual override principle.	64
Figure 8.18 Active electrical override strategy connected to the outside SMA wire.	65
Figure 8.19 Exploded view of the adaptive ventilation component.	66
Figure 8.20 Open and closed state of the SMA-driven ventilation component integrated in a CLT façade section.	67
Figure 8.21 Vertical section of the SMA-driven adaptive ventilation component in closed and open position.	68
Figure 8.22 Horizontal section of the SMA-driven adaptive ventilation component.	69
Figure 8.23 Front view of the SMA-driven adaptive ventilation component.	69
Figure 8.24 Adaptive ventilation component integrated in a CLT façade section.	70
Figure 9.1 Standard room layout and dimensions.	76
Figure 9.2 Dimensions for ventilation component in front view.	77
Figure 9.3 Reference room scenarios.	78
Figure 9.4 Critical apartment of Hartje Noord.	79
Figure 9.5 Residential tower Hartje Noord in Amsterdam.	80
Figure 9.6 Schematic overview of the case study simulation scenarios.	82
Figure 10.1 Percentage of not comfortable hours for different temperature thresholds.	85
Figure 10.2 Daily mean operative temperature for S0, S1, and S2 during the full summer period.	87
Figure 10.3 Daily maximum operative temperature for S0, S1, and S2 during the full summer period.	87
Figure 10.4 Daily hours above 24 °C for S0, S1, and S2 during the full summer period.	88
Figure 10.5 Daily mean air change rate for S1 and S2 during the full summer period.	89
Figure 10.6 DesignBuilder occupancy schedule for an office.	89
Figure 10.7 Air change rate in S2 during the full summer period with detected high peaks.	89
Figure 10.8 Occurrence of high air change rate peaks in S2 during occupied and unoccupied periods.	91
Figure 10.9 Daily mean outdoor air temperature during the full summer period, with the selected warm period highlighted.	92
Figure 10.10 Hourly outdoor temperature for selected warmest summer week (1 to 7 August).	92
Figure 10.11 Hourly operative temperature for S0, S1, and S2 during the selected summer week.	93
Figure 10.12 Hourly air change rate for S1 and S2 during the selected summer week.	94
Figure 10.13 S2 operative temperature, outdoor air temperature, and air change rate during the selected summer week.	94
Figure 10.14 Daily mean operative temperature for S1 and S2 and daily mean outdoor air temperature during the winter period.	96
Figure 10.15 Daily maximum air change rate for S1 and S2 during the winter period.	97

Figure 10.16 Daily mean operative temperature during the summer period.	99
Figure 10.17 Daily mean air change rate during the summer period.	99
Figure 10.18 DesignBuilder occupancy schedule for a living room.	100
Figure 10.19 Detected high ACH peaks in CS2.	101
Figure 10.20 CS2 occupied vs unoccupied high ACH peaks.	101
Figure 10.21 Daily cooling load during the summer period.	103
Figure 10.22 Hourly operative temperature for CS0, CS1, and CS2 during the selected summer week.	105
Figure 10.23 Hourly air change rate for selected summer week of scenarios CS0, CS1, and CS2.	105
Figure 10.24 CS2 air change rate plus cooling power for the selected summer week.	106
Figure B.1 Standard room layout and dimensions.	120
Figure B.2 Design options for one-sided ventilation in front view.	121
Figure B.3 Design options for two-sided ventilation in front view.	121
Figure C.1 Early design sketches of possible SMA-driven adaptive ventilation concepts.	123
Figure E.1 S2 operative temperature and outdoor air temperature during the selected summer week.	126
Figure E.2 S2 operative temperature and air change rate during the selected summer week.	126
Figure E.3 Hourly air change rate for S1 and S2 during the selected summer week with night-time periods indicated.	127
Figure E.4 S2 air change rate with night-time periods and occupied hours during the selected summer week	127

List of Tables

Table 5.1 Evaluation of smart materials based on selection criteria.	33
Table 6.1 Comparison of austenite and martensite phases.	35
Table 6.2 Comparison between constant stress and constant strain conditions.	36
Table 6.3 Advantages and limitations of SMAs.	37
Table 6.4 Advantages and limitations of thermo-bimetals.	38
Table 6.5 Advantages and limitations of hygro-morphic materials.	40
Table 6.6 Evaluation of SMAs, thermo-bimetals, and hygro-morphic materials.	41
Table 7.1 Possible façade applications for SMA integration.	44
Table 7.2 Design criteria for the SMA-driven ventilation component.	46
Table 8.1 Operational logic for passive ventilation system.	48
Table 8.2 Key results of testing the SMA wire.	51
Table 8.3 Phase transition temperatures and corresponding forces of SMA wire.	52
Table 8.4 Phase temperatures in practice SMA wire.	53
Table 8.5 Evaluation of actuation mechanisms based on the relevant design criteria.	55
Table 8.6 Displacement comparison for 90° rotation based on SMA strain.	59
Table 8.7 Final evaluation of the product design based on the design criteria.	71
Table 9.1 Climate file information used for the building performance simulations.	74
Table 9.2 Performance indicators.	75
Table 9.3 Free opening area with acoustic box.	77
Table 9.4 Reference room simulation scenarios.	79
Table 9.5 Case study simulation scenarios.	83
Table 10.1 Setpoint sensitivity results.	84
Table 10.2 Simulation results for the full summer period.	86
Table 10.3 Summary of detected high air change rate peaks in S2.	90
Table 10.4 Simulation results for the selected summer week.	92
Table 10.5 Model verification between Vabi and CS0 DesignBuilder results of a full year.	98
Table 10.6 Case study scenario comparison for the full summer period.	98
Table 10.7 Summary of detected high air change rate peaks in CS2.	101
Table 10.8 Cooling demand comparison between CS0 and CS2 for the full summer period.	102
Table 10.9 Simulation results of the case study for the selected summer week.	104
Table A.1 Technology Readiness Levels (TRL) of smart materials.	119
Table B.1 Required ventilation opening area for different ventilation types.	120

Nomenclatures

Abbreviations

Abbreviation	Definition
ACH	Air Changes per Hour
BENG	Bijna Energie Neutraal Gebouw
CLT	Cross-Laminated Timber
CO ₂	Carbon Dioxide
CS0	Hartje Noord reference scenario
CS1	Hartje Noord scenario with adaptive natural ventilation
CS2	Hartje Noord scenario with adaptive natural ventilation and active cooling
EMS	Energy Management System
HVAC	Heating, Ventilation and Air Conditioning
IAQ	Indoor Air Quality
NIR	Near Infrared Radiation
PCM	Phase Change Material
PV	Photovoltaic
RH	Relative Humidity
S0	Reference room without adaptive ventilation
S1	Reference room with one-sided adaptive ventilation
S2	Reference room with two-sided adaptive ventilation
SMA	Shape Memory Alloy
SMP	Shape Memory Polymer
TRL	Technology Readiness Level
UV	Ultraviolet Radiation

Symbols

Symbol	Definition	Unit
A	Opening area	m ²
F_{SMA}	Force generated by the SMA wire	N
F_{contra}	Return spring force	N
$F_{friction}$	Friction force	N
F_{weight}	Force due to the weight of moving elements	N
Q_{vent}	Ventilation airflow rate	L/s
r	Lever arm radius	mm
θ	Rotation angle	°
ε	SMA strain	%
ΔL	SMA contraction/displacement	mm
T_{indoor}	Indoor temperature	°C
$T_{outdoor}$	Outdoor temperature	°C
$T_{threshold}$	Ventilation control temperature	°C

1. Introduction

Background

The built environment plays a key role in affecting global sustainability since it uses approximately 40% of the total energy consumption, thereby significantly contributing global CO₂ emissions (Fathi & Fakhraeimanesh, 2025). Therefore, reducing energy demand in the built environment is widely recognised as a key strategy for mitigating greenhouse gas emissions, which is in line with United Nations Sustainable Development Goals related to energy efficiency, sustainable cities, and climate action (Scrucca et al., 2023).

In recent decades, there has been an increasing interest and reliance on active building systems, such as heating, ventilation, and air conditioning (HVAC). These systems are crucial for occupant comfort, and most importantly, they aim to manage and optimize a building's energy performance. HVAC systems account for approximately 30% of the total energy demand in buildings (Szolomicki & Golasz-Szolomicka, 2019). Hence, they contribute significantly to energy consumption and greenhouse gas emissions.

The building envelope, more precisely, its façade, has an important role in managing indoor and outdoor interactions. Façades significantly affect heat transmissions, solar gains, natural ventilation, diffusion, and daylight distribution. All these factors directly affect the indoor climate comfort in buildings (Halawa et al., 2018). Despite their central role, most of the contemporary façades remain static, and thus do not respond to changes in outside temperature, and, solar radiation, and fluctuating comfort demands. To flexibly adapt to these changing conditions, buildings still mostly depend on energy-intensive mechanical systems.

To reduce the dependence on and limitations of static façades new climate-adapted façade designs have been proposed. Although these new approaches hold great promise it should be recognized that most of these technologies depend on complex mechanical components, sensors, actuators, and controlled systems. Moreover, often, these system-based approaches are associated with high investment costs, increased maintenance requirements, and operational complexity, which constrains their feasibility and large-scale implementation (Loonen et al., 2013).

Motivation

The motivation for this research lies in the growing urgency for an overall reduction in energy use and carbon emissions in the built environment. Buildings are responsible for a large amount of global energy use. Therefore, improvement of the performance of building façades has the great potential to significantly reduce the energy demand needed by traditional mechanical systems that use substantial amount of energy.

Smart materials offer an innovative approach to façade design. They enable energy savings by adaptation at the level of the material itself rather than relying on complex mechanical systems. Their respond to environmental stimuli offers opportunities for more efficient and responsive building envelopes, with potential improvement in indoor climate conditions, while energy demand is reduced.

Moreover, numerous smart materials are being developed and applied in various fields, such as aerospace and product engineering. Yet, their contribution to potential architectural applications remains largely unexplored. This research is motivated by the need for investigating how such material innovations can be translated into the built environment, which supports the development of more sustainable, resilient, and future-proof buildings.

Research Gap

Several research gaps can be identified in the field of smart materials in adaptive building façades. Current research on smart materials for adaptive façades mainly focusses on material properties, conceptual ideas, or individual façade components. Although these studies have shown the potential of smart materials, few of them translate the behaviour of smart materials to façade systems and evaluate such a system on the effect on the indoor climate and energy demand.

In addition, there are no sufficient performance-based data for selecting the proper smart materials and applying them to façade systems. So, no or very little systematic, relevant information is available for designers or engineers to facilitate performance-based decision-making during early building façade design phases.

This research therefore attempts to provide a contribution to bridging the gap between smart material behaviour, façade integration, and building-scale performance evaluation.

Relevance

The relevance of this research is related to the growing and widely recognized need to reduce the energy consumption and CO₂ emissions in buildings. The building industry is one of the largest contributors to energy consumption globally. Hence, by improving building façade performance, the operational energy demand can significantly be reduced, and, in addition, the reliance on complex, energy demanding mechanical systems can be decreased.

Finally, this research is relevant for architectural and façade design practice. This is because it provides a critical analysis of the possibilities, limitations, and risks when designing adaptive façades with smart materials, including technical feasibility, performance reliability, and implications for façade design.

Research Questions

The main research question of this project is:

How can smart materials be integrated into adaptive building façades to improve indoor climate performance and reduce energy demand?

The supporting sub-research questions are:

1. What is the role of adaptive façades in improving indoor climate performance and reducing energy demand?

Addressed in Chapter 3.

2. What are smart materials and what types are available for adaptive façade applications?

Addressed in Chapter 4.

3. How can smart material behaviour be linked to façade functions that influence the indoor climate?

Addressed in Chapter 5.

4. Which smart materials show the greatest potential for passive adaptive façade integration, and what are their key properties, limitations and design implications?

Addressed in Chapter 6.

Research Objective

The main research objective is:

The objective of this research is to contribute to the integration of smart materials into adaptive building façades for improved indoor climate performance and reduced energy demand, by developing and evaluating an SMA-driven adaptive natural ventilation component through prototyping and building performance simulations.

The design and evaluation questions to support the research objective are:

1. How can Shape Memory Alloys be translated into a passive adaptive natural ventilation component?

Addressed in Chapter 7.

2. What operating logic, actuation mechanism and component geometry are required for the SMA-driven ventilation component?

Addressed in Chapter 8.

3. How can the adaptive ventilation component be represented in building performance simulations?

Addressed in Chapter 9.

4. What is the influence of the adaptive ventilation strategy on operative temperature, ventilation performance and cooling demand?

Addressed in Chapter 10.

Scope

This research focuses on the feasibility of smart materials in the design of adaptive building façades. Specifically, it aims to design a Shape Memory Alloy driven adaptive ventilation system and the development of a 1:1 mock-up of this system. Lastly, the research will evaluate the design impact of this system with building performance simulations.

Out of the scope is full product optimisation, long term durability testing, airtightness testing and acoustic validation or detailed market-ready engineering of the adaptive ventilation system.

Thesis Structure

This thesis is divided into two main parts. Part I introduces the theoretical foundation of the research by exploring adaptive façades, smart materials, and their potential application in building envelopes. The outcome of this part is the selection of a suitable smart material for further development. Part II focuses on the translation of the selected smart material into an adaptive façade component and evaluates its impact on indoor climate performance through building performance simulations.

Chapter 1 describes the background, problem statement, research gap, research questions, relevance, research objective and scope.

Chapter 2 presents the research methodology and explains the three research phases.

Chapter 3 introduces adaptive building façades and discusses the difference between static and responsive façades, as well as active and passive responsive systems.

Chapter 4 gives an overview of smart materials, their working principles, stimulus-response behaviour, possible façade applications and Technology Readiness Levels.

Chapter 5 links smart material responses to façade functions that influence the indoor climate. It also defines the selection criteria used to evaluate which smart materials are most suitable for façade integration.

Chapter 6 provides a deeper analysis of the selected smart materials: Shape Memory Alloys, thermo-bimetals and hygro-morphic materials. Based on this comparison, Shape Memory Alloys are selected for further design development.

Chapter 7 defines the design structure of Part II. It translates the material selection into a passive adaptive ventilation strategy and formulates the design criteria for the SMA-driven ventilation component.

Chapter 8 develops the adaptive ventilation component. It defines the operating logic, component dimensions, SMA actuation, actuation mechanism, geometry, open and closed positions, and evaluates the final design against the design criteria.

Chapter 9 describes the building performance simulation methodology. It explains the simulation software, climate file, ventilation control logic, performance indicators, reference room setup and Hartje Noord case study setup.

Chapter 10 presents the simulation results. It includes the setpoint sensitivity analysis, reference room results, winter period check, case study verification, scenario comparison, cooling demand analysis and detailed summer week analysis.

Chapter 11 discusses the main findings of the research and reflects on the limitations and uncertainties of the proposed SMA-driven adaptive ventilation system.

Finally, Chapter 12 concludes the thesis by answering the research questions and research objective. It also provides recommendations for further development and future research.

2. Methodology

This chapter describes the research methodology used to answer the main research question, research objective and supporting research questions. The methodology explains how the study moves from literature-based material investigation towards design development and performance evaluation. In this way, the chapter clarifies how the different research phases are connected and how each phase contributes to the final discussion and conclusion.

Research Framework

This research follows a mixed-method approach. It combines a literature review, design development, physical prototyping and building performance simulations. The methodology is divided into three phases: smart material investigation, ventilation system design, and performance evaluation. Each phase has an outcome that form the input for the next phase. This is summarized in Figure 2.1.

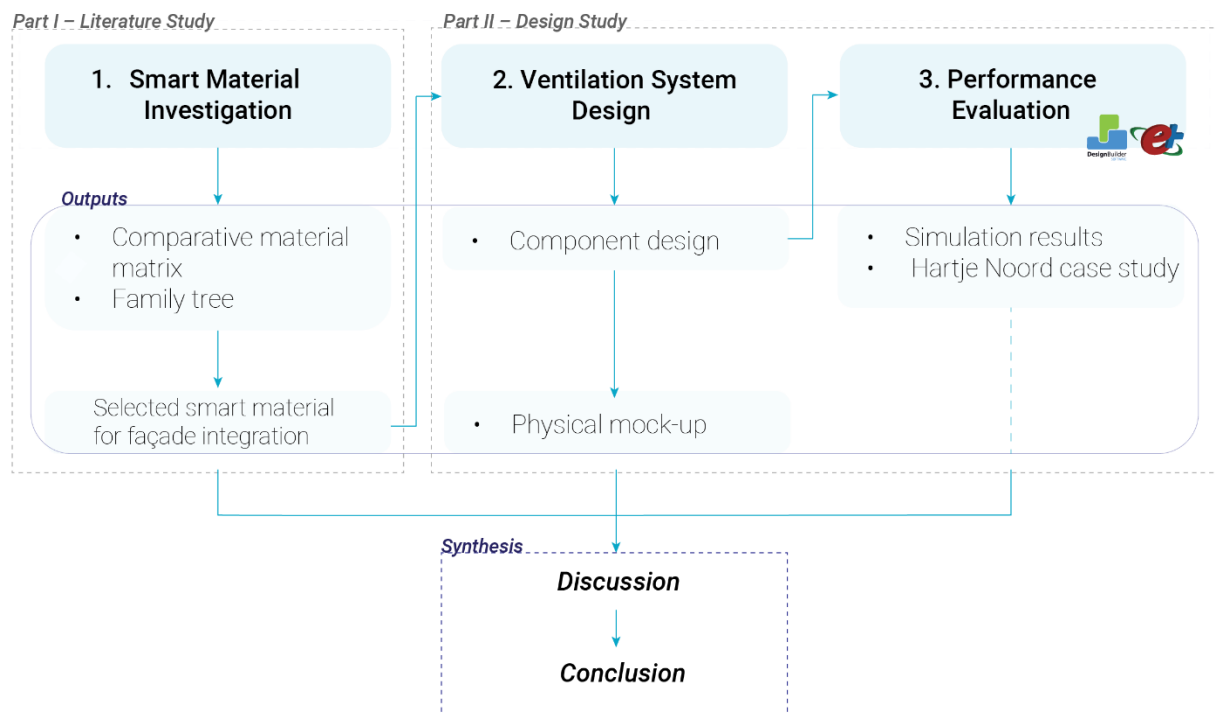


Figure 2.1
Methodological framework of the research process.

Smart Material Investigation

The first phase aims to identify smart materials that are suitable for adaptive façades. A literature review is carried out to understand the types of smart materials, their properties, behaviour, façade application, and Technology Readiness Levels (TRLs). From there a comparative material matrix and a family tree is conducted. Based on predefined selection criteria, the most suitable smart material is selected for further development.

Ventilation System Design

The second phase translate the selected smart materials into an adaptive façade application. A design study is conducted to develop a passive natural ventilation component. The second phase involves the ventilation strategy, the operating logic, design criteria, actuation mechanism and component geometry. The proposed design is further explored through the development of a physical 1:1 mock-up.

Performance Evaluation

The third phase evaluates the design impact of the proposed ventilation component through building performance simulations. These simulations are done using DesignBuilder and EnergyPlus. The simulations include evaluating the effect of the proposed adaptive ventilation strategy in a reference room. Later the proposed ventilation strategy is implemented in a case study from Arup: Hartje Noord. Furthermore, operative temperature, ventilation performance and cooling demand are considered the main performance indicators.

PART I

Literature Study

3. Adaptive Building Façades

In this chapter the important role of the façade will be discussed, as it is the interface between the in and outdoor climate. Furthermore, there will be an introduction to adaptive façades and their relevance for indoor climate and energy efficiency.

The façade serves as the main physical interface and boundary that separates the changing dynamic environment from the indoor environment (Addington and Schodek, 2005; Halawa et al., 2018). From an engineering perspective, it regulates energy exchange through heat transfer, daylight admission, airflow, and moisture control. Moreover, the façade must provide adequate sound insulation to shield the internal environment from external noise pollution (Bilow, 2012). Ultimately, this can be summarized to that the façade serves to optimize the indoor climate across four fundamental categories of occupant’s comfort (see Figure 3.1):

1. Thermal comfort
2. Visual comfort
3. Acoustic comfort
4. Air quality

In this way the façade should ensures a healthy and productive environment.

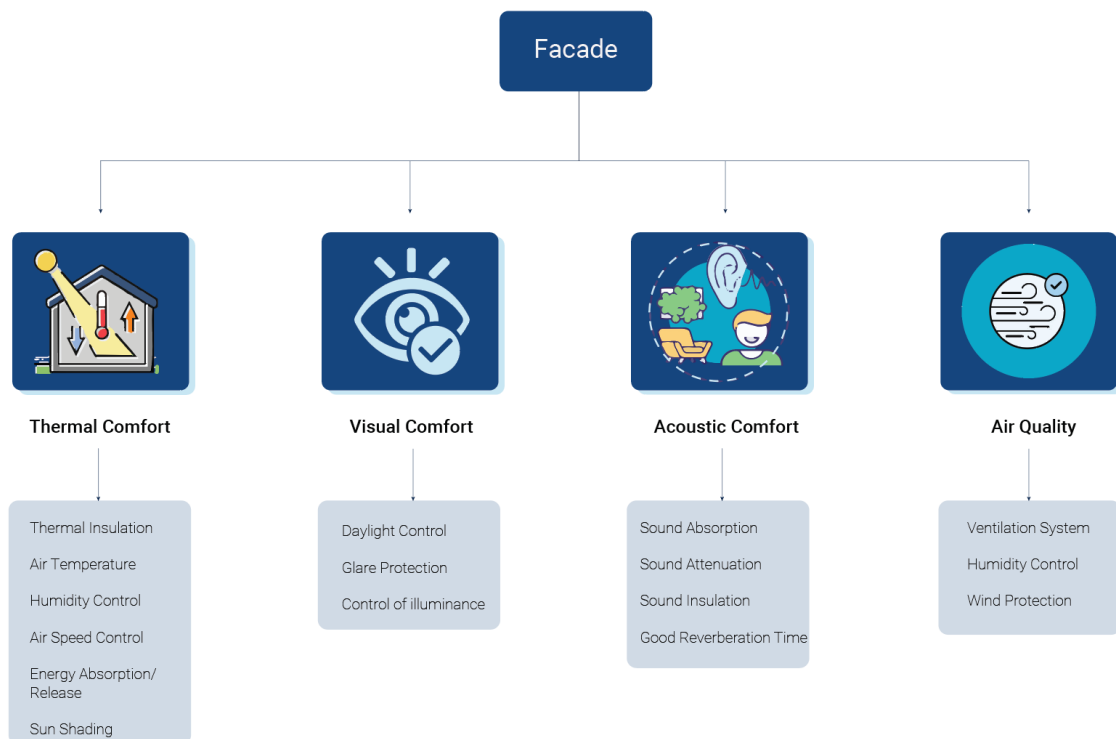


Figure 3.1
Façade function based on occupants’ comfort.
Note. Adapted from Persiani et al. (2016).

3.1 Static versus Responsive Façades

Despite the façade its key role in managing energy exchange, most conventional façades are still considered materially static. These façades are typically designed based on average or worst-case climatic conditions. Resulting in fixed U-values, permanent openings, and static shading systems that cannot respond to real-time environmental changes (Loonen et al., 2013). As a result, static façades often fail to maintain optimal indoor conditions, leading to unwanted solar gains in summer and heat losses in winter (Loonen et al., 2013; Riganti et al., 2025). This mismatch between fixed designs and dynamic environmental conditions increases the reliance on mechanical HVAC systems. These systems account for nearly half of total energy consumption in buildings and 10 to 20% of total energy consumption in developed nations (Pérez-Lombard et al., 2008). To compensate for these limitations, mechanical systems are frequently over-dimensioned, resulting in increased energy use, operational costs, and system complexity (Loonen et al., 2013).

To overcome these inefficiencies, there is a need to change the paradigm to adaptive façades. Adaptive façades have the capability to change their function, feature, or behaviour repeatedly over time. This is in relation to changing environmental factors, such as temperature, solar irradiance, moisture, and airflow (Loonen et al., 2013). In addition to this, the overall energy performance is greatly improved by the incorporation of responsive technologies, which have been proven to reduce the energy demand by up to 50% (Fathi & Fakhraeimanesh, 2025). Aside from the energy benefits, the impact of responsive façades is enormous for the overall occupant comfort and user experience.

3.2 Active versus Passive Responsive Façades

The evolution of low-energy building envelopes has traditionally followed two different paths: active technologies and passive design solutions. The basic difference between these two approaches is the type of energy input, system complexity, and autonomy.

Active systems require an external energy source and function through a control-driven system, including sensors, processors, and actuators. Thus, active façades afford a high degree of accuracy and programmability. This enabling them to meet complicated performance criteria such as a balance between daylight, glare, and thermal comfort (Akhras, 2024; Loonen et al., 2013). However, this high level of precision is accompanied by substantial sustainability and maintenance issues, as active façades are more energy- and maintenance-intensive (Halawa et al., 2018). Moreover, they are prone to technological failure and may require specialized expertise to maintain (Gosztanyi, 2022; Loonen et al., 2013). Figure 3.2 shows examples of active responsive façades.



Figure 3.2

Examples of active responsive façades.

Note. Image left from Architizer (n.d.); right from Homedit (n.d.).

By contrast, passive façades are not powered by an external energy source. Instead, they interact with the environment through intrinsic material behaviour, with the material serving as both sensor and actuator (Loonen et al., 2013; Holstov et al., 2015). Therefore, passive façades adapt autonomously in response to stimuli such as changes in humidity and temperature, thereby reducing the need for specialist control. Thus, the passive system is usually more reliable, requires less maintenance, and provides an energy-efficient approach compared to an active system. Nevertheless, the impossibility for manual interventions is considered as a downside.

A critical reflection on the practical application of adaptive envelopes indicates that hybrid systems could provide a pragmatic compromise. Hybrid façades are systems that combine the best of active and passive approaches by using a passive material response as the main mechanism and providing for a manual override or active assistance. Although hybrid systems can provide a remedy for some of the issues related to precision and control, they also have the potential to introduce unnecessary complexity and additional failure points (Lelieveld, 2013).

3.3 Conclusion

To conclude, because of the simplicity of passive façade systems and its energy efficiency, it is promising for sustainable responsive façade systems. For these reasons, this research focuses on passive systems, in which the adaptive capabilities of smart materials are employed. To provide a structured approach for selecting and implementing these technologies, the next chapter will discuss the classification of smart materials.

4. Smart Materials

This chapter presents the results of an extensive review of literature with the aim to provide a structured understanding of smart materials, their performance, and their characteristics. This will allow an evaluation of their possible application in the building industry. Importantly, it will help answering the research (sub)questions, including the grouping of smart materials, their principles of behaviour, as well as the limitations of the materials themselves, thereby providing the basis for the comparative material matrix.

4.1 Definition of Smart Materials

Smart materials are generally defined as materials that are capable of automatically and inherently responding to external environmental stimuli by dynamically changing one or more of their properties in a consistent, predictable way (Lelieveld, 2013). This contrasts with the behavior of conventional materials, which always respond in the same way to changing environmental conditions. Hence, smart materials are often seen as intelligent (smart), responsive materials.

The adaptive behaviour of smart materials may occur in response to environmental stimuli elicited by optical, electrical, magnetic mechanical, thermal, and chemical signals (Su & Song, 2021). The response is intrinsically driven by the material itself and thus does not require complex mechanics or external control systems. Depending on the nature of the external stimuli, smart materials respond by changing one of their key properties such as, for example, colour, shape or transparency (Lelieveld, 2013). Usually, the response of smart materials is reversible, meaning that they can revert to their normal state when the stimulus is no longer present (Costa, 2025). Thus, the smart materials are acting as both, sensor, processor and actuator (see Figure 4.1).

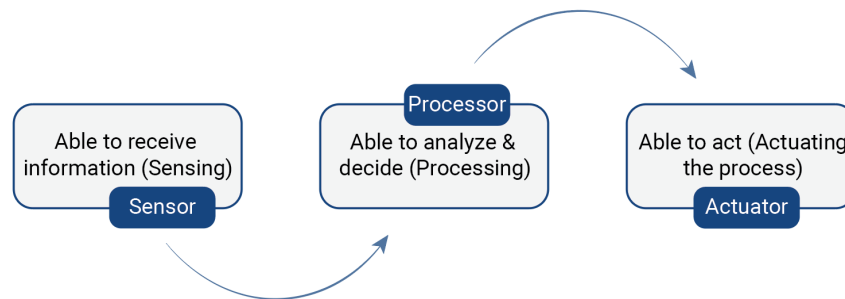


Figure 4.1

Smart materials components.

Note. Adapted from Jali (2025).

However, it should be noted that in some cases repeated activation and prolonged exposure to environmental stimuli may lead to material fatigue and aging, possibly reducing reversibility and impairing long-term performance. (Balcerak-Woźniak, 2024).

This study identifies several main categories of smart materials, grouped by stimulus type. These include thermo-responsive materials, light-sensitive materials, moisture-sensitive materials, electromagnetic reactive materials, mechanical stress-sensitive materials and chemically reactive materials (see Figure 4.2). Each of them describes a specific type of external stimuli of the environment of smart materials. Under each of the broad categories, sub-categories are provided in order to take into consideration the divergent response mechanisms and material properties of different materials (see Figure 4.3).

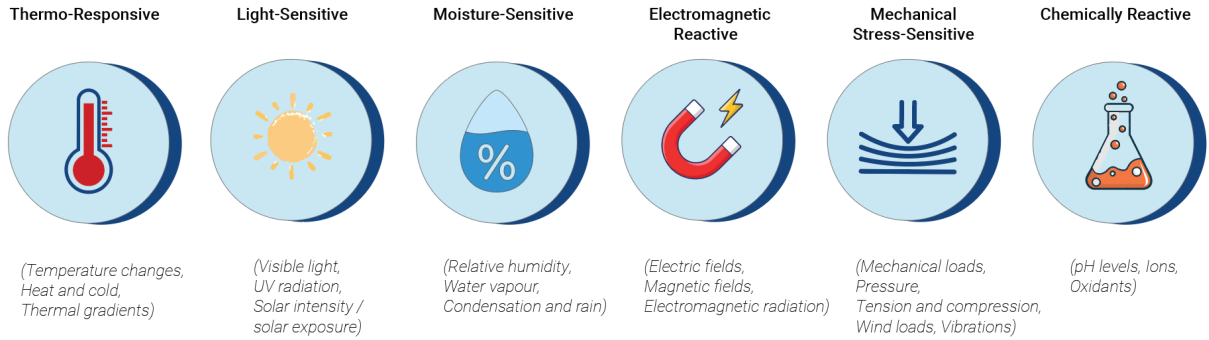


Figure 4.2
Main categories.

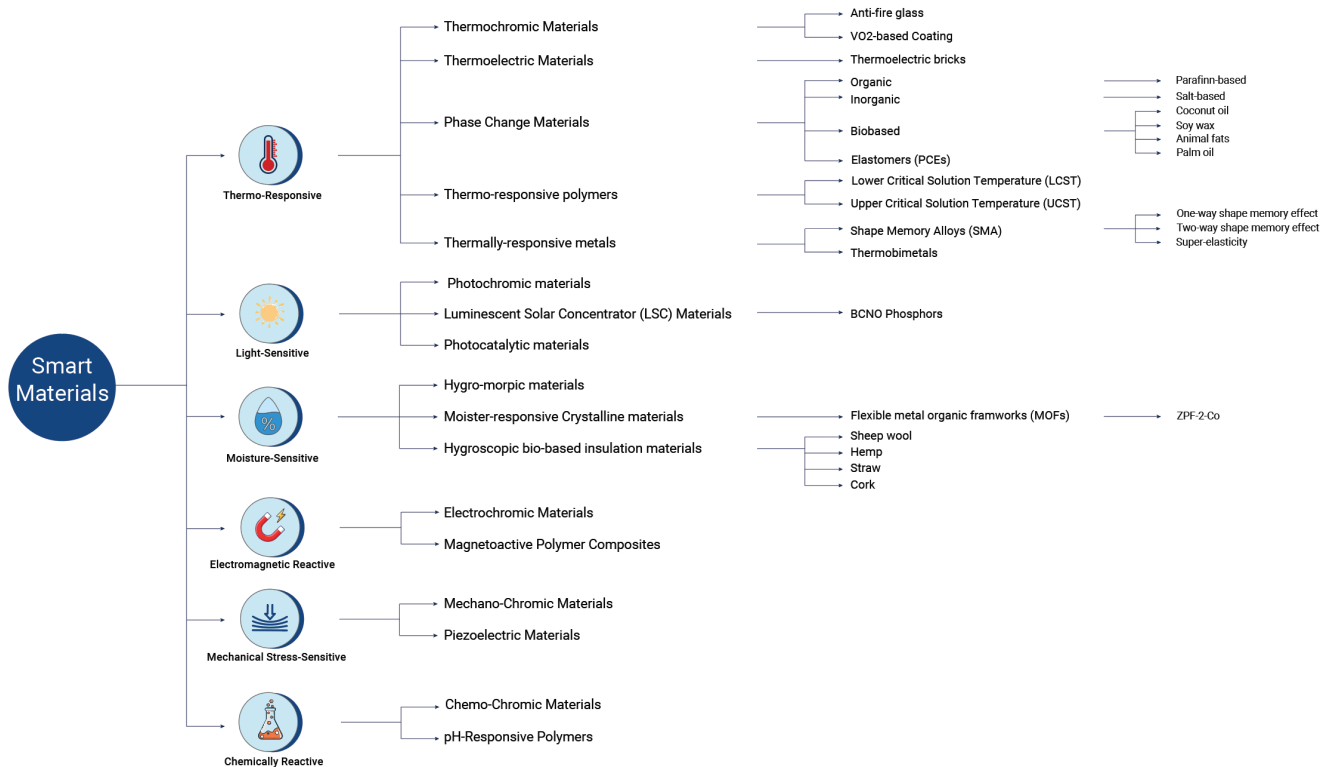


Figure 4.3
Family tree of smart materials discussed in this research.

In the next sections these main categories will be discussed. This includes how they respond, their applications and the Technical Readiness Level (TRL). Technical Readiness Level is a system ranging from 1 till 9. It is used to assess the maturity of technology. An TRL 1 represents basic research. While TRL 9 means that the technology is fully commercially available. In between these TRLs it describes different stages, ranging from proof of concept to full scale demonstrations. The TRL range helps to analyse the development of the smart materials. Furthermore, it shows their potential for applications in the building industry. Figure 4.4 summarizes the different TRL levels. For an overview of all the TRLs of the different smart materials see Table A.1 in Appendix A.

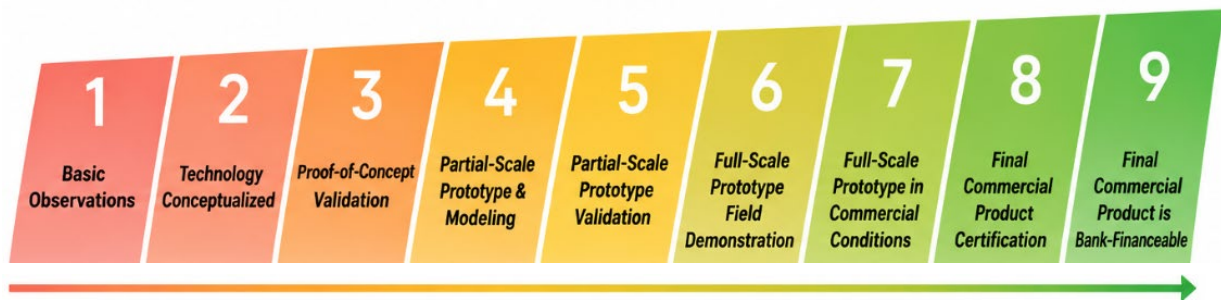


Figure 4.4
 Technology Readiness Levels (TRL) scale.
 Note. Adapted from WindHarvest (n.d.).

4.2 Thermo-Responsive Materials

Thermo-responsive materials are smart materials that change their properties based on temperature differences. In the next sections different thermo-responsive materials will be discussed, and their response, applications and their Technology Readiness Level (TRL). This is summarized in Figure 4.11.

Thermochromic Materials

Thermochromic materials are materials that respond to temperature fluctuations by changing their optical properties (see Figure 4.5). To be more precise, particularly their solar transmittance and reflectance. If the temperature is reaching a certain transition threshold, then the material will change its property's. This from a more transparent state to a more reflective state, particularly in the near-infrared (NIR) part of solar radiation. Therefore, solar heat gains are reduced while there is still transmission of visible light. In the façade industry, these kinds of materials are typically utilized as coatings in glazing systems. Through the passive control of solar radiation, by responding to temperature changes, these thermochromic materials could help decrease cooling needs in buildings and improve the overall building performance. Nevertheless, the use of these technologies is currently associated with certain drawback. Namely, low visibility and relatively costly production process (Kamalisarvestani et al., 2013).

Technologies that involve thermochromic properties, for example, VO₂ coatings, have already achieved a relatively mature stage of development. They can be viewed as almost ready for practical implementation and generally achieve a Technology Readiness Level (TRL) of 8 to 9 (Gosztonyi, 2022).



Figure 4.5
 Example of thermochromic material.
 Note. From Addington & Schodek (2005).

Thermoelectric Materials

Thermoelectric materials generate electricity by responding to temperature differences. This is based on the Seebeck effect, which converts a thermal gradient into electrical power. In terms of façade applications, thermoelectric materials have been introduced for use in building-integrated power

harvesting devices, like thermoelectric bricks (TEB), illustrated in Figure 4.6. The devices work through temperature gradients between building surfaces and can produce power continuously, if the temperature difference exists. The systems have solid-state operation and thus require little maintenance and offer long life expectancy. However, their use is mainly restricted to the production of electrical power rather than providing a dynamic façade system.

The development stage of thermoelectric materials in building-integrated devices is currently quite immature, having Technology Readiness Level (TRL) of 3-4. Even though the thermoelectric effect and module operation have been proven experimentally under controlled laboratory conditions and using numerical simulations for different climatic conditions, they still require further testing under actual building circumstances (Li et al., 2026).

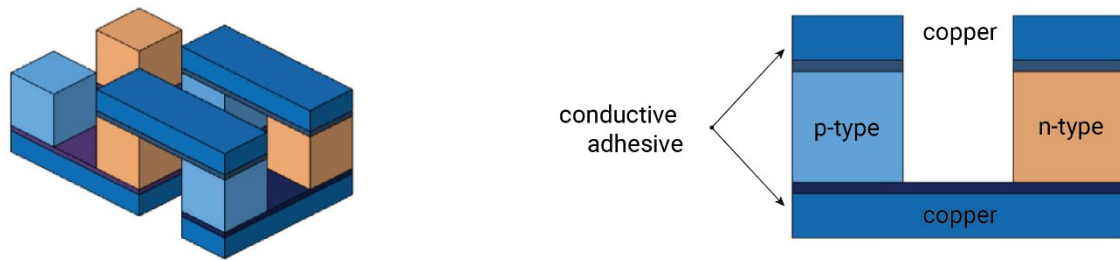


Figure 4.6
Detailed illustration of thermoelectric module.
Note. Adapted from Li et al. (2026).

Phase Change Materials (PCMs)

Phase Change Materials (PCMs) respond to temperature gradients, this by storing and releasing latent heat during their phase transition from solid to liquid, typically. This makes them act as “thermal batteries”. What helps to reduce temperature fluctuations in buildings and the reliance on HVAC systems (Barbhuiya et al., 2025).

The integration of PCMs into building elements such as walls, ceilings and floors serves to enhance the regulation of temperatures and stabilization of indoor conditions. Common types of PCMs include paraffin-based (organic) and hydrated salt-based (inorganic) materials. Paraffin-based PCMs are currently the market standers, this because of their chemical stable characteristics. Nevertheless, paraffin-based PCMs are highly flammable and have extremely low thermal conductivity, what are downsides. In contrast, inorganic hydrated salts offer higher thermal conductivity and heat storage capacity and are non-flammable, although their application is limited by issues such as phase segregation, supercooling, and corrosivity (Khdair et al., 2025).

Biobased PCMs utilize the same mechanism of storing and releasing heat based on temperature changes. These PCMs are commonly sourced from plant oils, such as coconut oil. These biobased PCMs have the advantages of reduced flammability levels and embodied carbon compared to paraffins. Nevertheless, they are still in at the beginning phase of development. Because of challenges related to environmental impact and resources (Baylis & Cruickshank, 2023).

Lastly, Phase Change Elastomers (PCEs) are more in an experimental phase whereby PCMs are combined with polymer materials to allow alterations in material properties, like stiffness (see Figure 4.7). Currently, these systems are studied in laboratories, including in the case of thermoelectric bricks, which assist in ensuring constant temperature differences while reducing the risk of any leakage (Ou et al., 2024).

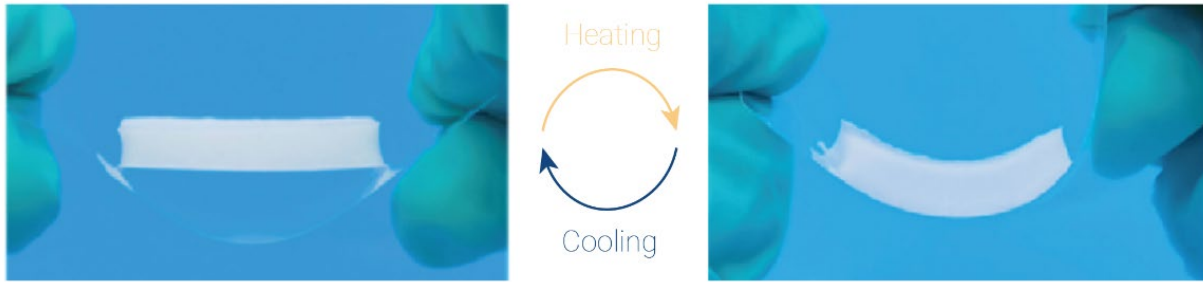


Figure 4.7

Flexibility changes of phase change composite elastomers before and after phase change.

Note. Adapted from Ou et al. (2024).

Phase Change Materials (PCMs) have achieved considerable technological maturity in the building industry achieving TRL scores between 8-9 in practical applications, whereas emerging solutions and prototypes lie at lower TRL scores (Gosztanyi, 2022). In summary, the main use of PCMs include thermal energy storage and regulation of temperature fluctuations in buildings.

Thermo-Responsive Polymers

Thermo-responsive polymers are an advanced class of smart materials, which shows changes in their physical or chemical properties. Including solubility, swelling behaviour, and hydrophilicity, according to the changes in temperature. When reaching the temperature threshold, these materials undergo a phase transition. This causes alterations in the material and can divided the material into two main groups, Lower Critical Solution Temperature (LCST) and Upper Critical Solution Temperature (UCST). To the fact that temperature is a parameter easily observable and controllable, these polymers find wide applications in medicine, electronics, and adaptive architecture (Balcerak-Woźniak et al., 2024).

A subgroup in thermo-responsive polymers includes Shape Memory Polymers (SMPs). They are programmed to remember one shape what make it able to change shape. This process is thermally activated and based on net points and molecular switches, illustrated in Figure 4.8 (Bengisu & Ferrara, 2018). According to Lelieveld (2013), shape memory polymers were implemented successfully in a prototype, thus reaching TRL of 4-6.

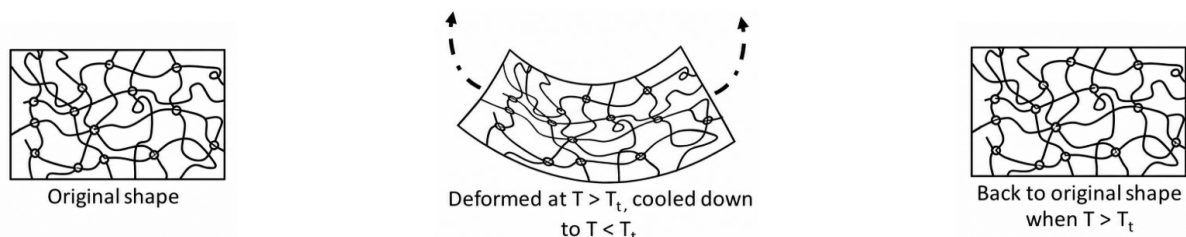


Figure 4.8

Thermally induced shape memory effect of Shape Memory Polymers (SMPs).

Note. From Bengisu & Ferrara (2018).

Thermally Responsive Metals

Thermally responsive metals are smart materials consisting of a metal or a combination of metals that respond to temperature changes with a mechanical or kinetic reaction. This reaction relies on internal phase changes or thermal expansion differences (Formentini & Lenci, 2018).

The largest family within thermo-responsive metals is Shape Memory Alloys (SMAs), such as Nitinol (Ni-Ti) wires. The response mechanism of these SMAs relies on a solid-state phase transformation. It consists of two types of phases: the austenite phase, which is the high-temperature rigid state with a

strongly connected molecular structure. And the martensite phase, which consists of the low-temperature weaker state that can easily be deformed. When the SMA is in its martensitic state is deformed and then heated above the austenite start temperature, it recovers its original, "remembered" shape with significant force (see Figure 4.9) (Addington & Schodek, 2005).

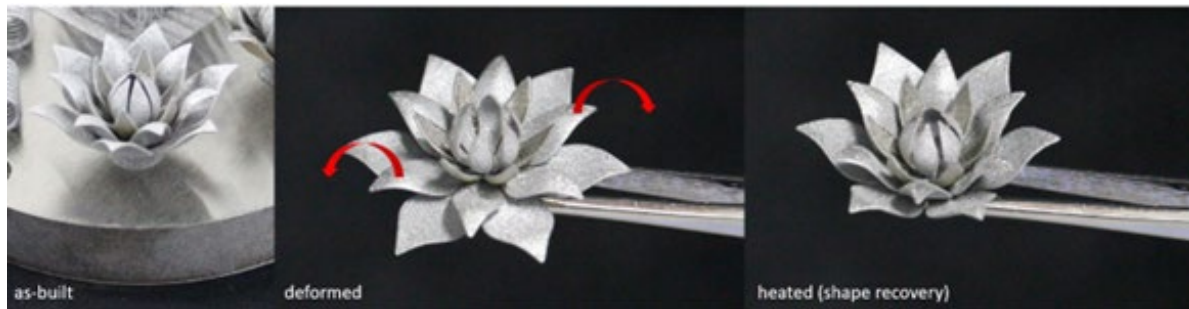


Figure 4.9

Shape memory effect with SMAs.

Note. From inspire AG (n.d.).

The mechanical behaviour in SMAs can be defined by three characteristics. First, one-way shape memory effect, here the recovery of a predetermined shape occurs only upon heating after plastic deformation at a low temperature. Secondly, the two-way shape memory effect, here the alloy is programmed to switch between high and low-temperatures shapes automatically as it cycles through thermal thresholds. Lastly, super-elasticity, this thermos-reversible process initiates a martensitic transformation under stress at temperatures above the austenite finish point. Large deformations up to 8 percent can recover instantaneously as stresses are removed without any change in temperature (see Figure 4.10) (Addington & Schodek, 2005).

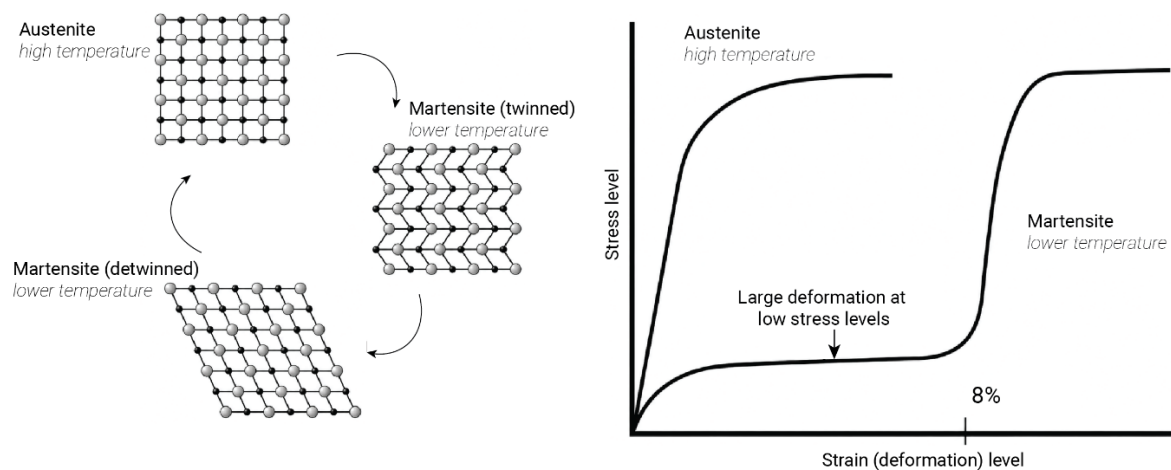



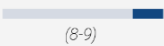



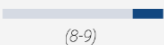



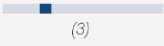


Figure 4.10


Shape memory alloys (e.g., Nitinol) that exhibit thermally induced shape memory effects.


Note. Adapted from Addington & Schodek (2005).


In façade applications SMAs function both as a sensor and actuator, providing movement without any external energy source. These alloys can be incorporated into adaptive façades, where panels respond to temperature fluctuations. For example, opening in warm conditions and close when the temperature drops. According to Formentini & Lenci (2018) the use of SMAs in adaptive buildings is still in a proof-of-concept stage, so it has a Technology Readiness Levels (TRL) of 3.


A second critical category of thermally responsive metals are thermo-bimetals. Thermo-bimetals are made from two metals whose expansion coefficients differ, leading to deformation when exposed to temperature variations. This allows them to perform continuously and autonomously. Thermo-bimetals are applied widely on a large scale in commercial settings, such as thermostats, reaching a TRL of 9 (Sung, 2011). But for façade integration thermo-bimetals are not classified as market ready but are well developed as prototype or laboratory level, reaching a TRL of 4 or 5 (Gosztonyi, 2022). In essence, thermally responsive metals allow mechanical actuations driven by temperatures.

Material	Function	Description	Application	TRL <i>Facade application</i>
Thermochromic		Solar transmittance & reflectance change with temperature	Glazing coatings	 (8-9)
Thermoelectric		Electricity generation via temperature gradients	Thermoelectric bricks	 (3-4)
PCM		Thermal energy storage through phase change	Walls, ceilings, floors	 (8-9)
SMP		Shape memory response to temperature change	Adaptive components	 (4-6)
SMA		Mechanical actuation based on phase transformation	Adaptive façades	 (3)
Bimetal		Thermal expansion for mechanical bending	Louvres, shading devices	 (4-5)

 Solar radiation modulation

 Temperature regulation

 Colour change

 Energy generation


 Mechanical actuation

Figure 4.11
Comparative material matrix of thermo-responsive materials.

4.3 Light-Responsive Materials

Light-responsive materials are smart materials that change their properties when exposed to lights or specific wavelengths, intensities. In the next sections different light-responsive materials will be discussed, and their response, applications and their Technology Readiness Level (TRL). This is summarized in Figure 4.15.

Photochromic Materials

Photochromic materials are known by their capability to a reversible colour change. These materials change the reflection of colours because of exposure to light, particularly radiation with a high UV content. When these materials absorb photons, their molecular structure is altered from a colourless inactivated state into an excited state that reflects longer wavelengths in the visible spectrum. This process is reversible and depends on the intensity of the light, illustrated in Figure 4.12 (Addington & Schodek, 2005).

For façade applications, photochromic materials are implemented because of the capacity to automatically change colour in response to the changes in the concentration of light (Loonen et al., 2013). This helps prevent glare and reduce solar heat gain without the need for external power or manual control (Addington & Schodek, 2005). The application of photochromic materials, such as switchable glass, in adaptive façades is a commercial product, reaching a TRL of 9 (Loonen et al., 2013). Nevertheless, it faced challenges regarding response times and material stability under long-term UV exposure (Addington & Schodek, 2005).

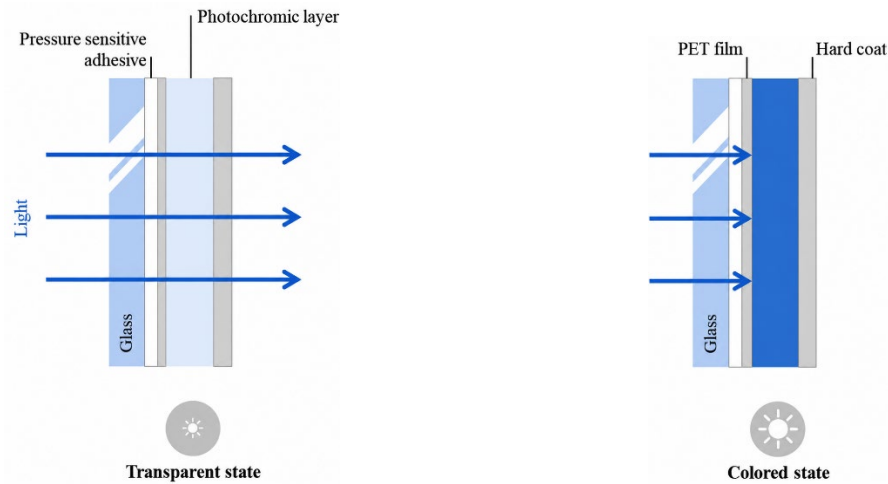


Figure 4.12
Schematic illustration of photochromic glazing.
Note. From Teixeira et al. (2025).

Luminescent Solar Concentrator (LSC) Materials

Luminescent solar concentrator (LSC) materials respond to light. This by absorbing shorter-wavelength radiation, often in the UV range, and re-emitted it at a longer wavelength. This process is also known as photoluminescence. When an electron is excited to a higher energy level and later returns to a lower energy state and will release light energy (see Figure 4.13). Emitted light is transmitted through the materials using the total internal reflection phenomenon to reach their edges, where it is absorbed by the PV cells and converted to electricity. Regarding façade implications, LSC are used as transparent alternatives to conventional silicon-based materials. They are mainly used to implement as Building Integrated Photovoltaics (BIPV), to provide both transparency and energy generation (Pitsika & Stathatos, 2026).

Technology readiness level (TRL) of LSC materials varies. But they are described by Halawa et al. (2018) as an emerging façade technology. Furthermore, LSC experience different critical factors for the use of commercial applications. Therefore, LSCs have a TRL of 4 to 6. In summary, LSC materials allow harvesting energy from light in transparent façade systems.

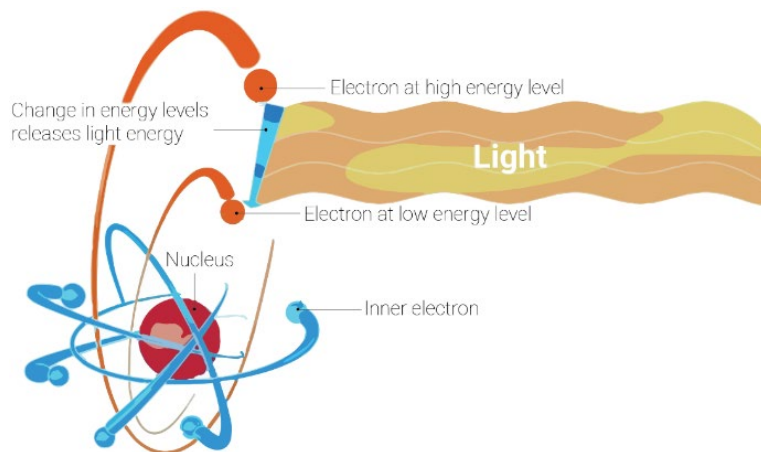


Figure 4.13
Schematic representation of photoluminescence, which forms the fundamental mechanism behind luminescent solar concentrator (LSC) materials.
Note. Adapted from Costa et al. (2025).

Photocatalytic Materials

Photocatalytic materials use the power of photons to trigger chemical reactions on their surface, with the breakdown of pollutants as a result. In this way the surface got cleaned. When a surface is exposed to UV radiation, this trigger's reaction in semiconductors like Titanium Dioxide (TiO₂). This is activating the oxidation process, what is an endless process (Lelieveld, 2013). This breaks down dirt, bacteria, and nitrogen oxides (NO_x) (see Figure 4.14).

For façade applications, photocatalytic materials are mostly applied on glass and panels. Their role is to provide self-cleaning and purify the air. Photocatalytic materials are characterized by super-hydrophilic property's, what results in removing dirt without any streaks (Boostani & Modirrousta, 2016). Hence, it can be argued that photocatalytic materials are currently at an intermediate level of development. They have Technology Readiness Levels (TRL) varying from 5 to 7. To conclude, photocatalytic materials facilitate photo-oxidation reactions for self-cleaning and air purification within the façade systems.

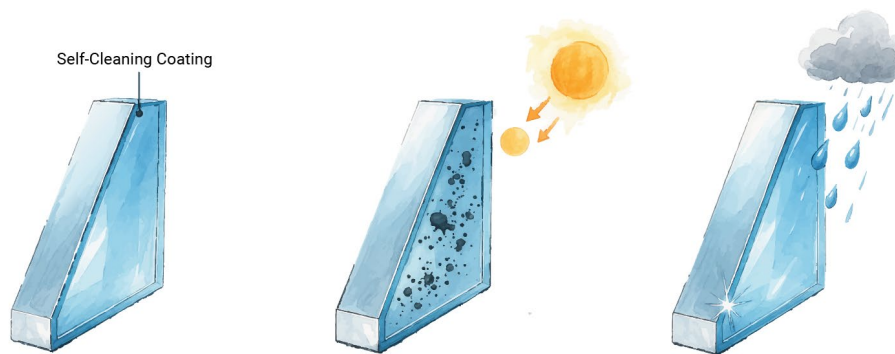


Figure 4.14

A self-cleaning glass system based on titanium oxide (TiO₂).

Note. Adapted from Boostani & Modirrousta (2016).

Material	Function	Description	Application	TRL <i>Facade application</i>
Photochromic		Colour change in response to UV radiation	Smart glazing	 (9)
LSC		Solar energy harvesting through light absorption	BIPV glazing	 (4-6)
Photocatalytic		Self-cleaning & air purification through UV activation	Coatings	 (5-7)

Solar radiation modulation

Temperature regulation

Colour change

Energy generation

Mechanical actuation

Figure 4.15

Comparative material matrix of light-responsive materials.

4.4 Moisture-Responsive Materials

Moisture-responsive materials are smart materials that change their properties when exposed to changes in relative humidity. In the next sections different moisture-responsive materials will be discussed, and their response, applications and their Technology Readiness Level (TRL). This is summarized in Figure 4.19.

Hygro-Morphic Materials

Hygro-morphic materials are smart materials that to response changing moisture levels by generating mechanical motion or reversible deformation in their volume, size, and stiffness. It is a passive responsive system, inspired by natural systems (Holstov et al., 2015). For example, the cones of conifer trees only open or close in the presence of moisture (see Figure 4.16).



Figure 4.16
Reversible moisture-driven closing (wet conditions) and opening (dry conditions) of spruce cones.
Note. From Vailati et al. (2018).

When exposed to humidity variations, hygro-morphic materials absorb or release moisture. This results in deformation in their volume. This phenomenon is usually implemented in bi-layer structures, what consist of an active and passive layer. Where the active layer has a large hygroscopic expansion coefficient while the passive one shows stability. The difference in their expansion coefficients leads to the material curvature (see Figure 4.17) (Holstov et al., 2015).

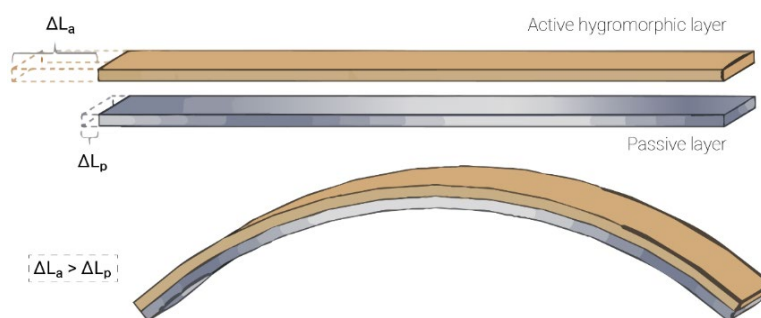


Figure 4.17
Principle of the response of hydromorphic composites based on active and passive layer.
Note. Adapted from Holstov et al. (2015).

For the application in adaptive façades, hygro-morphic materials respond to humidity levels. For instance, they may open when the air is dry to improve natural ventilation and close when it rains to ensure protection from weathering (Holstov et al., 2015). At the moment, Hygro-morphic materials are still in the initial stages of their implementation in architectural design, and their Technology Readiness Level (TRL) varies from 1 to 7 (Gosztanyi, 2022).

Moisture-Responsive Crystalline Materials

Moisture-responsive crystalline materials are smart materials responding to changes in relative humidity through structural changes. Upon exposure to moisture, these crystalline materials undergo phase changes. Resulting in changes in the volume of the unit cells. For instance, a change in phases from the beta to the alpha phase leads to a volumetric change of the unit cells by as much as 16.2% (Yang et al., 2021).

For adaptive façade applications, it could play a role in harvesting water from the air and acting as actuators. Further development of the concept entails coupling the system with piezoelectric material capable of converting mechanical changes into electrical energy. This can provide a self-sustained wireless sensing in smart buildings (Yang et al., 2021).

The technology is still at an early stage of development and its Technology Readiness Level (TRL) ranges from 3 to 5. Even though proof-of-concept and pilot-scale experiments have proved successful, development of practical applications is still ongoing (Yang et al., 2021). Generally, the materials have the capability of producing humidity driven mechanical changes with application in energy systems and sensing.

Hygroscopic Bio-based Insulation Materials

Hygroscopic bio-based insulation materials, such as sheep wool, hemp, flax, straw, and cork, undergo absorption or desorption of moisture depending on fluctuations in air humidity (Barbhuiya et al., 2025). See Figure 4.18 for peat and moss as examples of hygroscopic biobased insulation materials. The absorption and desorption processes are associated with the storage and release of latent heat, which positively impacts the thermal performance of façades (Hameury, 2005).






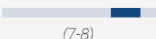
These materials are used in sustainable construction and building retrofit projects in order to provide for a stable indoor climate and prevent any risks associated with excessive indoor humidity or mold development (Barbhuiya et al., 2025). The hygroscopic bio-based insulating materials are utilized in construction and can be characterized by relatively high technological maturity, so the TRL is 7-8. Overall, these materials allow regulating air humidity passively.



Figure 4.18

Examples of hygroscopic bio-based insulation material: peat (left), moss (right).

Note. From Fedorik et al. (2021).

Material	Function	Description	Application	TRL <i>Facade application</i>
Hygro-morphic		Deformation due to moisture changes	Ventilation elements	 (1-7)
Crystalline		Phase change in response to humidity	Sensors, energy systems	 (3-5)
Bio-based insulation		Moisture & heat buffering for improved thermal performance	Insulation materials	 (7-8)






 Solar radiation modulation	 Temperature regulation	 Colour change
 Energy generation	 Mechanical actuation	

Figure 4.19
Comparative material matrix of moisture-responsive materials.

4.5 Electromagnetic Responsive Materials

Electromagnetic responsive materials are smart materials that change their properties when exposed to an external magnetic or electric field. In the next sections different electromagnetic responsive materials will be discussed, and their response, applications and their Technology Readiness Level (TRL). This is summarized in Figure 4.22.

Electrochromic Materials

Electrochromic materials are smart materials that change their optical characteristics like transmission, absorption, and reflection of light in responds to electrical inputs (see Figure 4.20). When a voltage is applied, ions are reversibly inserted or extracted within an electroactive layer. This leads to a change between transparent (bleached) and a dark (coloured) appearance (Riganti et al., 2025).

Electrochromic materials are used in façade systems primarily in glazing assemblies for dynamic control of solar radiation. They provide shading to minimize solar gains during summertime while allowing heat gains during wintertime. Electrochromic materials differ from passive systems as they need an external power supply, the electrical input. Despite requiring electricity and having higher installation costs, electrochromic materials help to minimize peak heating loads and provide comfort indoor (Roostaei Firouzabad & Razi Astaraei, 2024).

Electrochromic glazing has been applied wildly in the construction sector. Furthermore, it has reached a high level of technological maturity. Reaching a TRL between the 8 and 9 (Gosztanyi, 2022). In summary, electrochromic materials undergo optical properties changes driven by electrical inputs.

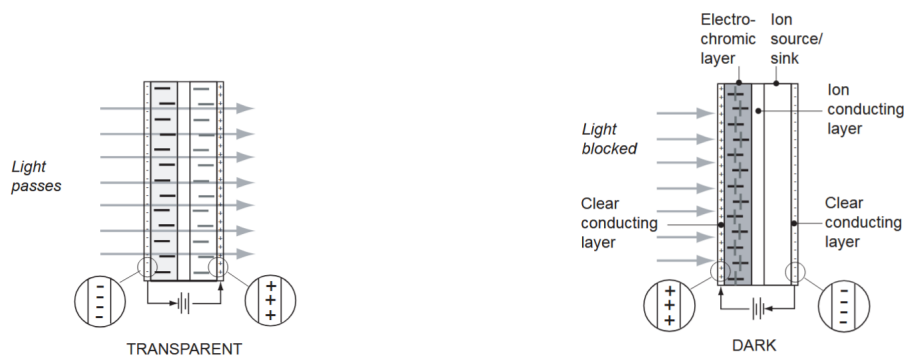


Figure 4.20
Electrochromic glass.
Note. From Addington & Schodek (2005).

Magnetoactive Polymer Composites

Magnetoactive polymer composites are smart materials that change their properties or shape in response to magnetic fields (see Figure 4.21). These materials consist of magnetic nanoparticles into a polymer matrix. The interaction among dipoles leads to a deformation of the material under exposure to magnetic fields. Depending on the type of particles that are used, the response differs. Either irreversible changes in material properties may be observed, or deformations that remain permanent (Balcerak-Woźniak et al., 2024).

In terms of applications, such materials are typically involved in technologies like soft robotics, microvalves, or systems for drug delivery. That require remote activation by means of applying a magnetic field. In large scale architecture, these materials are used for smart infrastructure, where the materials can be used to provide self-sensing functions and programmable deformation in interactive surfaces. Furthermore, these smart materials are beyond the proof-of-concept stage, therefore reaching TRL of 5-6 (García et al., 2023). Thus, these materials allow controllable mechanical effects in adaptive systems driven by magnetic fields.

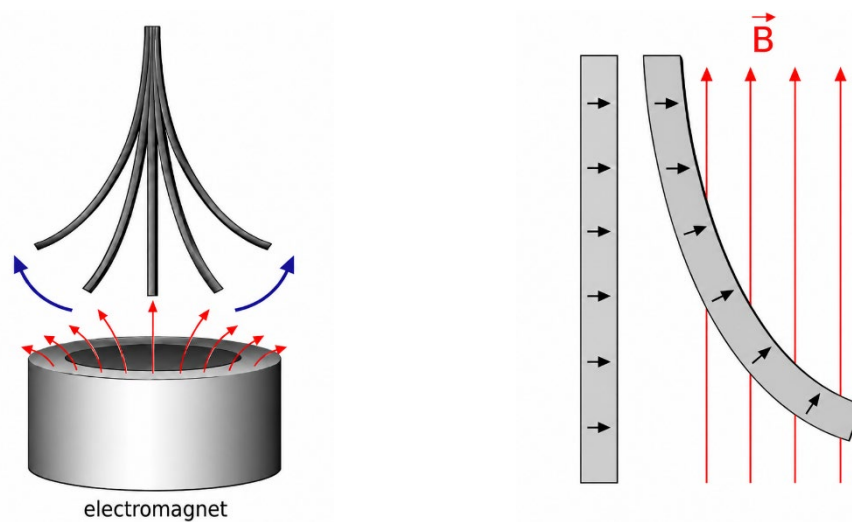


Figure 4.21
Deformation of a soft magnetoactive actuator under a magnetic field.
Note. From García et al. (2023).

Material	Function	Description	Application	TRL <i>Facade application</i>
Electrochromic		Optical change in response to electrical inputs	Smart glazing	 (8-9)
Magnetoactive polymer		Shape change via magnetic fields	Smart infrastructure	 (5-6)

Solar radiation modulation

Temperature regulation

Colour change

Energy generation

Mechanical actuation

Figure 4.22
Comparative material matrix of electromagnetic-responsive materials.

4.6 Mechanical Stress Responsive Materials

Mechanical stress responsive materials are smart materials that change their properties when exposed to mechanical stress. In the next sections different mechanical stress responsive materials will be discussed, and their response, applications and their Technology Readiness Level (TRL). This is summarized in Figure 4.24.

Mechano-Chromic Materials

Mechano-chromic materials are smart materials that alter their optical properties, like colour, when exposed to mechanical stress and deformations, illustrated in Figure 4.23 (Addington & Schodek, 2005). These materials consist mostly of polymer-based composites. The technology of mechano-chromic materials is less complex than the technology of electrochromic glass because it has faster response and simpler construction. But there is one drawback to the technology because it requires only slight mechanical deformation to produce substantial optical effects.

Mechano-chromic materials can be used in façade design to provide temperature control and manage the accumulation of solar energy inside the building, depending on the deformation of structure or the mechanical stresses it experiences. These materials are still in the prototype stage and needs laboratory validations and experimental research. Thus, mechano-chromic materials reach a TRL from 4 to 7 (Li et al., 2025). Thus, with the help of mechano-chromic materials, it is possible to achieve mechanical-driven optical adaptation of façades.

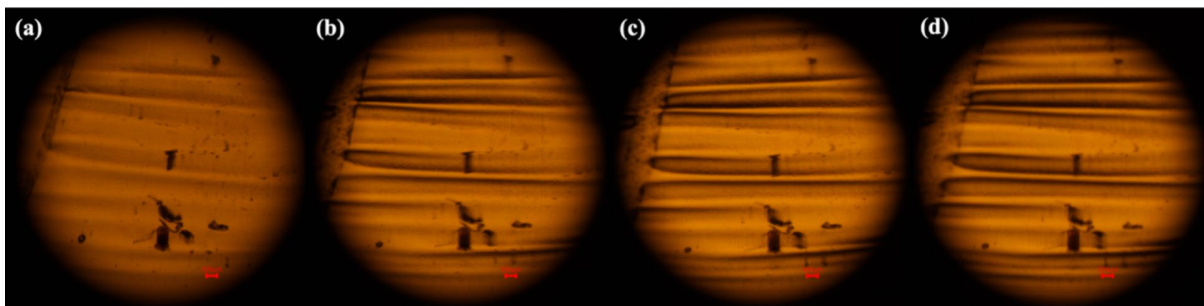


Figure 4.23

Optical microscopy images of a mechano-chromic film under increasing strain: (a) released state, (b) 5% strain, (c) 10% strain, and (d) 15% strain.

Note. From Li et al. (2025).





Note. Scale bars represent 100 μm .

Piezoelectric Materials

Piezoelectric materials are smart materials that generates electrical energy under response of mechanical stress (Jali, 2025). As the mechanical forces are applied to these materials, they generate electrical energy immediately. Furthermore, it causes a slight mechanical deformation, what is an inverse effect.

In façade applications, piezoelectric elements are used to harvest energy from wind forces and vibrations. This for powering self-sufficient wireless sensors. Moreover, these materials can operate as integrated sensors for structural health monitoring. By monitoring cracks, corrosion, or strain within building components (Chen et al., 2019). Additionally, they can work as actuators to dampen vibrations or to drive kinetic façades, for example shading devices (Gosztanyi, 2022). Large-scale applications for energy harvesting and active control purposes in façades are currently limited to prototypes and lab validation stages. Therefore, reaching a TRL of a range from 4 to 7.

The advantages of using piezoelectric in façades include high power densities and capabilities as sensors and actuators. Their disadvantages include low mechanical deformations and instability and fatigue issues along with high actuating voltages (Chen et al., 2019).

Material	Function	Description	Application	TRL <i>Facade application</i>
Mechano-chromic		Colour change due to mechanical stress	Facade design	 (4-7)
Piezoelectric		Generates electricity through mechanical stress	Energy harvesting, sensors	 (4-7)






 Solar radiation modulation	 Temperature regulation	 Colour change
 Energy generation	 Mechanical actuation	

Figure 4.24

Comparative material matrix of mechanical stress responsive materials.

4.7 Chemically Responsive Materials

Chemically responsive materials are smart materials that change their properties or features when exposed to a change in chemically environments. In the next sections different chemically responsive materials will be discussed, and their response, applications and their Technology Readiness Level (TRL). This is summarized in Figure 4.27.

Chemo-Chromic Materials

Chemo-chromic materials are smart materials that change colour when exposed to specific chemical environments. They are usually incorporated into coatings or films, which enables them to function autonomously by detecting the presence of certain chemicals or gases in the environment, see Figure 4.25 (Addington & Schodek, 2005).

For façade applications, chemo-chromic materials present a passive way of detecting environmental changes and communicating them visually. One important limitation for façade use is the problem of degradation caused by exposure to UV light (Addington & Schodek, 2005). These materials are an emerging technology. While simple chemical indicators, such as litmus paper, may be said to be mature. Thereby reaching an TRL of 9. For façade applications are in a much earlier stage of development, reaching an TRL between 3-5.



Figure 4.25

Chemochromic material example.

Note. From OliKrom, n.d.

PH-Responsive Polymers

PH-responsive polymers are smart materials that change in properties based on Ph-changes in the environment, see Figure 4.26. They generally react through the expansion or shrinkage of volume, changes in solubility, or a variation in colour (Balcerak-Woźniak et al., 2024). For façade applications, pH-responsive polymers could respond by releasing corrosion inhibitors, when exposed to local pH levels. Furthermore, pH-sensitive polymer materials remain in the process of development, and TRLs range from 3 to 6 (Zhang et al., 2025).

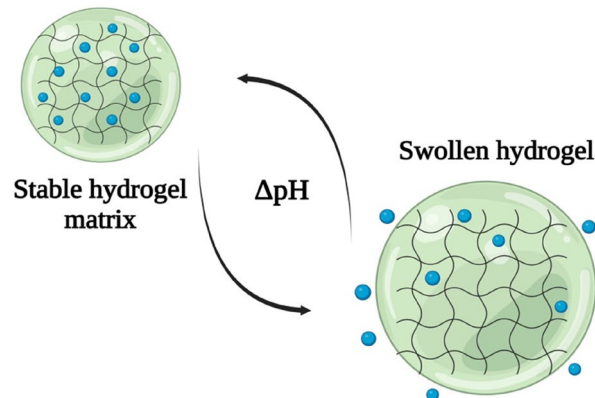


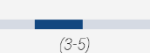

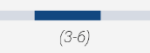


Figure 4.26

Swelling/de-swelling of drug-loaded hydrogel matrix, resulting from the change in ambient pH.

Note. From Singh & Nayak (2023).

Material	Function	Description	Application	TRL <i>Facade application</i>
Chemo-chromic	 	Colour change in response to chemical environments	Coatings, films	 (3-5)
PH-responce polymers		Shape/volume change due to pH levels	Corrosion inhibitors	 (3-6)






 Solar radiation modulation	 Temperature regulation	 Colour change
 Energy generation	 Mechanical actuation	

Figure 4.27

Comparative material matrix of chemically responsive materials.

4.8 Conclusion

This chapter provided an overview of smart materials, their behaviour, characterises and possible applications in the building industry. Smart materials are defined as materials that change one or more properties in responds to environmental stimuli in a predictable way. The evaluated smart materials were categorized according to their stimuli. Six main categories where defined: thermo-responsive, light-responsive, moisture-responsive, electromagnetic responsive, mechanical stress responsive and chemically responsive materials. For each category, the response mechanism, possible façade application and TRL were discussed.

To conclude, the overview illustrates that smart materials differ in their response, maturity and limitations. Therefore, the classification and comparative materials matrix make the basis for the translation of smart materials into adaptive façades.

5. From Smart Materials to Façade Integration

This chapter bridges the gap between material properties and architectural application. The information from the comparative material matrix will be used to translate smart materials into façade functions. First, specific façade functions are defined. Which have an immediate impact on the indoor climate. Secondly, these façade functions are linked to material responses of the smart materials. This is the hinge between the literature-based material exploration and selecting promising smart materials for further research.

5.1 Façade Functions Relevant to Indoor climate

The function of the façade is the most direct interface between the outdoor and indoor environment (Addington and Schodek, 2005; Halawa et al., 2018). For this research, the functions of the façade are organized based on the main categories of indoor comfort, thermal comfort, visual comfort, and acoustic comfort. Although acoustic comfort is relevant façade function. It is not further addressed in this research. Because acoustic comfort has no direct impact on the indoor climate.

5.1.1 Thermal Comfort

Thermal comfort is related to the ability of the façade to control heat transfer. A primary function is the thermal regulation through the reduction of heat losses (Barbhuiya et al., 2025). This is ensured by thermal insulation, expressed by the U-value. A high level of airtightness is also required to reduce uncontrolled air leakage. Furthermore, the façade should also limit unwanted heat gains during summer, mainly caused by solar radiation. This is mostly because of heat gains through solar radiation (Barbhuiya et al., 2025). In addition to heat transfer, thermal buffering by storing heat and releasing it at another time is also a strategy of heat regulation. Materials with a high thermal capacity, such as concrete, can store heat and release it during cooler periods, for example during the night. This results in reducing excessive heat in buildings (Liu et al., 2025).

Moreover, natural ventilation is a strategy to remove this excessive heat in buildings. In this way the façade is not only limiting the heat gain through solar control, airtightness, and insulation. But also contributing to passively cool the indoor climate, when the outdoor conditions are favourable, by air exchange and increasing thermal comfort.

The performance of all these thermal functions is related to aspects as indoor temperatures, the total overheating hours, and the energy demand in buildings. This establishes a direct relationship between different façade design strategies and thermal comfort, within the building.

5.1.2 Visual Comfort

Key aspects of visual comfort are daylight control, glare protection, and the regulation of indoor illuminance. Sufficient daylight can make occupants feel more comfortable. The windows transparency, properties, and shading strategies measure the total amount of light that enters a building. Besides from daylight control, the façade must also address the issue of visual discomfort due to glare (Halawa et al., 2018). High levels of luminance or large luminance near openings areas may impact occupants' comfort negatively. Furthermore, this may lead to the use of blinds and artificial lighting systems.

5.1.3 Indoor Air Quality

The indoor air quality is also controlled by the façade to allow controlled ventilation while at the same time preventing unwanted air leakage (Barbhuiya et al., 2025). Ventilation makes sure that fresh air is entering the building, while at the same time removing CO₂ and other pollutants, such as dust and bacteria. Failure of these leads often to Sick Building Syndrome (SBS). This is negatively impacting

occupants' productivity and health (Bilow, 2012). Ventilation could be applied with several techniques. Such as natural ventilation, with windows, gaps or shafts, through mechanical systems or the combination of both approaches.

Besides ventilation for indoor air quality, ventilation can also be used as a cooling strategy to reduce overheating. In this case, the aim is not only to supply fresh air, but also to remove excess indoor heat when outdoor conditions are favourable. The façade plays a key role in the path of airflow as well as the size of the openings (Roostaei Firouzabad & Razi Astaraei, 2024). These parameters influence the effectiveness of ventilation.

Moreover, moisture levels are also part of indoor air quality, as they directly influence humidity levels. In this way they influence comfort and the risk of mould growth. The façade regulates the movement and exchange of moisture through different methods. Such as, diffusion of water vapor across the façade. Furthermore, the use of moisture buffering in building materials, like massive timber. Which can absorb excess moisture and release it during humid conditions (Hameury, 2005). This plays a crucial role in ensuring the relatively humidity levels remain comfortable, this is between 30% and 65%. Thereby enhancing general thermal comfort (Bilow, 2012).

5.2 Linking Smart Materials Responses to Façade Functions

This section links material responses to façade functions what are relevant to the indoor climate. This is based on the classification and the comparative material matrix of smart materials, what is presented in chapter 4. The aim is not to explain the materials again, but to identify which stimulus–response mechanisms are relevant at façade and building scale.

5.2.1 Thermo-Responsive Materials

Thermo-responsive smart materials have mainly been used in ensuring thermal comfort. Because these smart materials have the capacity to moderate solar energy, store thermal heat or causes actuation, which can provide sun shading or a ventilation system. This helps the indoor climate to reduce the risks of overheating (Barbhuiya et al., 2025). Two types of thermo-responsive materials can be differentiated for façade applications, namely property changing and shape changing response smart materials.

First, property changing responses, this includes the modification of the optical properties of façades in responds to thermal variations, this is considered as solar radiation modulation function. Materials just as glazing and coatings change their transmittance, reflectance, absorptance, or emittance properties (Kamalisarvestani et al., 2013). For example, thermochromic materials react by changing from their transparent properties, which facilitate the admission of solar energy during the winter months, to being opaque, therefore reflecting unwanted energy during the summer months (Mu et al., 2024).

Secondly, shape changing responses, based on thermal variations there occurs a change of geometry of the façade element. This can result in temperature regulation or mechanical actuation as a function. These thermo-responsive façades usually have the following two effects:

1. Shifting of thermal peaks: excess thermal energy available in the building envelope is temporarily stored as latent heat using Phase Change Materials (PCMs). This capability of façades results in flatten the temperature fluctuations peaks (Baylis & Cruickshank, 2023).
2. Reduction of cooling loads: through mechanical actuation of certain smart materials, such as SMAs or thermo-bimetals, dynamic shading or ventilation systems can function passive. Thereby reducing indoor temperatures during warm periods.

Thermo-responsive materials establish a direct correlation between temperature-driven material properties and various façade functions, like solar control, thermal regulation, and energy buffering.

These materials can reduce the cooling need and the peak demands. How these thermo-responsive materials can potentially influence different façade function is illustrated in Figure 5.1.

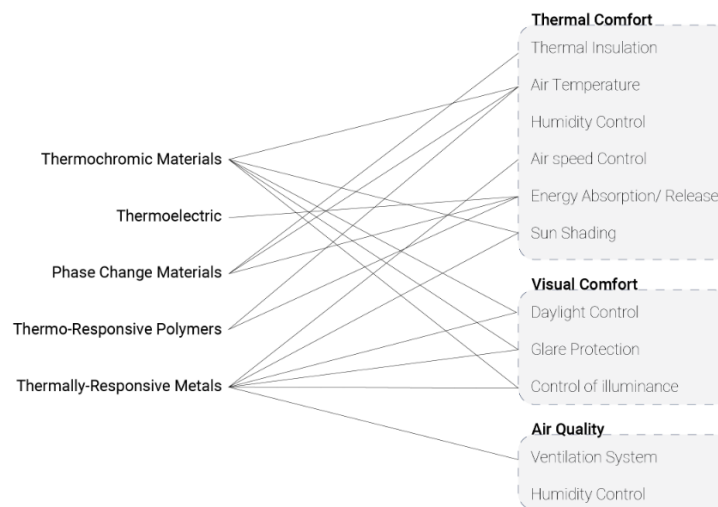


Figure 5.1
Schematic mapping of thermo-responsive material responses to façade functions.

5.2.2 Light-Responsive Materials

Light-responsive materials have a reversible change in their optical properties in response to exposure of light. These materials have the ability to improve the thermal comfort of the room due to the reduction of solar gains. What leads to lowering cooling demands. Nevertheless, there is a conflict between occupants’ comfort, daylight, and energy consumption of a building. When light-responsive materials have a high solar control and glare mitigation, this can lead to compromises in the level of available daylight. Which can result in a higher demand of electric lighting. What is negatively influencing the benefits of the decreasing in cooling loads, because of the reduction of solar radiation entering the room (Halawa et al., 2018).

To conclude, light-responsive smart materials have the ability in a façade to alter visual comfort and sunlight control. However, performance evaluation is necessary, in terms of the trade-offs between comfort, daylight, and the energy demand. How these light-responsive materials can potentially influence different façade function is illustrated in Figure 5.2.

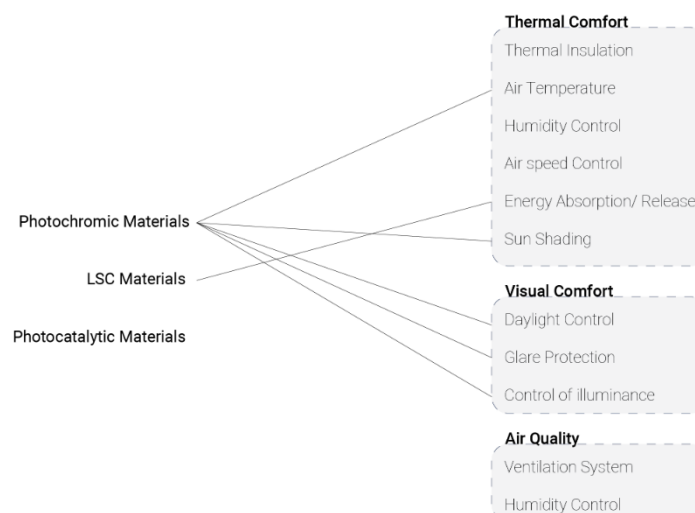


Figure 5.2
Schematic mapping of light-responsive material responses to façade functions.

5.2.3 Moisture-Responsive

Moisture-responsive smart materials are related to façade functions regarding air quality and natural ventilation. They have the ability to close and open autonomously, resulting in altering ventilation paths without the need for complex mechanical systems. An example of using this technique as a cladding is Norwegian boathouses in Nordmøre. During dry conditions the wood curls up, allowing natural ventilation. This is a reversible process, so during wet weather the wood bents back (see Figure 5.3) (Holstov et al., 2015).

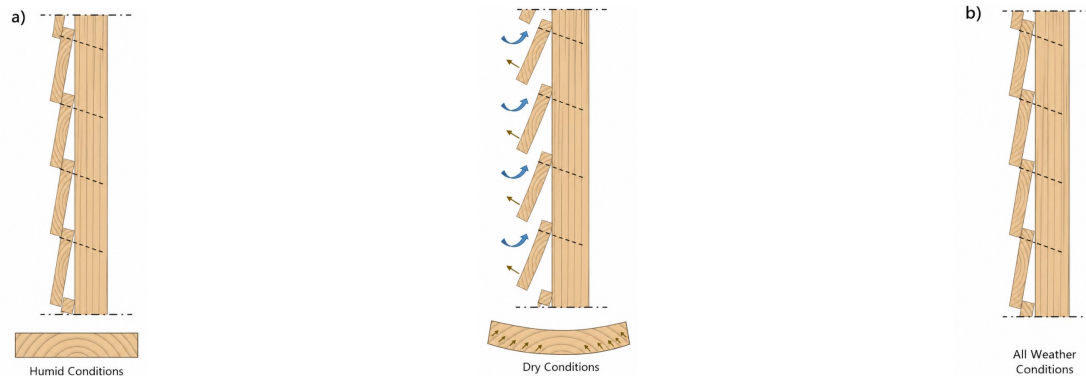


Figure 5.3
Boathouses in Nordmøre, Norway, enhance natural ventilation in dry weather.
Note. From Holstov et al. (2015).

In addition to passive actuation, hygroscopic materials such as heavy timber structures what are directly exposed to an indoor climate provide moisture buffering (Hameury, 2005). They absorb excess humidity and release it when the conditions become drier. This to regulate the daily or seasonal variation in humidity. Moisture buffering will enhance indoor air quality by helping to maintain indoor relative humidity within the comfortable range of 30% to 65%. Furthermore, it has a relation in enhancing occupant thermal comfort (Bilow, 2012). These moisture-responsive systems are based on inherent intrinsic material behaviour. It has sensing and actuation functions, allowing passive adaptation at façade scale while minimizing technical complexity and maintenance. On the other hand, their behaviour is highly dependent on climate conditions. So, their effectiveness is highly linked to particular climate zones (Holstov et al., 2015). How these moisture-responsive materials can potentially influence different façade function is illustrated in Figure 5.4.

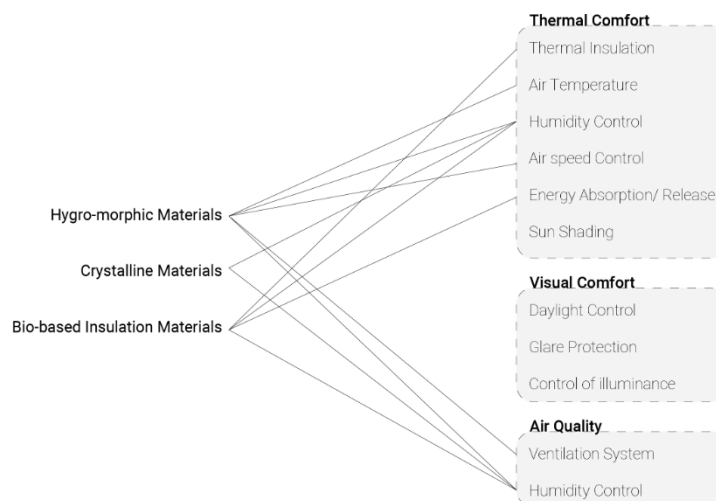


Figure 5.4
Schematic mapping of moisture-responsive material responses to façade functions.

5.2.4 Electromagnetic Responsive Materials

Electromagnetic responsive, such as electrochromic glazing, have high impact on the building performance. Because, due to their role in controlling solar heat gain, providing visual comfort, and modifying daylight transmission. Which are all crucial aspects of the indoor thermal environment. These materials can filter electrical radiation during peak season, while allowing heat gain during winter (Riganti et al., 2025). This kind of adaption has a high degree of precise control of solar heat gains and glare protection. Field test shows a reduction of 40% in the cooling loads. Nevertheless, electrochromic glass needs an external energy source, so it is an active system. Resulting that this type of technology comes with additional complexity (Barbhuiya et al., 2025).

In conclusion, electromagnetic responsive materials may have the potential in adaptive façades for improving visual comfort and reducing solar heat gains. The effectiveness of this system depends on the amount of control that can be archived. And how well this technique is implemented in the building based on the local climate. Therefore, the implementation of these materials must evaluate based on the specific performance requirements and the local climatic context to ensure an optimal balance between technology and sustainability. How these electromagnetic responsive materials can potentially influence different façade function is illustrated in Figure 5.5.

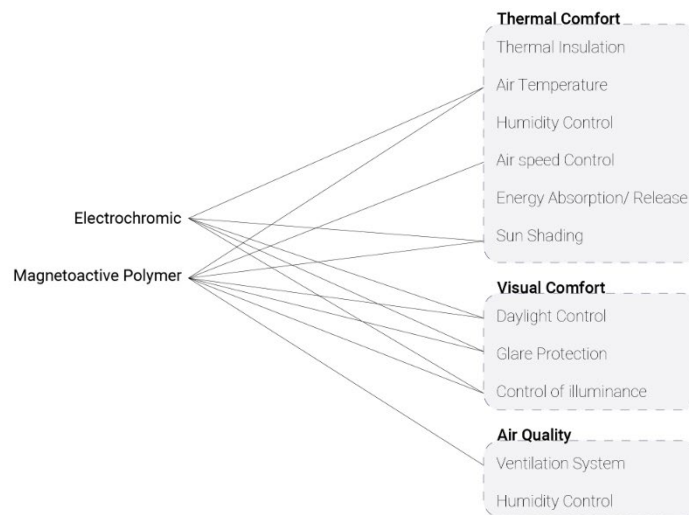


Figure 5.5
Schematic mapping of electromagnetic responsive material responses to façade functions.

5.2.5 Other Main Categories

This study aims to investigate the impact of smart materials on the indoor climate. Specific materials in these groups are excluded for further investigation. This because, materials like mechano-chromic and piezoelectric, are mainly used for structural health monitoring, precision sensing, and generating energy (Chen et al., 2019; García et al., 2023). Furthermore, these materials have a limited or no functional influence in the regulation on the indoor climate. Similarly, smart materials that responds to chemical changes have a promising aspect for improving the indoor air quality, by detecting chemical pollutants (Balcerak-Woźniak et al., 2024). However, these materials have a limited impact on the overall indoor climate. Such as controlling thermal conditions, airflow or solar gains. Therefore, will these materials be excluded for further research for the implementation in a façade.

5.3 Selection Criteria for Smart Materials for Façade Integration

To select the right smart materials for further research, they need to fulfil certain selection criteria. This to evaluate how these materials can be integrated into an adaptive façade design. Furthermore, to test how this is influencing the indoor climate. This section defines the selection criteria for evaluating smart materials. The result of this evaluation is presented in Table 5.1.

At first, the smart material should directly influence the indoor climate. Secondly, the response of the smart material is expected to be passive and reversible. Furthermore, the materials should have a Technology Readiness Level (TRL) of a 7 or lower. This is because materials with an TRL of 7 and lower are tested in real world conditions but are not yet commercial. So, these materials are still under development. What makes them suitable and interesting for further research and integration for adaptive façades. Additionally, for successful integration of smart materials in façade applications, the materials response thresholds must be aligned with the local climatic context and microclimate of the location of the case study. These design criteria are also summarized in Figure 5.6.



Figure 5.6
Design criteria for smart materials.

Table 5.1
Evaluation of Smart Materials Based on Selection Criteria

Smart material	Direct influence on indoor climate	Passive & reversible	TRL ≤ 7 (limited façade application)	Climate alignment	Suitable for further research
Thermo-responsive materials					
Thermochromic materials	Yes	Yes	No	Yes	No
Thermoelectric materials	No	No	Yes	Limited	No
Phase Change Materials (PCM)	Yes	Yes	No	Yes	No
Thermo-responsive polymers	Limited	Yes	Yes	Yes	Limited
Shape Memory Alloys (SMA)	Yes	Yes	Yes	Yes	Yes
Thermo-bimetals	Yes	Yes	Yes	Yes	Yes
Light-responsive materials					
Photochromic materials	Yes	Yes	No	Yes	No

Smart material	Direct influence on indoor climate	Passive & reversible	TRL ≤ 7 (limited façade application)	Climate alignment	Suitable for further research
Luminescent solar concentrators	No	Yes	Yes	Limited	No
Photocatalytic materials	Limited	Yes	Yes	Yes	Limited
Moisture-responsive materials					
Hygro-morphic materials	Yes	Yes	Yes	Yes	Yes
Moisture-responsive crystalline materials	Limited	Yes	Yes	Yes	Limited
Bio-based hygroscopic materials	Yes	Yes	No	Yes	No
Electromagnetic responsive materials					
Electrochromic materials	Yes	No	No	Yes	No
Magnetoactive polymer composites	Limited	No	Yes	Limited	No
Mechanical stress responsive materials					
Mechano-chromic materials	Limited	Yes	Yes	Limited	Limited
Piezoelectric materials	No	No	Yes	No	No
Chemically responsive materials					
Chemo-chromic materials	No	Yes	Yes	Limited	No
pH-responsive polymers	No	Yes	Yes	Limited	No

Note. “Yes” indicates that the material meets the selection criterion; “No” indicates that it does not meet the criterion; “Limited” indicates a partial or indirect contribution. TRL = Technology Readiness Level.

5.4 Conclusion

To conclude, according to the criteria discussed in Table 5.1, a selection of smart materials can be classified as suitable for further research. Smart materials such as, Shape Memory Alloys (SMAs), thermo-bimetals, and hydromorphic materials, fit all the proposed selection criteria. Which include, direct impact on the indoor climate, passively and reversible, and must have an TRL below a 7.

However, materials with a relatively high TRL (TRL>7) for example, thermochromic, photochromic, and electrochromic materials. Or materials without in direct influence on the indoor climate, including piezoelectric and chemo-chromic materials, can be considered as less suitable for further investigation within the scope of the research. In the following chapter there will be a deep dive in the selected smart materials.

6. Material Deep Dive

This chapter will dive deeper into smart materials that were promising for façade integration, based on the selection criteria. The threshold and actuation forces of shape memory alloys, thermo-bimetals, and hygro-morphic materials, will be mentioned. Furthermore, their advantages and limitations will be discussed. Finally, these materials are evaluated and compared to determine which material is most suitable for further development in this research.

6.1 Shape Memory Alloys (SMAs)

Shape Memory Alloys (SMAs) are a class of smart metallic materials that can remember a predetermined shape, driven by temperature. The next sections will discuss the SMAs thresholds, actuation forces, and advantages and limitations.

6.1.1 Martensitic Transformation

The functional intelligence of SMAs is based on a diffusion less solid-state phase transformation known as the martensitic transformation. This transformation takes place between two different crystalline phases, namely the austenite and martensite phase.

The austenite phase take place during high temperatures. The molecules in the SMA are well ordered in a crystal structure (Lelieveld, 2013). This results in a relatively strong and stiff materials. Which has a low deformability (Addington and Schodek, 2005). In contrast, the martensite phase, what occurs during low temperatures. When it is relatively soft, ductile, and easily deformable (Lelieveld, 2013). The comparison between the austenite and martensite phase is summarised in Table 6.1.

Table 6.1

Comparison of Austenite and Martensite Phases

Property	Austenite Phase	Martensite Phase
Temperature range	High temperature	Low temperature
Crystal structure	Ordered, stable	Twinned / reoriented
Mechanical behaviour	Strong and stiff	Soft and ductile
Deformability	Low	High
Shape memory state	Original (memorized) shape	Deformed state possible
Responds to stress	Elastic deformation	Easily reoriented under stress

6.1.2 Temperature Threshold

A characteristic of SMAs is the ability to program the transformation temperature. These temperatures thresholds can be adjusted with a high degree of accuracy using two main approaches. The first one depends on the chemical composition of the alloy. For instance, in Nickel-Titanium (Nitinol), a change of only 1% in Nickel concentration can cause a change of up to 100 °C in the transformation temperature. Secondly, applied stress had also an influence on the threshold of the alloys. Based on the Clausius-Clapeyron theorem, the transformation temperatures rise with an increase of applied stress on the material. This is particularly important for façades engineering. As the material weight or external wind pressure will cause a natural change in the activation temperatures of the SMA actuators (Formentini & Lenci, 2018).

Following existing research on adaptive building envelopes, the recommended SMA is Nitinol (Ni-Ti). Nitinol is preferred over copper-based alloys because of its enhanced corrosion resistance, increased ductility, and higher deformation recovery (up to 8%, versus the 4 to 5% of the copper-based alloys) (Lelieveld, 2013). Nitinol is usually programmed to activate between 10 °C and 110 °C (Bengisu & Ferrara, 2018).

6.1.3 Actuation Force

SMA is well known for providing maximum actuation stress relative to strain, among all known smart material. They produce very high recovery stresses (around 700 MPa) during the phase transformation from martensite to austenite. Due to this high force-to-weight ratio, SMA can act as very powerful actuators in a remarkably small size. The force produced depends on the size of the SMA (wire, spring, or strip), its cross-sectional area, and the internal stress. Larger dimensions will lead to higher forces. However, the stress-strain relation should be kept into account (Lelieveld, 2013).

6.1.4 Metal Fatigue

Metal fatigue in Shape Memory Alloys (SMAs) is directly related to applied strain and loading conditions. Higher or uneven strain results in degradation and lowering the lifespan of the alloy. So, SMA function best in a linear shape instead of bending. Because there is a much higher strain on the inside in comparison with the outer layer of the wire in bending conditions through the cross section (see Figure 6.1).

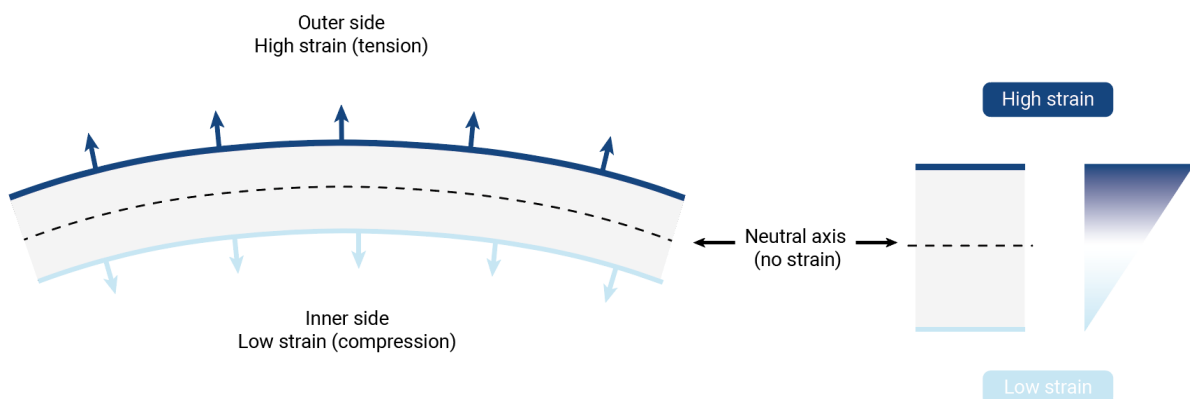


Figure 6.1
SMA wire in bending.

Furthermore, there is a difference in constant stress or strain. Research from Scire Mammano & Dragoni (2014) showed during constant strain tests that even during low strain values, it results in poor fatigue life. Failure for strain values ranging from 1% to 5% happens after about 7,000 to 19,000 cycles, where higher strains result in fewer cycles. It implies that there is no safe strain value within which many cycles are possible. However, when subjected to constant stress tests, much better fatigue life is possible. Fatigue life in this case extends to almost 500,000 cycles with a stress level of 100 MPa. It illustrates that if strain is not controlled and SMA is allowed to equally deform. It is possible to have a relatively high fatigue life. This needs to be considered when designing with SMAs. These differences between constant stress and strain are summarized in Table 6.2.

Table 6.2
Comparison Between Constant Stress and Constant Strain Conditions

Condition	What is kept constant	What changes	Effect on SMA Performance
Constant stress	Force (stress)	Deformation (strain)	Longer lifespan
Constant strain	Deformation (strain)	Force (stress)	Faster fatigue

Note. Constant stress conditions result in improved durability, whereas constant strain conditions may lead to material fatigue faster.

6.1.5 Advantages & Limitations

There are different advantages and limitations in using SMAs for façade integration, this is summarized in Table 6.3. Advantages of SMAs are self-actuated and energy free kinetic motion. It works as both sensor and actuator. Resulting in no need for complex electronic sensors and wiring. Thereby ensuring noiseless and maintenance-free performance (Formentini & Lenci, 2018). Furthermore, SMAs have a very high recovery stress in relation to their size.

Contrary, SMAs show fatigue over time. SMAs are sensitive for degradation with increasing cycles. Especially when subjected to high forces or excessive thermal loading (Lelieveld, 2013). Additionally, the transition time between heating and cooling cycles (usually 15-25 °C) may cause control difficulties. Furthermore, the activation thresholds are sensitive to unwanted inputs, such as direct solar radiation on the surface. Which can cause the material to reach 50°C to 60°C despite the room temperature being pleasant (Formentini & Lenci, 2018). Moreover, SMAs have a relatively slow response compared to other actuators. This is because SMAs are thermally activated by the ambient temperature, this is often not rising very rapidly (Costa et al., 2025).

Table 6.3
Advantages and Limitations of SMAS

Advantages	Limitations
Self-actuated, energy-free motion	Fatigue over time with increased cycles
Acts as both sensor and actuator, eliminating complex wiring	Sensitivity to temperature transitions (15–25°C)
Noiseless, maintenance-free performance	Slow response compared to other actuators
High recovery stress-to-size ratio	Sensitive to environmental factors (e.g., solar radiation)

6.2 Thermo-bimetals

Thermo-bimetals are smart materials consisting out of two different metals with different thermal expansion coefficients. It relies on a reversible shape change effect. When the thermos-bimetal is exposed to a rise in temperature, the layer with the high expansion rate will increase in size. This process is faster than the layer with the low expansion rate. This difference in expansion will cause the entire material to bend. When the material cooled down, the effect will reverse (Bengisu & Ferrara, 2018).

6.2.1 Temperature Response Range

The temperature range and the responsiveness of these metals is based on the alloy pair, and the thickness of the laminate. For example, to reach a maximum deflection in the range of -18 to 49 degrees, TM2 (or ASTM 36-10) is used as thermo-bimetals. What consist of Invar (64% iron and 36% nickel) as the low-expansion material and a nickel-manganese alloy as the high-expansion material. This material is useful in relation to façades, as these thresholds matches environmental changes. Nevertheless, material weight and friction can cause large deviations in the temperature response thresholds. For example, prototypes designed to activate at 21,1°C have been known to activate only at 29,4°C due to the resistance of the assembly (Sung, 2010).

6.2.2 Actuation Force & Displacement

Thermo-bimetals are known to produce a small deflection with a relatively low force, compared to SMAs (Lelieveld, 2013). The amount of displacement depends on the dimensions, the thickness, and the point of clamping of the sheet. Furthermore, the ambient temperature is also relevant. Although they cannot produce the high recovery stresses necessary for the movement of heavy structural panels, their low-force curling is very useful for lightweight parts. The displacement is continuous and directly proportional to the temperature difference. Enabling a gradual opening and closing instead of a simple "on/off" switch (Sung, 2010).

6.2.3 Advantages & Limitations

The main benefit of thermo-bimetals is their autonomy and simplicity. Simultaneously playing the roles of sensor and actuator without requiring external power and electronic control. So, offering noiseless actuation. However, thermo-bimetals have some challenges. For example, thermo-bimetals have a low actuation force (Lelieveld, 2013). Additionally, thermo-bimetals are prone to oxidation and rusting. Unless they are specially treated with materials that are resistant to corrosion, such as chrome or copper (Sung, 2010). Furthermore, limitations such as metal fatigue, creep and material degradation because of thermal cycling needs to be considered for the long-term performance (Singh et al., 2024). These advantages and limitations are summarized in Table 6.4.

Table 6.4
Advantages and Limitations of Thermo-bimetals

Advantages	Limitations
Autonomy and simplicity	Low actuation force
Acts as both sensor and actuator without external power or electronic control	Prone to oxidation and rust without corrosion-resistant treatment
Noiseless actuation	Susceptible to metal fatigue, creep, and material degradation from thermal cycling

6.3 Hygro-morphic Materials

Hygro-morphic materials are a type of smart materials that exhibit physical transformation, such as swelling or shrinking. This in direct responds to changes in humidity. These materials are often inspired on principles from nature. Such as moisture-driven opening and closing of conifer cones. Which can be considered as a “no-tech strategy” for climate responsive designs (Holstov et al., 2015).

6.3.1 Hygroscopic Expansion

The principle of hygro-morphic movements is based on hygroscopicity. This is the ability to transfer moisture by absorbing and desorption. In the case of wood, this is achieved by the uptake of "bound water" into the cell walls. Resulting in the transverse expansion of the cellulosic microfibrils and the hemicellulose matrix. This expansion is very anisotropic because of the vertical orientation of wood cells. In the case of Scots pine, for example, the maximum expansion of 8-12% is in the tangential direction, while the expansion in the longitudinal direction is negligible at 0.1% (see Figure 6.2). The difference in the expansion forces in the active and passive layer of the material make it to bend or curl (Holstov et al., 2015).

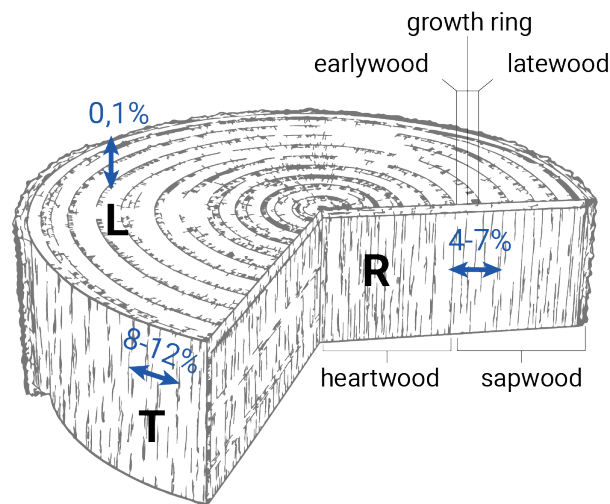


Figure 6.2

Cross-section of a tree trunk showing growth rings and wood grain directions, highlighting tangential, radial, and longitudinal orientations.

Note. Adapted from Holstov et al. (2015).

6.3.2 Relative Humidity Response Range

The behaviour of hygro-morphic materials is controlled by the Equilibrium Moisture Content (EMC). Which is the point at which the material stops to gain or lose moisture depending on the surrounding Relative Humidity (RH) and temperature. The ambient temperature has the less influence, but it influences the relative humidity (Holstov et al., 2015). Principles from nature have shown that they open to release seeds when RH falls to 40% and close completely when RH increases to 80-90% (Bengisu & Ferrara, 2018). The Netherlands is characterized by a temperate oceanic climate, with an annual average relative humidity of approximately 78 % (KNMI, 2023). So, if these hygro-morphic materials will be used in façade applications they would likely remain in a closed state for almost the whole year. Unless they are programmed to respond at a specific humidity threshold what is suitable for the oceanic climate in the Netherlands. Hydromorphic materials can be calibrated to express a different response, while exposed to the same conditions (Holstov et al., 2015). Without this calibration ventilation openings will most of the time staying closed, in a humid surrounding.

This pre-programmed behaviour can be adjusted during the fabrication of the hygro-morphic materials and can be done with different methods. First, by pre-conditioning the wood into a specific moisture content during production process. This it is setting the initial shape of these composites. Furthermore, the layers can be joined in a curved shape while the wood is saturated. This can cause that the panel is programmed to assume a straight (closed) shape specifically at a higher relative humidity and bend open as it dries. Furthermore, pre-stressing can be applied. By applying tension to the passive layer or compressing the active layer during assembly period this can manipulate the force and exact moment the materials start to curve (Holstov et al., 2017).

However, the outdoor air in the Netherlands is humid in the winter. The indoor temperature due to heating systems makes the indoor environment ideal for hygro-morphic activation. Because the RH decreases substantially when the air is heated. For example, outdoor air at -8°C and 100 % RH can decrease to about 15 % RH when heated to 20°C indoors, illustrating how heating reduces relative humidity even if absolute moisture stays constant (World Health Organization, 2009). Because the hygro-morphic wood reacts to the RH in the immediate environment. It will activate when exposed to this dry indoor air, even when it is cold and damp outside.

6.3.3 Actuation Magnitude

The degree of actuation, measured by the radius of curvature or displacement, depends on the stiffness and thickness ratios of the active and passive layers. The radius of curvature is inversely proportional to the total thickness of the composite. Hence, thinner panels are much more sensitive but also prone to wind damage. The rate of response is controlled by the slow process of molecular diffusion and water movement across cell walls. For example, a wood bilayer composite takes about 2 hours and 15 minutes to reach 80% of the total change in curvature in responds to a change in relative humidity (Holstov et al., 2015).

6.3.4 Advantages & Limitations

The use of hygro-morphic materials had advantages and disadvantages, this is summarized in Table 6.5. Benefits of using hygro-morphic materials are passive autonomy, energy free, and noiseless actuation. Furthermore, Natural hygro-morphs such as wood are cost-effective, carbon-negative, and light weight with good mechanical properties (Holstov et al., 2015). In addition, it functions as both sensor and actuator and controller. Since they do not have complex electronic systems, they are less likely to technically fail (Gosztonyi, 2022).

Nevertheless, there are also some relevant limitations. For example, hygro-morphic materials have a relatively slow response. This time lag can make them unsuitable for using in situations that require a fast response. Furthermore, one of the major challenges for hygro-morphic wood composites is durability. In addition, if the material is exposed to higher moisture levels for a longer period, it makes the materials vulnerable to degradation because of fungi. Moreover, photodegradation of lignin by UV radiation and surface erosion can cause a significant reduction in the life span of thin wood composites. Lastly, wood treatments that enhance fire or weather resistance often cause an irreversible loss of hygroscopicity (Holstov et al., 2015).

Table 6.5
Advantages and Limitations of Hygro-morphic Materials

Advantages	Limitations
Passive autonomy, energy-free, noiseless actuation	Slow response due to time lag in moisture absorption
Cost-effective, carbon-negative, and lightweight	Vulnerable to degradation by fungi if exposed to high moisture levels for prolonged periods
Functions as sensor, actuator, and controller	UV degradation of lignin and surface erosion reduces lifespan
No complex electronic systems, reducing risk of failure	Fire or weather resistance treatments can cause loss of hygroscopicity

6.4 Evaluation of Selected Smart Materials

This section compares the selected smart materials, SMAs, Thermo-bimetals, and hygro-morphic materials. This evaluation is based if they are suitable for further façade integration. These three promising materials offer passive actuation. But they differ in response mechanism, force, speed and durability. This comparison and evaluation is summarized in Table 6.6.

SMAs are selected as the most suitable smart material for an adaptive façade. This is because they provide high actuation forces compared to their weight. Furthermore, they generate controlled movement in response to temperature changes. However, metal fatigue and thermal cycling must be considered. This means that the SMA should mainly be used in linear movement and excessive strain should be avoided.

Thermo-bimetals and hygro-morphic materials show potential. Nevertheless, their lower actuation force, slow response, or stronger climate dependency makes them less suitable for adaptive façade integration.

Table 6.6
Evaluation of SMAs, Thermo-bimetals, and Hygro-morphic Materials

Property	SMAs	Thermo-bimetals	Hygro-morphic Materials
Actuation	Thermal phase change (martensite ↔ austenite)	Thermal expansion difference between layers	Moisture-driven expansion or contraction
Energy use	Energy-free, thermal activation	Energy-free, thermal activation	Energy-free, moisture-driven
Speed of response	Slow	Slow	Very slow
Force	High	Low	Low
Durability	Prone to fatigue and thermal cycling	Prone to oxidation, rust, and fatigue	Vulnerable to fungi and UV degradation

6.5 Conclusion

This chapter dived deeper into the smart materials that fulfilled the selection criteria. Shape Memory Alloys (SMAs) is selected as best suitable smart material for the implementation into an adaptive façade component. This because of their high recovery force and energy free actuation. Metal fatigue and thermal cycling are limitation of SMAs. Therefore, careful design must be considered.

In the next chapter an adaptive façade will be developed using Shape Memory Alloys (SMAs) as smart material. The goal of this adaptive façade component is to improve the indoor climate. This research demonstrates one feasible option of integration of SMA in a façade, to enhance the indoor climate. Nevertheless, many other alternatives exist and could be explored. Therefore, part II further develops one possible application by examining how Shape Memory Alloys can be integrated into a façade system and how this integration can be tested in relation to the indoor climate and the building performance.

PART II

Design Study

7. Design Structure

Part II of this research is structured as a design study. The aim of this design study is to translate the findings from the literature review into a passive adaptive façade concept. Furthermore, to explore the qualitative impact of this adaptive façade concept on indoor climate and building performance.

Based on the material selection in the previous chapter, Shape Memory Alloys are selected for further design development. This chapter translates this selection into a façade design direction by defining how SMA can be integrated into an adaptive natural ventilation system to support passive cooling and reduce indoor overheating.

The design process starts from the selected smart material and the chosen ventilation strategy. These two inputs form the basis for the design development in Chapter 8, where the adaptive ventilation component is further defined through its operating logic, component dimensions, actuation mechanism, and geometry. Together, these steps lead to the development of a passive adaptive ventilation component, which is further elaborated in Chapter 8 and later tested in the case study. Figure 7.1 gives an overview of the design structure used in Part II.

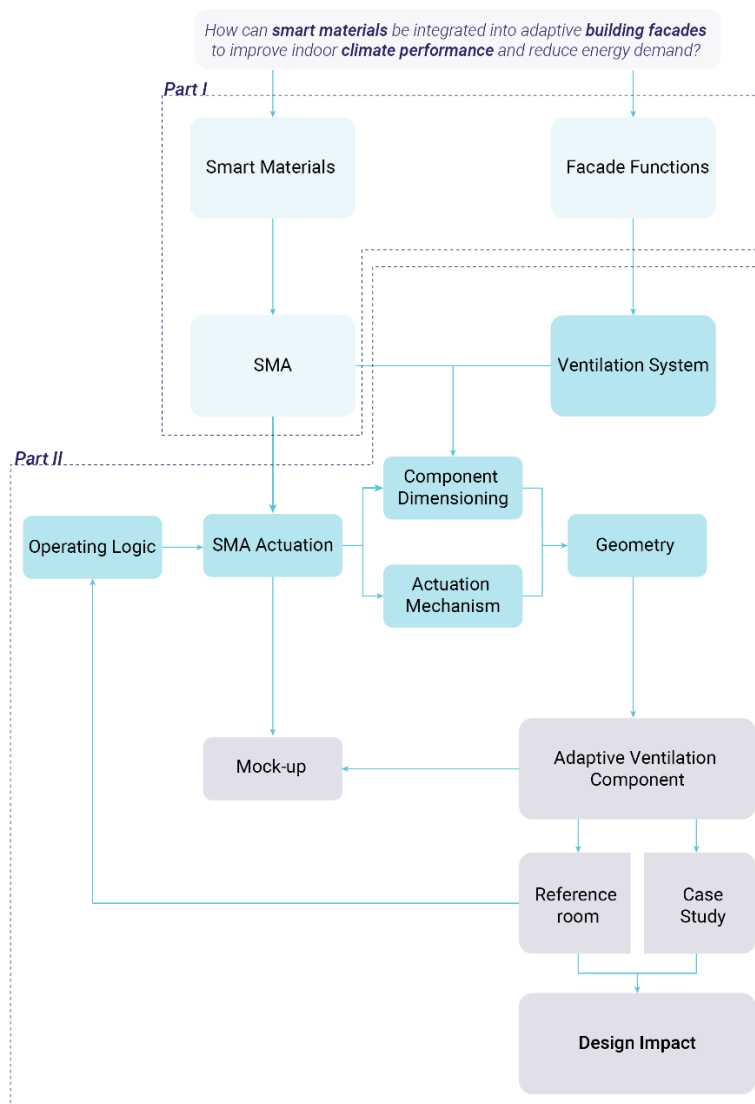


Figure 7.1
Design structure of Part II.

7.1 Smart material as Design Input

Based on the literature review, Shape Memory Alloys are used as the smart material for further design development. SMA is relevant because it can respond to temperature changes. This by changing in shape, for example by contracting. Which allows the material to generate movement without motors or external control systems.

However, the material properties also create important design conditions. As mentioned in the literature, SMA have a longer lifespan of its used in linear movement instead of bending, to reduce metal fatigue. Therefore, the façade system should be designed in a way that translates this linear movement into a controlled movement.

7.2 Passive System Strategy

After defining SMA as the material input, the next step is to determine in which type of façade system this material can be meaningfully integrated to improve the indoor climate. In this research, the system should remain passive. Meaning that the response is generated by the material behaviour itself rather than by motors, sensors or active control systems, as explained in the literature.

There are different potentially option to integrated smart materials into façade systems. The aim of this research is to explore a possible design direction through which the smart material behaviour can contribute to indoor climate performance.

Furthermore, the façade controls the exchange between indoor and outdoor conditions. Therefore, the smart materials, in this case the SMA, should be implemented in a way it has a clear relation to contribute to indoor climate performance. The following section evaluates which façade system is the most suitable as a design case for the integration of SMA.

7.2.1 Façade system selection

The literature review showed that thermally responsive materials, including Shape Memory Alloys, can influence several façade-related indoor climate aspects. This indicates that SMA could potentially be integrated into different types of adaptive façade systems. Table 7.1 provides a short comparison of possible façade applications for SMA integration.

For this research, a passive adaptive ventilation system is selected as the façade system for further development. This choice is made because ventilation has a direct relation to air exchange, air speed and indoor temperature. In addition, the limited linear contraction of SMA can be translated into a clear opening and closing movement, which makes ventilation suitable for SMA-based actuation.

The selected ventilation system is therefore not presented as the only possible application of SMA in façades, but as a design case to explore how SMA actuation can contribute to indoor climate improvement.

Table 7.1
Possible façade applications for SMA integration

Façade application	Indoor climate relation	Suitability for this research
Adaptive sun shading	Reduces solar gains and influences daylight, glare and illuminance	Relevant, but mainly related to solar and visual comfort
Adaptive ventilation	Influences air exchange, air speed and indoor temperature	Selected, because it directly links SMA movement to measurable indoor climate effects

Façade application	Indoor climate relation	Suitability for this research
Adaptive insulation	Influences heat transfer through the façade	Less suitable, because it requires a change in thermal resistance rather than a simple opening movement

7.2.2 Climate Relevance of Adaptive Ventilation

The design for an adaptive façades is specified for Temperate Oceanic Climate (CFB) in the Netherlands. This type of climate features mild winter seasons and cool to warm summers, but it is currently undergoing a dramatic change due to global warming (Gosztonyi, 2022). Although summers in the Netherlands are known for their mild temperatures with an average of 17,3 degrees (KNMI, n.d.). Recent summers have shown a dramatic increase in temperature peaks, often reaching 35°C (KNMI, 2022).

Current building regulations in the Netherlands, known as BENG, require high U-values. Based on the level of insulation and airtightness to meet winter energy targets often leads to an "internal heat lock" in the summer. This means that the built-up heat from internal gains and solar radiation cannot be dissipated through the highly insulated building envelope. Leading to the necessity for dynamic adaptation (Gosztonyi, 2022). Ventilation, especially night ventilation, can offer a suitable solution for this internal heat lock. Therefore, in this research an adaptive natural ventilation system, what responds to temperature changes, will be designed based on the actuation on shape memory alloys.

7.2.3 Natural Ventilation

Natural ventilation is the process of supplying and removing air from a building through openings in the building envelope, without the use of mechanical fans. Airflow relies on two physical mechanism, pressure and buoyancy differentials. Pressure differentials occurs when the building is interacting with wind. The wind creates a high-pressure area on the windward face and a low-pressure area on the leeward face. When there are openings on the high-pressure zone, the wind will enter the building on that side. The air will leave the building on the openings on the low-pressure areas. Buoyancy driven ventilation is due to the difference in temperature. Warm air is less dense than cooler air. The air naturally moves upward and escapes through high-level building apertures.

7.2.4 Ventilation Principles

In analysing natural ventilation for a responsive façade, three main approaches were identified. Namely single-sided, cross, and stack effect ventilation (see Figure 7.2).

Single-sided ventilation is a passive ventilation strategy where the exchange air between indoor and outdoor take place through openings on only one side of the façade. This ventilation strategy is mostly inefficient (Khdair et al., 2026). According to Bilow (2012), when single-sided ventilation is used, there are restricted room depths of approximately 2.5 times the room height.

Secondly, cross ventilation, also known as two-sided ventilation, is a passive cooling technique that uses the benefits of a pressure gradient. Caused by openings on multiple sides, usually opposite ones. This technique ensures a constant air change by providing a clear path from an opening to an outlet. Its effectiveness is widely acknowledged in terms of airflow and air distribution. In regions with warm climates, night-time cross-ventilation has the effect of reducing indoor temperatures up to 6.5°C, compared to no ventilation (Khdair et al., 2026).

Cross ventilation is more efficient than single-sided ventilation, here the room depth can increase by up to 5 times the room height because of the resulting draft. Furthermore, analytical models and simulations have confirmed that single-sided systems offer functional but lower Air Change Rates (ACH) values compared to cross-ventilation systems. To illustrate this, it has been noted that the Air Change Rates value can be increased by more than 200% if the single-sided system is converted to a cross-ventilation system (Khdair et al., 2026).

Lastly, stack-effect ventilation which mechanism is based on a physical law that warm air is less dense than cool air. The air inside a building or a façade cavity, when warmed, will naturally rise and exit out of openings on the upper levels of a building. This process will, in turn, draw in cool air from the outside and into the building through openings on the lower levels. Thereby developing a continuous and autonomous airflow (Khdair et al., 2026).

Out of the three primary strategies of natural ventilation, the stack effect is deemed the most appropriate for integration, based on the airflow. Although cross-ventilation also sounds promising, it is highly dependent on the orientation of the building and the internal passage (Khdair et al., 2026). The stack effect, on the other hand, is wind and orientation independent (Formentini & Lenci, 2018). Therefore, stack-effect ventilation supports the criteria of passive operation and façade integration more effectively than the other ventilation strategies.

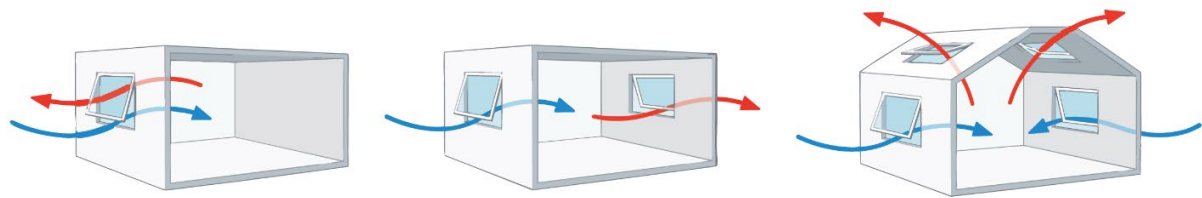


Figure 7.2

Natural ventilation strategies.

Note. From left to right: single-sided ventilation, two-sided ventilation, and stack effect ventilation.

7.3 Design Criteria

The design criteria for a passive, adaptive ventilation system can be divided into hard criteria and soft criteria. Hard criteria are strict requirements needed so that natural ventilation can occur. Soft criteria are not strictly required for basic operation. The soft criteria improve the quality, reliability and feasibility of the design. All the design criteria, their type, and requirements are summarized in Table 7.2. When design choices are made in the following sections, the relevant criteria are used to evaluate the options and justify the choices.

Table 7.2

Design criteria for the SMA-driven ventilation component.

Design criterion	Type	Requirement
Passive operation	Hard	The component must operate without motors or external energy input.
Temperature-responsive behaviour	Hard	The component must respond to temperature changes through SMA activation.
Reversible movement	Hard	The component must be able to open and close repeatedly.

Design criterion	Type	Requirement
Limited SMA deformation	Hard	The SMA wire must mainly work in linear contraction and avoid bending or excessive strain.
Façade integration	Hard	The component must be suitable for integration within a façade build-up.
Ventilation capacity	Hard	The component must provide sufficient opening area for passive ventilation.
Limited number of components	Soft	The mechanism should contain as few moving parts as possible.
Stable movement	Soft	The moving parts should move in a controlled and predictable way.
Efficient force transmission	Soft	SMA contraction should be translated into movement with limited losses.
Airtight closed state	Soft	The closed position should reduce unwanted infiltration as much as possible.
Durability	Soft	The design should minimise friction, wear and mechanical complexity.

7.4 Conclusion

This chapter outlines the design structure of Part II. Shape Memory Alloys were selected as the material input for further design development. While adaptive natural ventilation was selected as the façade strategy because of its direct relation to air exchange, indoor temperature and passive cooling.

The relevance of adaptive ventilation was further supported by the Dutch climate context, where warmer summers and highly insulated building envelopes can increase the risk of internal heat build-up. This makes a temperature-responsive ventilation system a relevant passive strategy to support heat dissipation and improve indoor climate conditions.

Based on the comparison of ventilation principles, stack-effect ventilation was selected as the most suitable strategy for the passive adaptive façade component. This strategy supports passive airflow and is less dependent on wind direction or façade orientation than cross ventilation.

The formulated design criteria provide the basis for the next design phase. Chapter 8 uses these criteria to develop the adaptive ventilation component in terms of operating logic, geometry, component dimensions and SMA-based actuation mechanism.

8. Adaptive Ventilation Component Design

This chapter develops an adaptive ventilation component based on the design criteria formulated in Chapter 7. The aim is to translate the selected smart material, Shape Memory Alloys, into a passive adaptive ventilation component.

First, the operational logic of the system is defined as well as the dimensions of the ventilation component. Furthermore, the SMA actuation principle will be tested and discussed. Different actuation mechanism will be considered. After this, the geometry of the component is defined by specifying the lamellas, crank arms, pins, yokes, route of the SMA wires and return spring. Lastly, the complete component is evaluated according to the design criteria. This to identify which requirements are achieved and which aspects still require further testing.

8.1 Required Operating Logic

To improve the indoor climate and building performance the adaptive ventilation component must open and close according to predetermined threshold that vary according to summer and winter season.

Summer (daytime)

During the summer months, the main aim is to ventilate the building to ensure that the building does not overheat. At the same time, the building should be kept comfortable for their occupants. Hence, the ventilation system should be able to open and close depending on inside and outside temperature conditions.

The system should open when the temperature inside the building is higher than 24°C, because this exceeds the comfort temperature (W/E adviseurs, 2018). At the same time, it should open when the outside temperature is below this 24°C (see Figure 8.1). This allows the system to take advantage of the lower temperatures to provide cooling inside the building. However, the system should always remain closed if the outdoor temperature is greater than the indoor temperature to prevent overheating. These values are used as initial reference points. The simulations presented in Section 10.1 determine the most effective setpoints for optimizing the indoor climate.

Summer (nighttime)

Night ventilation is a passive cooling technique that makes use of the natural storage capacity of a building's thermal mass to regulate the internal temperature (Bilow, 2012). It uses the cooler air at night to remove the build-up heat during the day. The success of this strategy also depends on a large diurnal temperature swing (Halawa et al., 2018). In temperate oceanic climate zones (Cfb), such as The Netherlands, night ventilation is a common and recommended strategy to counter summer overheating (Gosztanyi, 2022). The practical implementation includes issues such as burglary protection for open windows at night (Bilow, 2012).

To be effective, a strategic operating logic is a requirement. This strategy is often used in office buildings, which are usually unoccupied at night and, therefore, can use high ventilation rates without causing discomfort to the occupants. The use of simple schedules, however, is often risky, as it might draw air that is warmer outside the building, which might then increase the cooling load. In more complex systems, temperature-controlled ventilation is used, which is effective if the temperature outside, T_{out} , is lower than the temperature inside, T_{in} , by at least 1°C (see Table 8.1) (Alvarez Gutiérrez et al., 2025). To prevent overcooling, ventilation should be stopped once the indoor temperature drops below the threshold of 24°C.

Winter Conditions

In the winter, the main objective of the system will change from cooling to maintaining the energy efficiency of the buildings by preventing heat loss through ventilation or infiltration. If the ventilation system is opened during the winter, there will be significant loss of energy. Especially for buildings that are well insulated. Therefore, there must be a mechanism to manually override the system to close it completely (see table 8.1). This to reduce heat losses during the winter. Figure 8.1 illustrates a schematic overview of when the system is operating.

Table 8.1
Operational Logic for Passive Ventilation System

Season/Condition	Condition	Action
Summer (daytime)	$T_{in} > 24^{\circ}\text{C}$ and $T_{out} < 24^{\circ}\text{C}$	Open
Summer (night ventilation)	$T_{out} < T_{in} - 1^{\circ}\text{C}$	Open
Winter	Overruled	Overruled

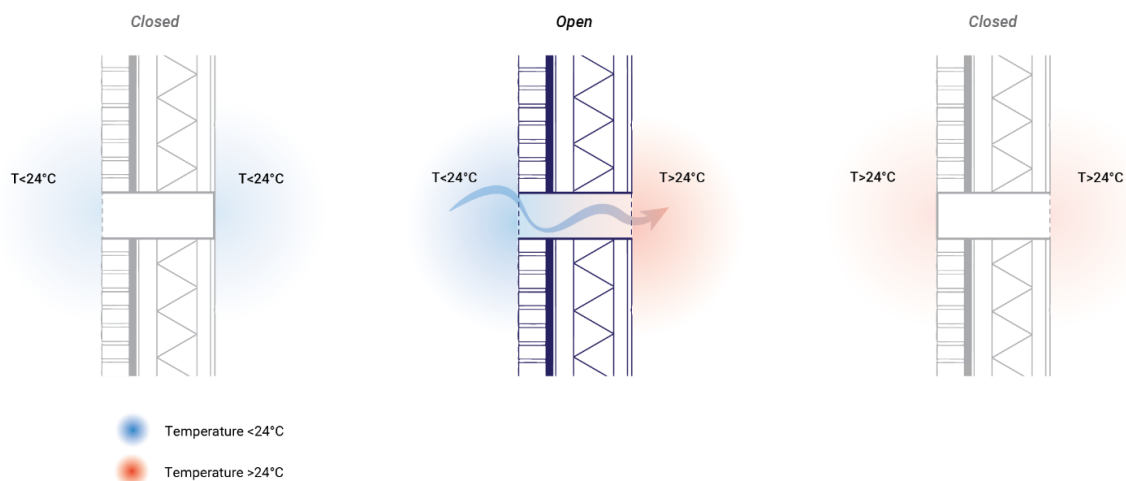


Figure 8.1
Operating principles of passive ventilation system.

8.2 Component Dimensioning

This section defines the basic dimensions of the adaptive ventilation component. As shown in Appendix B, the required ventilation opening area depends on the room size and the selected ventilation strategy. Furthermore, it shows that the required ventilation opening area can be achieved through different sizes and configurations. Therefore, the adaptive ventilation system is not designed as one fixed opening for a specific room. Instead, it is designed as a modular façade component, when a higher airflow rate is needed, multiple units can be added across the façade. This to reach the desired ventilation capacity.

For this research, one adaptive ventilation component is designed with fixed dimensions of 500 mm by 150 mm, as illustrated in Figure 8.2. The width of 500 mm is mainly based on the required SMA wire length. Since SMA contraction is limited to a small percentage of its original length, a longer wire can provide a larger linear displacement. A component width of 500 mm therefore allows the SMA wire to be used over a sufficient length. While at the same time keeping the component suitable for façade integration and 1:1 prototyping. Furthermore, the height of 150mm was selected to keep the ventilation component compact. Nevertheless, it offers enough space for rotating ventilation elements.

Moreover, to reduce the noise transmission through the open system, the ventilation components must include an acoustic ventilation box. However, the presence of such an acoustic box will limit the

effective free opening area of the component. This compared to the gross geometric opening. This results in a reduction of the effective airflow area of the component. This must consider in the building performance simulations in Chapter 9.

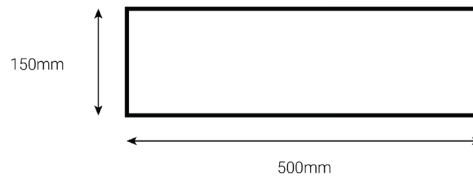


Figure 8.2
Dimensions for ventilation component in front view.

8.3 SMA Actuation

This section further develops the SMA actuation principle for the adaptive ventilation system. Design criteria, formulated in Chapter 7, who are related to SMA actuation are temperature-responsive behaviour, reversible movement, limited SMA deformation and durability. Since the SMA wire is the driving force in the ventilation system, its mechanical and thermal behaviour directly influences the reliability of the opening and closing movement.

To meet these criteria, the SMA wire should mainly work through linear movement rather than in a bending deformation. This reduces the risk of metal fatigue and supports the durability over time. In addition, the wire needs to function in a semi-free moving configuration, instead of being completely fixed. This allows the wire to contract during heating against a contra-force. This to be stretched again during cooling by this contra force. Based on metal fatigue discussed in Section 6.2.3, low stress values and limited strain are preferred for long-term performance. Therefore, the design aims to keep the SMA strain below 4%.

8.3.1 Experimental Testing of the SMA wire

For developing the prototype testing the ordered SMA wire, with a diameter of 0,88 mm is necessary. First the wire was preheated to reach its austenite shape, also known as its recovered shape. After cooling down the material, it was placed in the test setup where it has been pre-strained up to 4% elongation (see Figure 8.3).

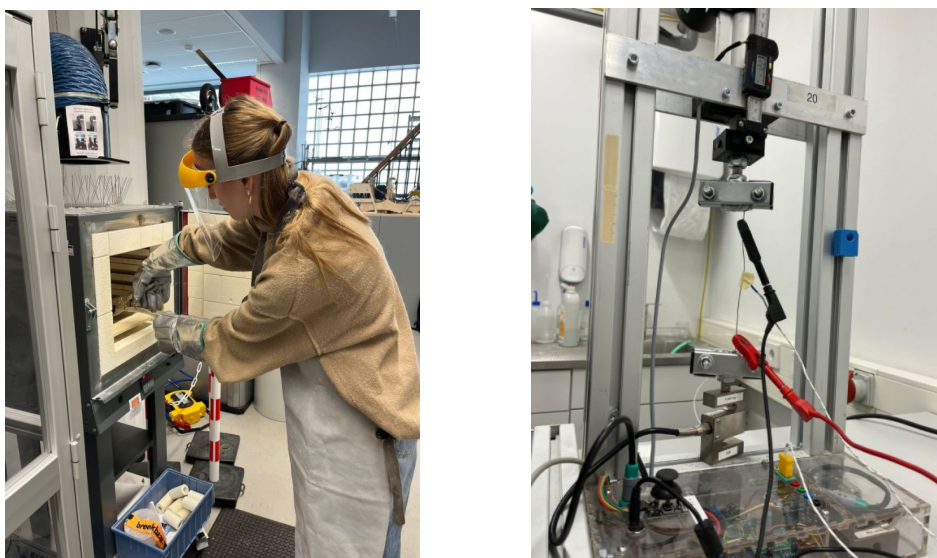


Figure 8.3
Progress images of experimental testing of SMA wire.

The setup measured how much stress is needed to reach a 4% elongation. The results, what are shown in Figure 8.4, illustrates a non-linear behaviour of the stress-strain response of the SMA wire. The stress rises more subtle at the more low strain levels. This in comparison with the more strongly rise in This indicates that the wire becomes stiffer as the applied strain increases stress levels at higher strain, also known as the austenite phase. The maximum stress is reached at around 125 MPa. This to reach the maximum strain level, what was pre-strained to a 4% elongation.

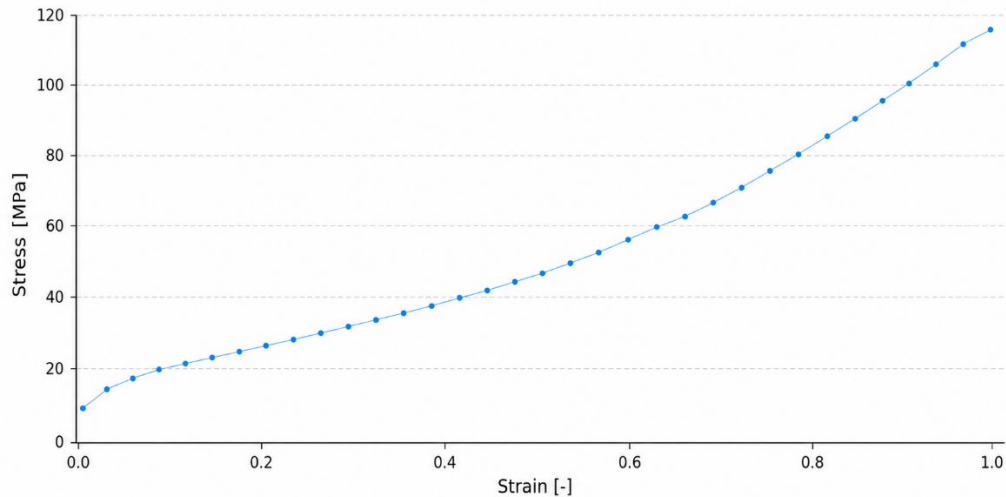


Figure 8.4
Stress–strain response of the SMA wire during tensile loading up to 4% elongation.

After the stress-strain response, the force-temperature of the SMA was tested, shown in Figure 8.5. The figure presents a clear hysteresis loop, what is a characteristic of SMAs. The top curve illustrates the heating process. Where the force increases with the temperature, while the wire contracts. This starts from approximately 50 degrees and reaches its limit around 200 N between 60 and 75 degrees. In contrast, the bottom curve shows the cooling process, wherein the decrease in force and a decrease in temperature occurs. A significant difference occurs at the same temperature between the heating and cooling processes. For instance, at 60 degrees the force gained by heating is at its maximum value. While during cooling, the force is quite low.

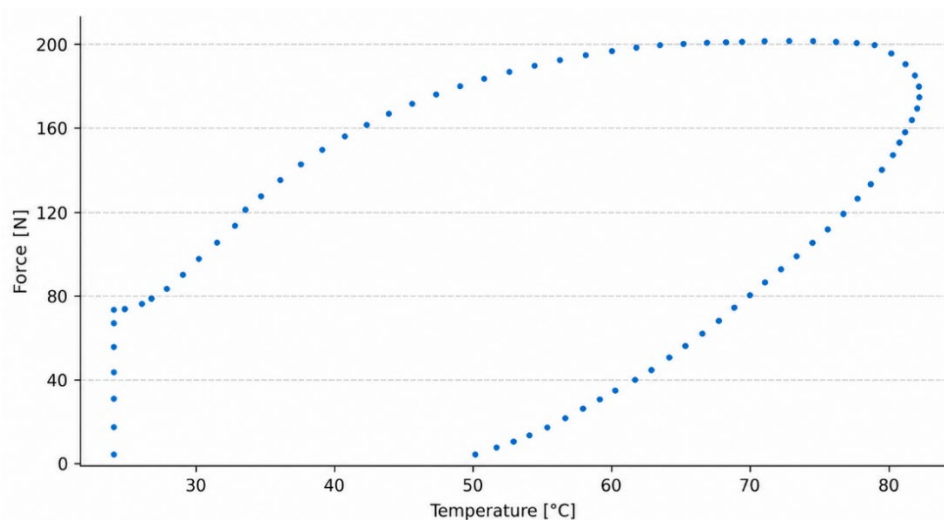


Figure 8.5
Force-temperature response of SMA wire.

The hysteresis loop has an important role in terms of designing the actuation mechanism. Since it determines the operating temperature and actuation force that can be achieved. The test shows that the SMA wire can generate a relatively high force during heating. However, the contra force must be stronger than the SMA when it is cooling down, to deform the wire again. The key findings of these experiments are summarized in Table 8.2.

Table 8.2
Key Results of Testing the SMA Wire

Parameter	Value	Unit	Notes
Wire diameter	0.88	mm	Measured
Cross-sectional area	0.61	mm ²	Calculated
Test type	Tensile (relaxation)	–	Based on experimental setup
Initial temperature	23.7	°C	Start of test
Applied pre-strain	4,0	%	Initial elongation
Maximum extension	6.07	mm	Measured displacement
Maximum force	203.6	N	Peak measured force
Maximum stress	334.8	MPa	Calculated from cross-section
Activation temperature	~50	°C	Onset of force increase
Peak temperature range	~60–76	°C	Maximum force region
Residual force (room temperature)	~70	N	After cooling
Hysteresis behaviour	–	–	Difference between heating and cooling
Actuation force range	~0–200	N	Based on temperature-dependent behaviour

8.3.2 Phase Transition Behaviour

Based on the force-temperature graph the phase transition (M_f , M_s , A_s , A_f) temperatures of the tested SMA wire can be estimated, which is summarized in Table 8.3. These phase transitions describe when the SMA changes between the martensite and austenite phases. The estimated temperatures and corresponding forces are summarised in Table 8.3.

Table 8.3
Phase Transition Temperatures and Corresponding Forces of SMA Wire

Phase	Temperature (°C)	Force (N)	Interpretation
M_f	55°C	~0 N	Force is largely reduced during cooling

Phase	Temperature (°C)	Force (N)	Interpretation
M_s	80°C	~160 N	Force starts to decrease during cooling
A_s	30°C	~85 N	Start of force increase during heating
A_f	70°C	~200 N	Force reaches maximum level during heating

Note. These values are approximate estimates based on the force-temperature graph.

Based on the force-temperature response, the phase transition temperatures of the tested SMA wire can be estimated. During heating, the force starts to increase at approximately 30°C, which is related to the austenite start temperature, A_s . the force reaches its limit at around 70°C, with 200 N, corresponding to the austenite finish temperature, A_f . During cooling the force start to decrease around 80°C, which indicates the martensite start temperature, M_s . Around the 55°C, the force is largely reduced again. This indicates the martensite finish temperature M_f . In this stage the SMA wire is flexible again and can be deformed by the contra-force. From here the cycle can start over again.

These results are useful for understanding the hysteresis behaviour of the SMA wire and for dimensioning the contra-force in de mock-up. The contra-force must be lower than the SMA force during heating, so that the wire can contract. On the other hand, the contra-force must by higher than the remaining SMA force during cooling. This that the wire can stretched again. To return to the deformed original position.

8.3.3 Translation to Practical Operating Temperatures

The tested SMA wire was used to understand the mechanical and thermal behaviour for the mock-up. However, the adaptive ventilation component should respond to indoor and outdoor conditions. Therefore, the final system is based on a SMA wire with an austenite finish temperature of 24°C, according to Section 8.1. So, when the SMA wire is reaching this temperature threshold, it is fully contracted. This is summarized in Table 8.4 and Figure 8.6.

Table 8.4
Phase Temperatures in Practice SMA Wire

Phase	Temperature (°C)
M_f	18°C
M_s	20°C
A_s	22°C
A_f	24°C

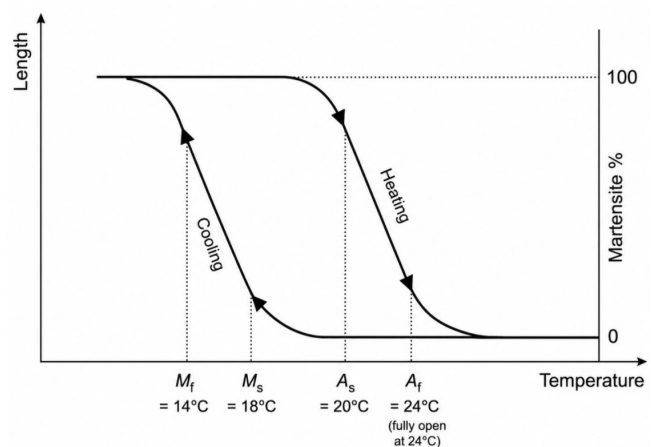


Figure 8.6
Phase temperatures of SMA wire in practice

For the practical application, an SMA wire with a target austenite finish temperature of approximately 24°C is assumed. This means that the wire starts to contract around the austenite start temperature of 22°C and reaches its fully contracted state at 24°C. During cooling, the wire does not immediately return to its original length due to hysteresis. The reverse transformation starts around the martensite start temperature of 20°C and is completed at the martensite finish temperature of 18°C. At this point, the wire is fully deformable again and can be stretched by the contra-force. Note that these values are assumed phase temperatures. They are used to define the operating range of the adaptive ventilation component in practical setting.

Furthermore, due to the hysteresis of the SMA wire, the ventilation system may stay open even when indoor temperatures drop below 24 °C. In practice, this means the system could remain open for long periods, even the whole summer, causing ventilation to occur when it might not be needed. This is a practical limitation of the system and could be studied further in the future how this may influence the indoor climate.

8.4 Actuation Mechanism

This section discusses how the linear movement of the SMA wire can be converted to the rotational movement of the ventilation elements. Since the SMA wire should mainly contract in linear direction. Therefore, the actuation mechanism must transfer this movement without any extra deformation or bending of the SMA wire. The most relevant design criteria for selecting the mechanism are limited SMA deformation, limited number of components, stable movement, efficient force transmission and durability.

8.4.1 Exploration of Mechanisms

Several actuation mechanisms were considered. This to translate the linear contraction of the SMA wire into rotation of the ventilation elements. The following mechanisms were considered: direct actuation, pulley system, and scotch yoke mechanism, as shown in Figure 8.7. Early design sketches were used to explore façade integration, opening principles and SMA actuation layouts. These sketches informed the development of the selected lamella-based Scotch yoke mechanism and are included in Appendix C.

Direct Actuation

With direct actuation is the SMA wire directly attached to the lamella, with an arm offset the as. In this way the SMA is transforming its linear deformation into a rotation. This actuator design is simple and compact and eliminates additional complex parts. Nevertheless, it offers insufficient control over the motion and the force transmissions. Moreover, direct actuation is not optimal in transferring forces. Within this system, it is not making optimise use of force versus displacement of the SMA wire. Consequently, despite its simplicity, direct actuation seems less suitable for this application.

Pulley System

The pulley-based actuator system uses a combination of cables and wheels for redirecting the force of the SMA. This method provides increased flexibility in routing and directing the actuation force. Even though this system offers increased flexibility, it also has some limitations. Such as, friction losses and slack in the cable. This can negatively affect the performance of the pulley system. In addition, incorporating pulleys into a façade system might prove difficult due to their size.

Scotch Yoke Mechanism

Whitin the scotch yoke mechanism converts linear movement in rotation, this is based on a sliding yoke and a rotating pin, what is connected to the lamellas. The linear contraction of the SMA is connected to the sliding yoke, what results in rotation of the lamellas. This system allows a precise movement control what makes it suitable for applications.

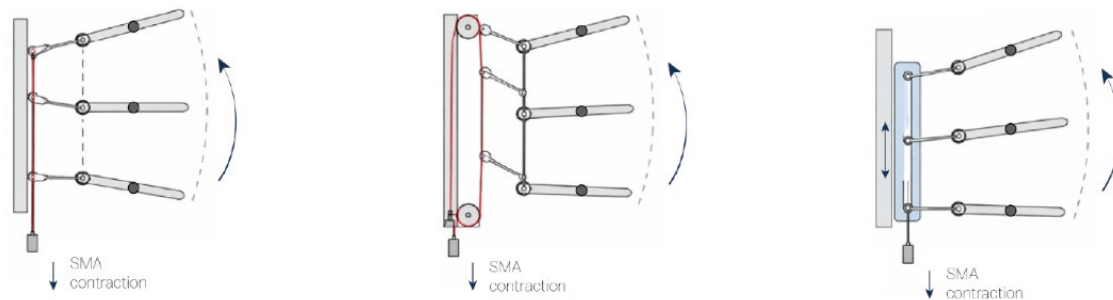


Figure 8.7

Actuation mechanisms for lamella rotation.

Note. From left to right: direct actuation, pulley system, Scotch yoke mechanism.

8.4.2 Evaluation of Mechanisms

The three mechanisms, direct actuation, pulley system, and Scotch yoke mechanism are evaluated according to the relevant design criteria, this is summarized in Table 8.5.

The direct actuation method scores well on the limited number of components, because it is mechanically simple and compact. However, the stable movement, the efficient force transmission, and the limited SMA deformation criteria get relatively poor results. This because the SMA wire is connected to the rotating elements directly. Furthermore, the pulley system allows more freedom in routing the SMA wire, but therefore there are more components needed. More components can result in friction losses. This makes it less favourable in terms of durability and mechanical reliability.

Table 8.5

Evaluation of actuation mechanisms based on the relevant design criteria.

Design criterion	Direct actuation	Pulley system	Scotch yoke mechanism
Limited number of components	++	-	+
Stable movement	-	o	++
Efficient force transmission	-	o	++
Limited SMA deformation	-	+	++
Reversible movement	o	+	+
Durability	o	-	+
Compact façade integration	++	-	+

Note. ++ = performs well, + = sufficient, o = neutral/uncertain, - = weak.

The Scotch yoke mechanism scores overall the best on the set design criteria. The Scotch yoke mechanism allows the SMA wire to contract in a mostly linear movement. This supports the criteria of limited SMA deformation. At the same time, the sliding yoke creates a controlled movement and allows multiple moving elements to be actuated simultaneously. This improves stability and force transmissions compared to direct actuation. Therefore, the Scotch yoke mechanism is selected as the final actuation principle. How actuation principle works in detail is explained in the next section.

8.5 Geometry and Component Design

This part explains how the selected Scotch yoke mechanism is implemented into the geometry of the design of the adaptive ventilation component. This section focuses on all the parts that make the movement, of opening and closing the ventilation system, possible. These parts include, the lamellas, the yoke, the pins, the SMA wire and the contra force. Together, these parts form the mechanical system of the ventilation component.

8.5.1 System Overview

The adaptive ventilation component uses the selected Scotch yoke mechanism to translate the linear contraction of the SMA wire into the rotation of the ventilation elements. In this system, each lamella has its own axis of rotation. To each axis a crank with on the end a pin is connected. All these pins will be attached to the yoke. This makes it possible to rotate all lamellas simultaneously, what makes it more stable and uniformly.

The whole mechanism works as follows: as soon as the SMA reaches its temperature thresholds in the austenite phase, the SMA wire starts to contract. The force of the SMA will be transferred from horizontal to vertical through a pulley. This pulls on the yoke. The yoke has as many holes as lamellas, where a pin is placed in. As the yoke moves, the pins rotate the cranks and therefore rotate the lamellas. In this way, the linear motion of the SMA will be translated into rotation of each lamella uniformly.

When the temperature drops and is below the threshold of the SMA wire, the force in the SMA wire also reduces. A spring, connected to the yoke, will slide the yoke back to the original position. In this way the SMA wire will be deformed again, in the martensite phase. The wire will increase in length, so the original position is recovered. So, the cycle can start over again.

Thus, the whole operation mechanism works as an internal group of interacting cause-and-effect forces. Wherein the SMA acts as the primary source of the force. Driving a chain of reaction of movements in a purely passive way, so no external force is required for activation. The mechanism minimizes unnecessary mechanical or structural components. See Figure 8.8 for the moving components of the system were the SMA responds to the outdoor conditions.

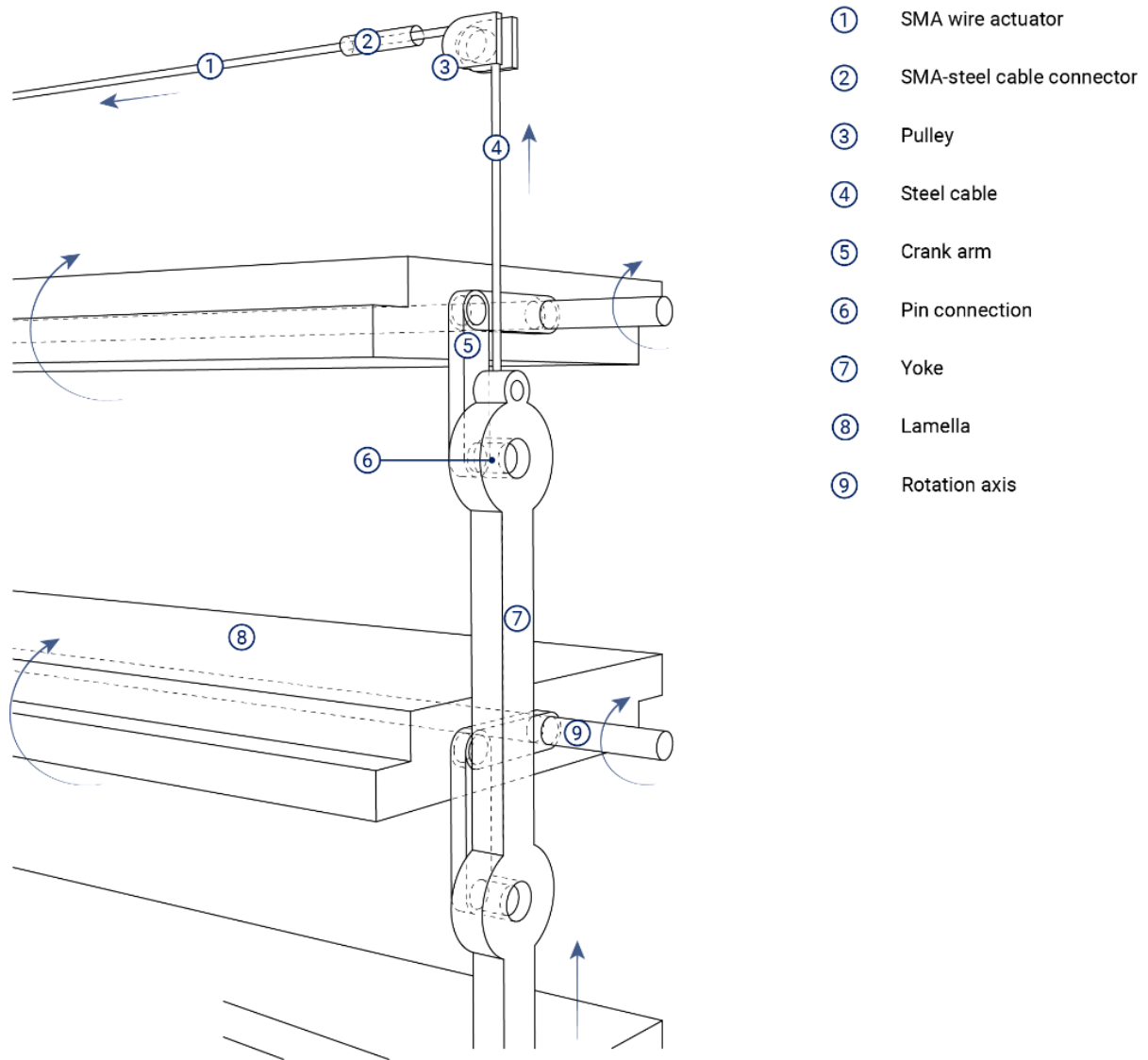


Figure 8.8
Mechanism overview of the SMA driven ventilation component, responding to outside conditions.

8.5.2 Lamella Design

The ventilation component includes three rotating lamellas. With a length of 493 mm, a height of 50 mm, and a thickness of 10 mm. These dimensions are based on the component size of 500 mm by 150 mm.

To ensure better airtightness in closed conditions, the design of the lamellas have an interlocking system. This ensures that the lamellas fit well into the other securely. This is done by adding grooves at the end of each lamella. The grooves have a measurement of 5 mm by 5 mm on each side. In the middle of each of the lamellas is the axis places in the centre. This provides a balanced mechanism during closing and opening. See Figure 8.9 for a cross section of one lamella and its dimensions.

The lamellas are designed as hollow aluminium profiles to reduce weight and still being stiff. This is a suitable material what is lightweight and has a high durability and is well resisted to environmental conditions. The open ends of the profiles should be closed to prevent water, dirt, or insects from entering the lamella.

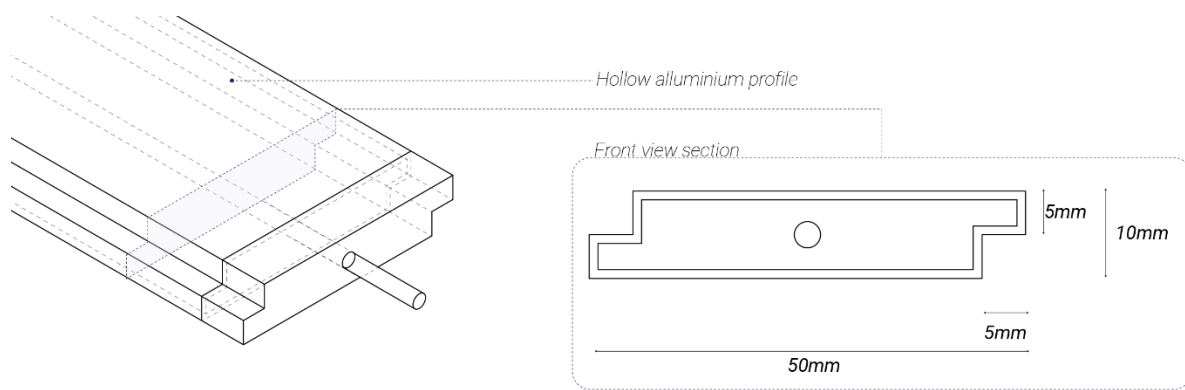


Figure 8.9
Key dimensions of lamella in cross-section.

8.5.3 Mechanism Geometry

The mechanism geometry consists out of crank arms with connected pins at the end, what is placed in the sliding yoke. First the crank with pin will be explained then the sliding yoke will be discussed.

Crank with Pin

The crank with pin is used as a lever. The crank and pin are connected to the axis of each lamella. This configuration with dimensions is illustrated in Figure 8.10. The bigger the distance from the axis of rotation to the pin, the smaller the forces needed. However, how greater the crank arm, the more deformation of the SMA wire needed. This principle is also illustrated in Figure 8.11. Therefore, the system must be designed so that there is a good balance between force and deformation of the SMA wire needed.

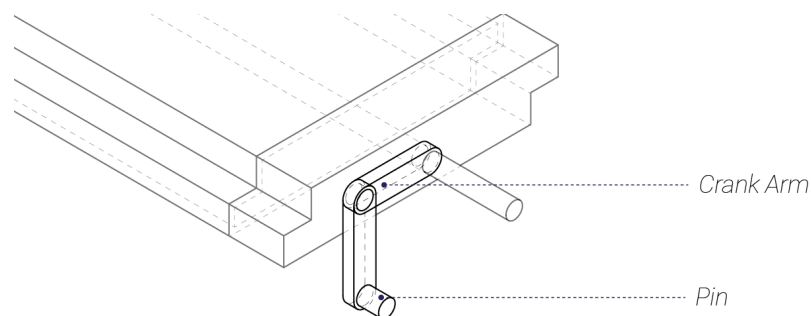


Figure 8.10
Crank arm and pin attached to the lamella rotation axis.

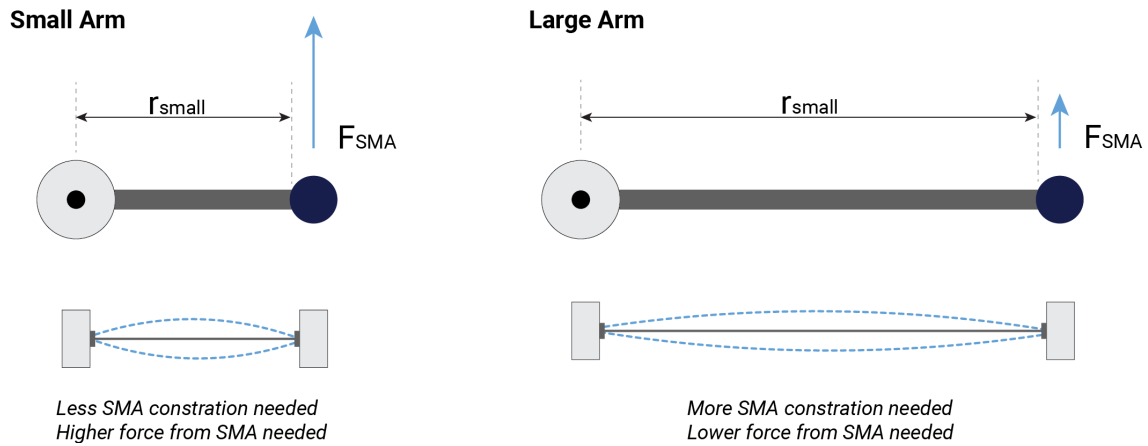


Figure 8.11
Influence of lever arm length on force and SMA contraction.

Moreover, the lamellas need to make a rotation of 90 degrees, to go from a closed position to an open position and vice versa. The required contraction of the SMA wire depends on the length of the crank arm and the angle of rotation, this can be calculated with Equation 8.1.

Equation 8.1

$$\text{Displacement} = r \times \theta$$

Where the displacement is the contraction needed from the SMA wire in mm, r is the length of the crank arm in mm, and θ the angle in radians.

In this research a crank arm of 10 mm is selected. Furthermore, to ensure a better life span of the SMA wire it is better to keep the strain as low as possible. 3 till 4 percent strain is in an acceptable range. For example, with a 3% strain on a 480 mm SMA wire, the maximum displacement is limited to 14,4 mm. This is not sufficient for the 90-degrees rotation with a crank arm of 10mm. On the other hand, with a greater strain of 4%, the displacement will increase to 19,2 mm. This is sufficient to rotate the lamellas from open to a closed situation. These results are summarized in Table 8.6.

Table 8.6
Displacement Comparison for 90° Rotation Based on SMA Strain.

SMA Strain	SMA Length	Max Displacement	Required Displacement	Sufficient for 90° Rotation?
3%	480 mm	14.4 mm	15.7 mm	Not Sufficient
4%	480 mm	19.2 mm	15.7 mm	Sufficient

To conclude, a crank arm length of 10 mm is selected. This results in a required SMA displacement of 15.7 mm to achieve a 90-degree rotation of the lamellas. With an SMA wire length of 480 mm, 3% strain is slightly insufficient, while 4% strain provides enough displacement. Therefore, 4% strain provides a workable balance between the required force and the deformation of the SMA wire. Although lower strain would be preferable for long-term durability.

The Yoke

The yoke is used to facilitate the rotation of the lamellas, see Figure 8.12 for the design of the yoke. The yoke has three holes for each pin of the three crank arms connected to the axis. Moreover, the yoke has small loops at both the ends. These loops are used to connect the spring, for contra force, and the steel wire that is attached to the shape memory alloy. To ensure that there is no clash between the sliding yoke and the lamella's axis during the linear movement, the pin is offset from the central axis.

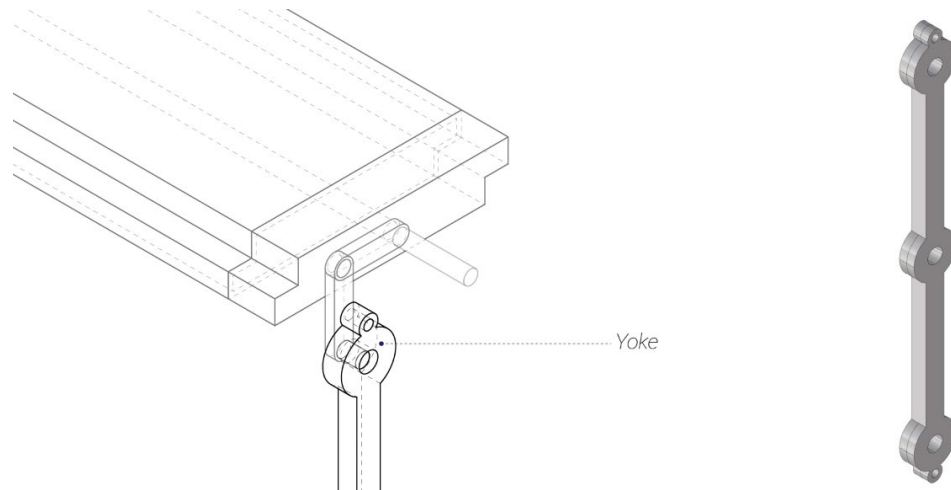


Figure 8.12
Design of the yoke.

8.5.4 SMA Wire Routing and Acting Forces

This part discusses the wire routing and the driving force of the mechanism. The mechanism consists out of, lamellas, crank arms, pins, and a sliding yoke. They provide the possibility of open and closing the ventilation system. However, they still need a driving force that result in a movement of these parts. The SMA wire is this driving source.

SMA Wire Routing

The SMA wire is partially embedded within the component to minimize direct exposure to airflow. This could possibly influence the temperature the wire is experiencing. What could lead to unwanted actuation, due to local cooling or heating from the passing air. Figure 8.13 illustrates several potential ways to further shield the SMA wire from airflow and maintain consistent actuation.

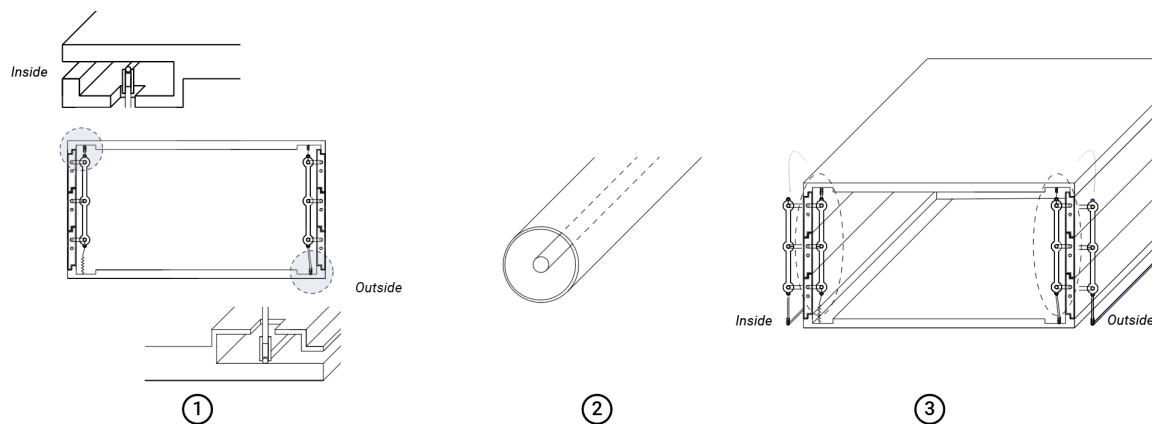


Figure 8.13
Potential strategies to protect the SMA wire from direct airflow.

This figure shows 3 different approaches to protect the SMA wire from airflow, to ensure consistent actuation. In Concept 1, the SMA wire is placed in a small compartment within the component, with openings to the inside and outside. This setup allows the actuator to respond to both indoor and outdoor temperatures while being shielded from wind and direct sunlight. Concept 2 encloses the SMA wire in a protective tube, ensuring more stable actuation. In Concept 3, the mechanism is positioned outside the main box. In this configuration, the SMA wire on the outside is exposed to wind and sunlight. Furthermore, when the system is open, cold outside air can still flow along the indoor SMA wire, which may affect its actuation.

Overall, Concept 1 appears to be the most effective approach. It provides the SMA wire with protection from wind and direct sunlight while still allowing it to respond accurately to both indoor and outdoor temperatures, ensuring reliable and consistent actuation.

Acting Forces

When the SMA wire increases in temperature it starts to contract. The SMA is placed horizontally, while the yoke is moving vertically. Therefore, a pulley is used to convert the horizontal contraction into vertical movement of the yoke. The yoke and SMA wire are connected with a steel cable. As the yoke moves, the pins and crank arms rotate the lamellas. To make this movement reversible a spring is connected to the yoke.

In this system there are several different forces active. These forces are influencing the SMA wire and the rotation of the lamellas. The force generated by the SMA wire is temperature-dependent and, as discussed in Section 6.1.3, also depends on the wire diameter. As mentioned in Section 8.3, the force generated by the tested SMA wire (diameter 0.88 mm) differs per temperature. When the SMA wire is at low temperature, in its martensite phase, it generates approximately 70 N. When the temperature rises the force increases to reach a maximum of 200 N, in its Austenite phase. These forces are essential to rotate the lamellas.

The spring is used as contra-force to push the yoke backwards when the SMA wire is cooled down and reduces its force. When the SMA wire is converting from the austenite phase into the martensite phase during temperature decreasing, the material is becoming soft again and can be deformed by the spring. So, the original position of the mechanism is restored. This contra-force must be greater than the 70N and lower than 200N. Other forces that have an influence are the own weight of the lamellas and the friction in the moving parts. This can be summarized in a force balance given in Equation 8.2. This mechanism, including the force and displacement of the SMA wire on both phases is illustrated in Figure 8.14. This figure highlights how the SMA responds to outdoor conditions: as the temperature rises to 24 °C, the SMA contracts, pulling on the yoke and rotating the lamellas from the open to the closed position.

Equation 8.2

$$F_{contra} > 70 + F_{friction} + F_{weight}$$

But also:

$$F_{contra} < 200 - F_{friction} - F_{weight}$$

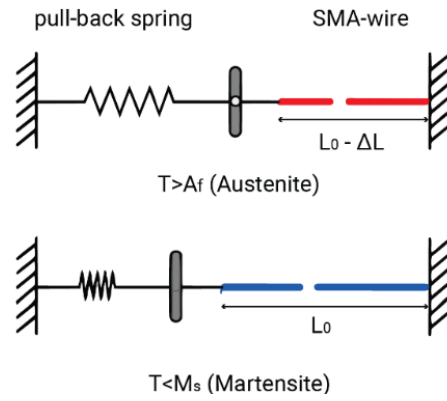
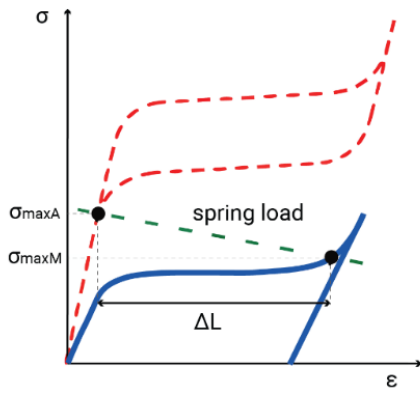
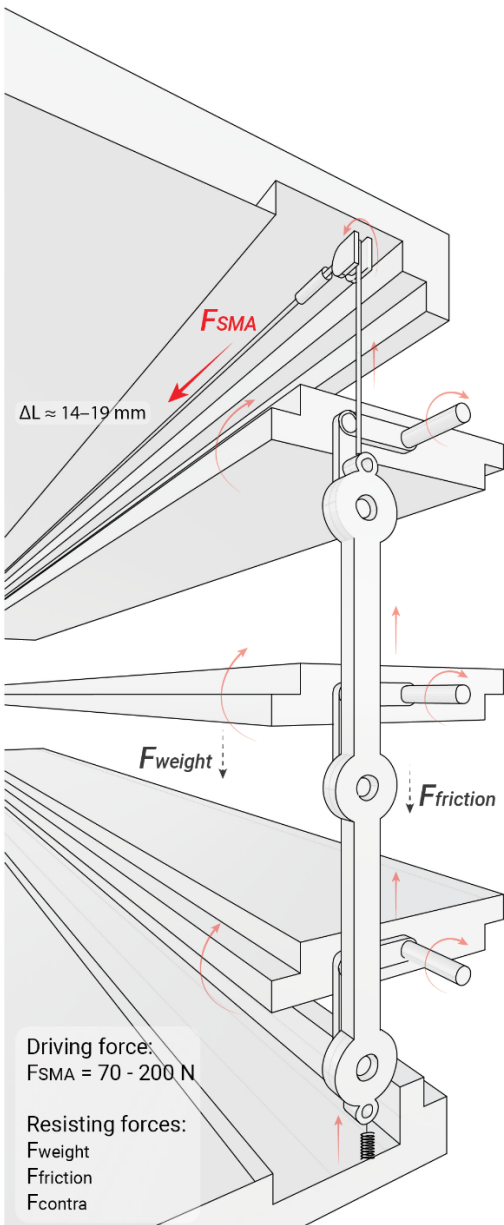


Figure 8.14
Force-displacement behaviour of SMA wire.

Temperature Rising



Temperature Dropping

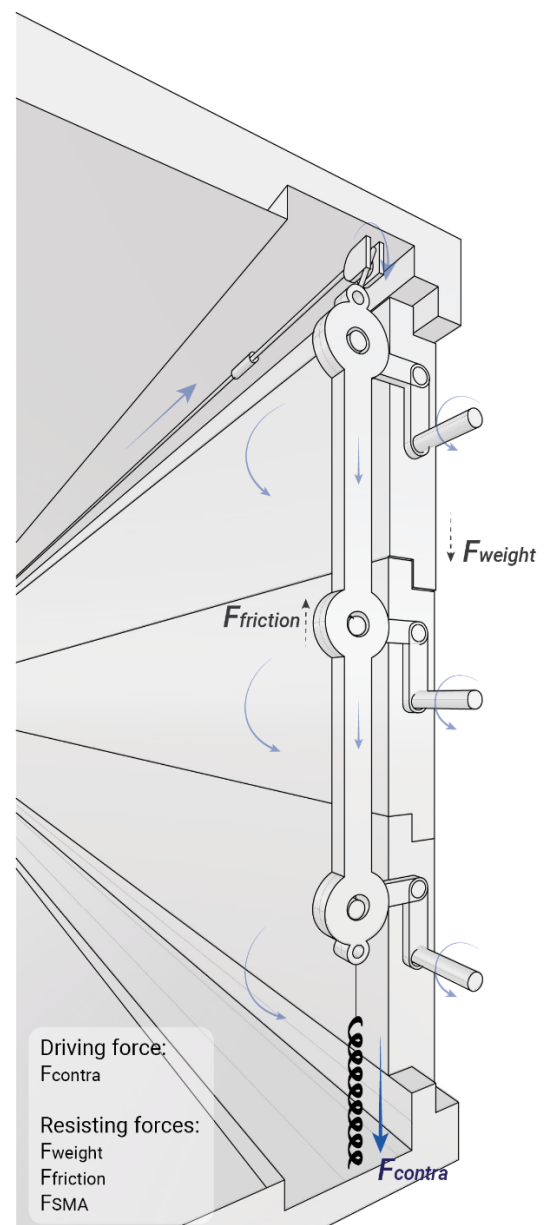


Figure 8.15
Force balance of the SMA-driven mechanism during heating and cooling responding to outdoor conditions.

Figure 8.16 illustrates the integrated mechanism in both the open and closed position. The system is actuated by two SMA wires that respond to different temperature conditions. One SMA wire responds to the outdoor temperature, while the other responds to the indoor temperature. Because these wires are positioned on opposite sides of the mechanism, they create opposing forces that control the vertical movement of the linkage system. In this way, the system responds passively to both indoor and outdoor conditions.

The figure also shows the main active forces in the system, including the SMA actuation force, the counterforce, friction, and the weight of the moving elements. Together, these forces determine the resulting motion of the lamellas.

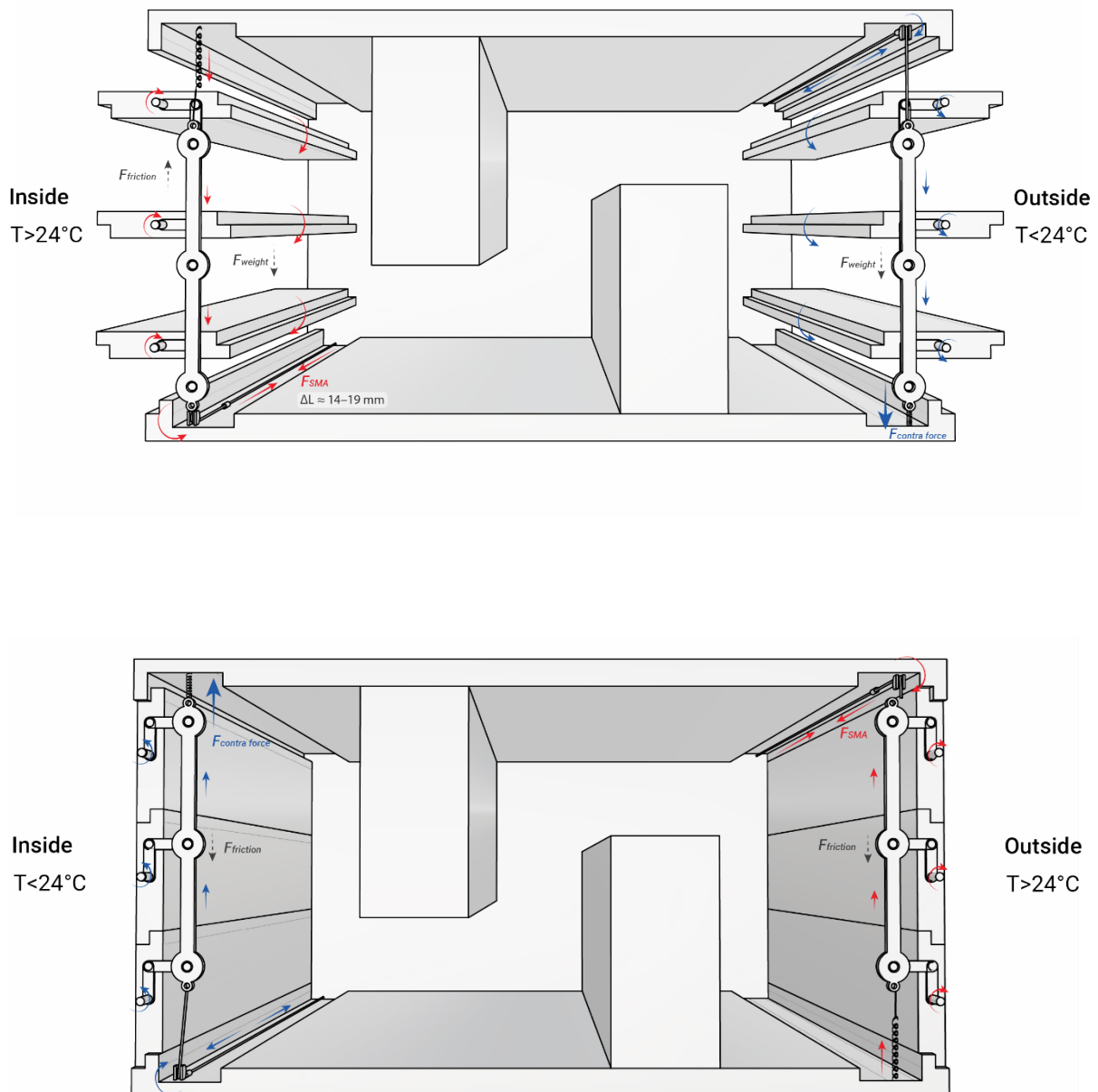


Figure 8.16

SMA-driven mechanism showing all active forces in both open and closed positions, with one side responding to outdoor and the other to indoor temperature.

8.5.5 Manual Override Mechanism

Although the ventilation component is designed to operate passively through SMA actuation, a manual override is needed to allow user control during winter or with unwanted high air change rates. This prevents unnecessary heat loss, draught, or ventilation when the system should remain closed. Two override strategies are considered, a passive mechanical override and an active electrical override. The passive option is most consistent with the design criteria, because it keeps the system simple and does not require external energy.

The passive override consists of an indoor slider connected to the sliding yoke. By moving the slider, the user can manually move the yoke and rotate the lamellas into the closed position. Since the yoke controls all lamellas at the same time, the user can close the full component with one simple movement. With a crank arm of 10 mm, the required yoke displacement for the rotation of the lamellas is approximately 15.7 mm. This system is illustrated in Figure 8.17.

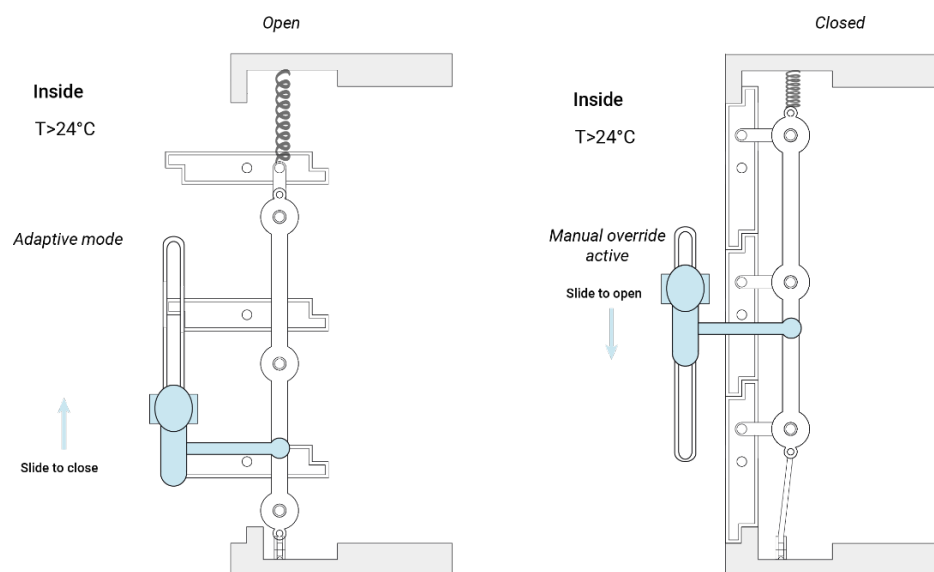


Figure 8.17
Manual override principle.

An active electrical override could be considered as an alternative strategy. In this option, the user presses an indoor button, which sends an electrical signal to the outside SMA wire. The wire is then electrically heated, contracts, and pulls the yoke into the closed position. This allows the component to be actively closed. Even when the outdoor temperature is not high enough to activate the outside SMA. This system is summarized in Figure 8.18.

The required energy could be supplied by façade-integrated photovoltaic materials or a small PV panel, potentially combined with a battery for short-term storage. This links the override strategy to light-responsive energy-harvesting materials discussed in Chapter 4.

However, this option adds components such as wiring, a push button, PV material and energy storage. It therefore increases system complexity and reduces the fully passive character of the design. For this reason, it is considered a possible future development rather than the main override strategy.

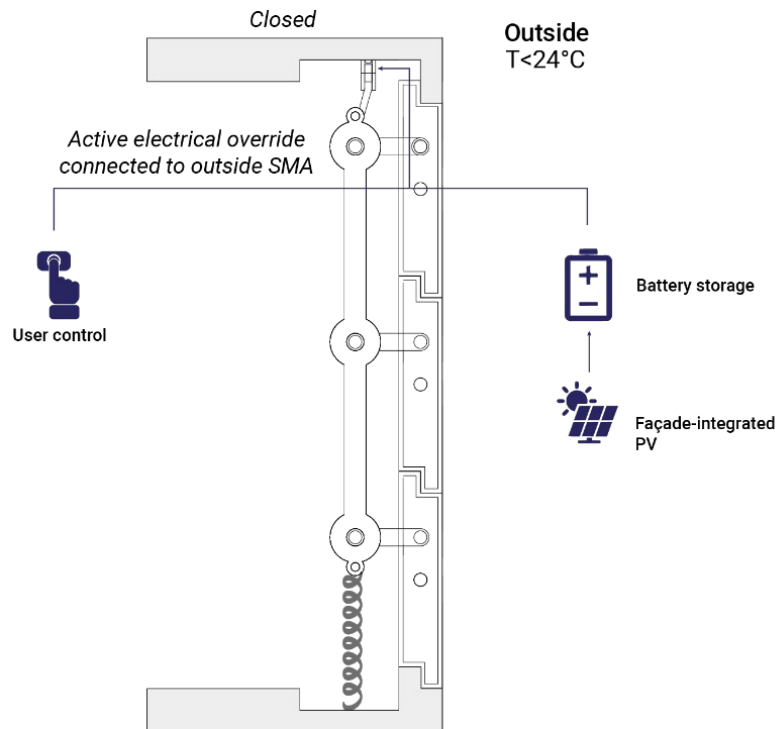
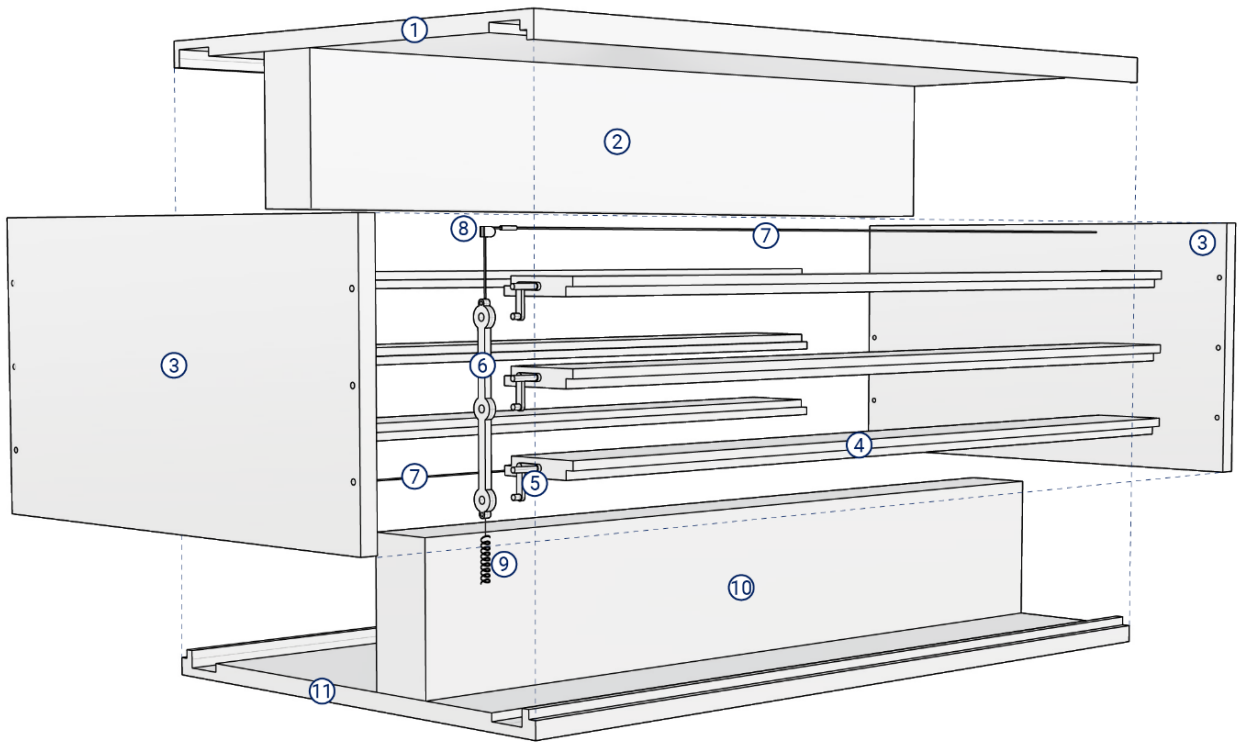


Figure 8.18
Active electrical override strategy connected to the outside SMA wire.

8.6 Final Component Design

This section presents the final design of the SMA-driven adaptive ventilation component through technical drawings and renders. The drawings bring together the previously discussed design elements, including the lamellas, actuation mechanism, SMA wire routing, return spring, acoustic box and façade integration. Together, they show how the mechanical working principle is translated into a façade component.

The final component is shown through an exploded view, vertical section, horizontal section, and façade integration render. The vertical section shows the open and closed positions and clarifies the airflow path through the component. The horizontal section illustrates the internal layout of the component and the position of the lamellas and side profiles. The façade integration drawings show how the component could be implemented within the CLT façade build-up.



- | | | | | | |
|---|-----------------------------|---|---------------------------|---|-----------------------------|
| ① | Top cover | ⑤ | Lamella actuation linkage | ⑨ | Contra-force spring |
| ② | Upper acoustic guide module | ⑥ | Yoke | ⑩ | Lower acoustic guide module |
| ③ | Side panel | ⑦ | SMA wire actuator | ⑪ | Bottom cover |
| ④ | Lamellas | ⑧ | Pulley | | |

Figure 8.19
Exploded view of the adaptive ventilation component.

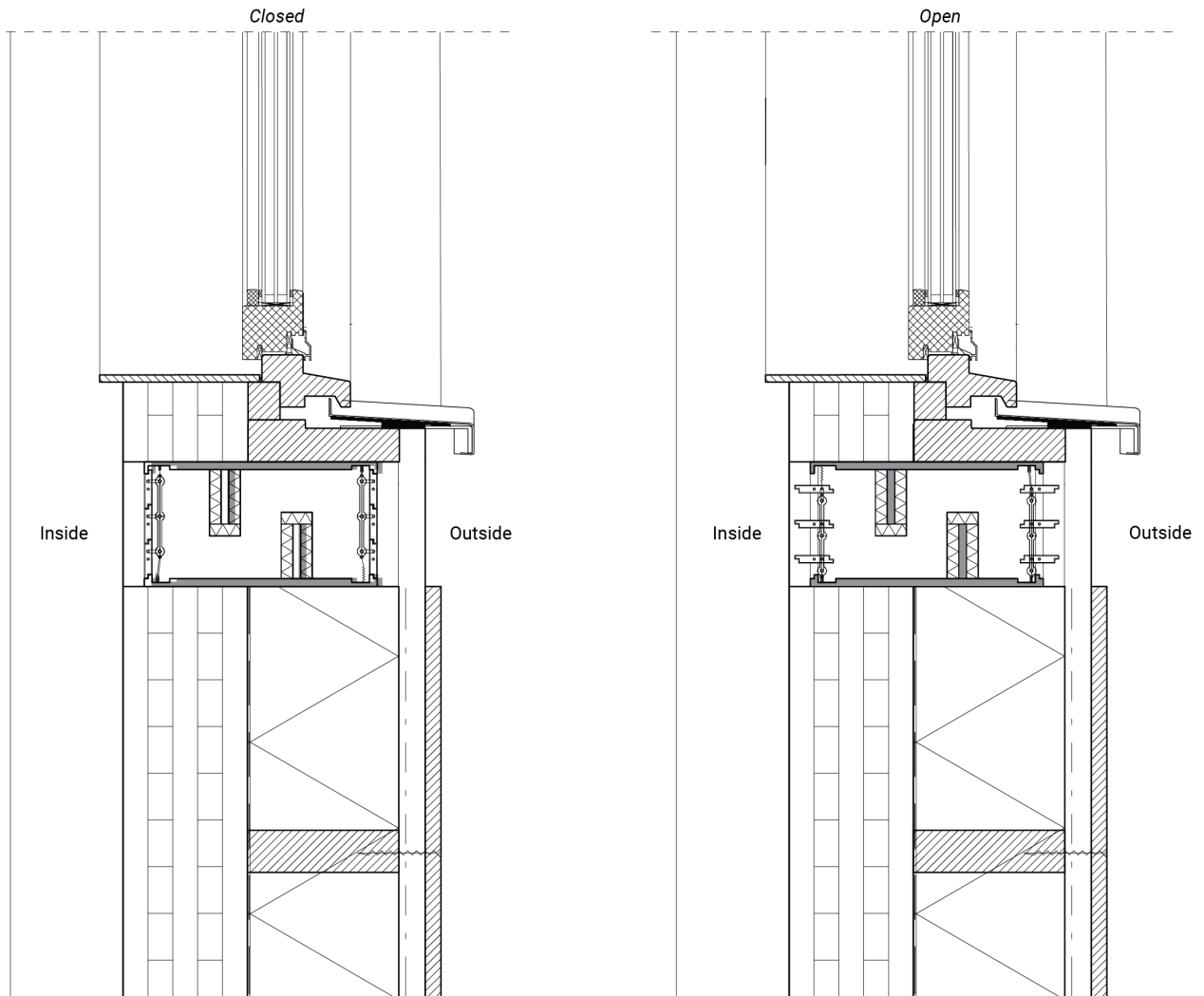


Figure 8.20
Open and closed state of the SMA-driven ventilation component integrated in a CLT façade section.

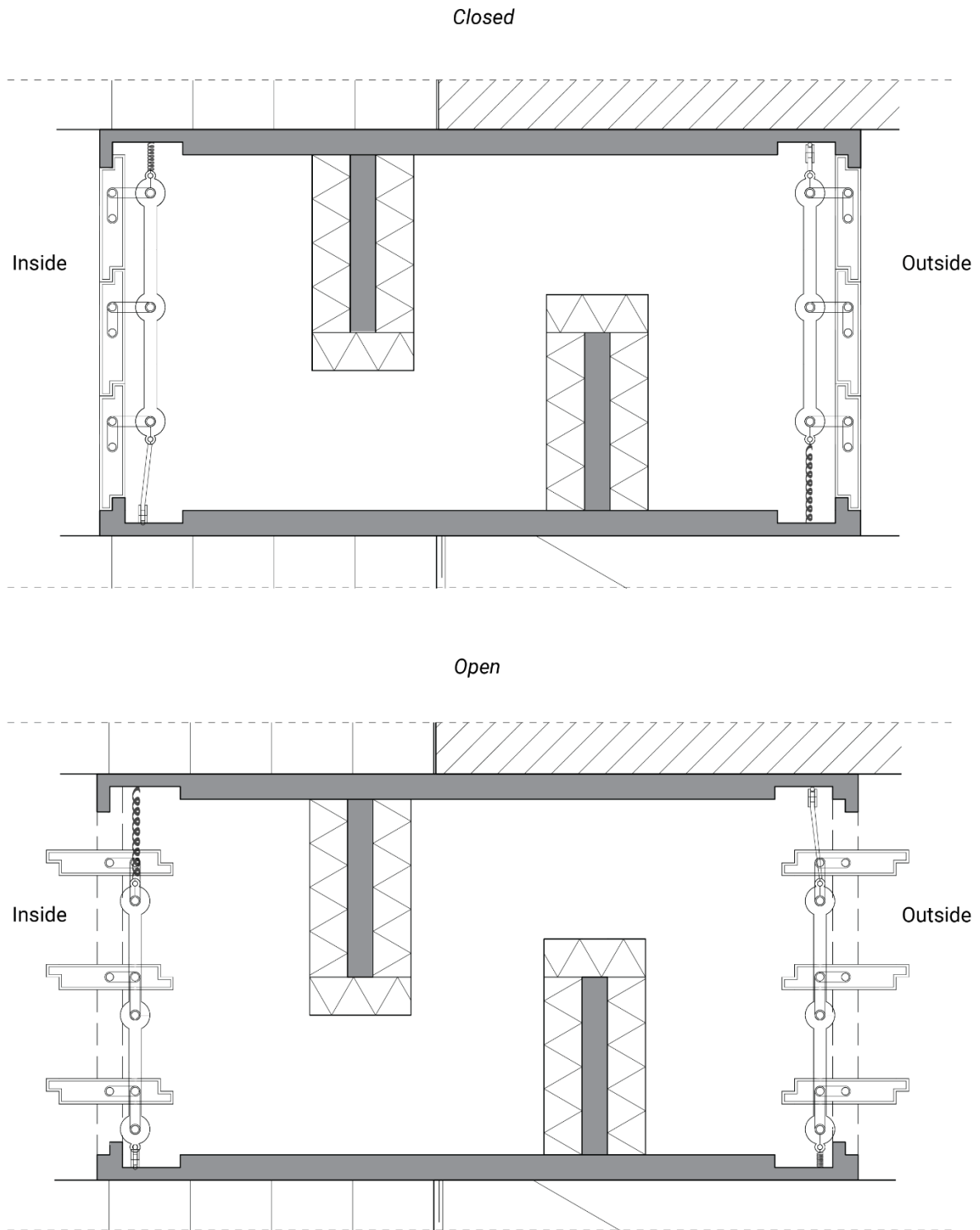


Figure 8.21
Vertical section of the SMA-driven adaptive ventilation component in closed and open position.

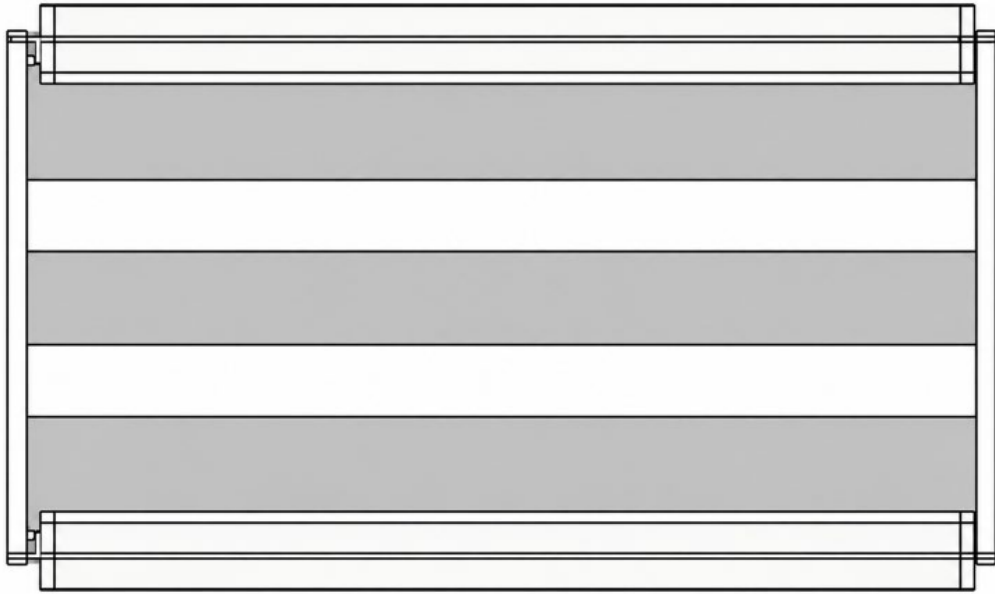


Figure 8.22
Horizontal section of the SMA-driven adaptive ventilation component.

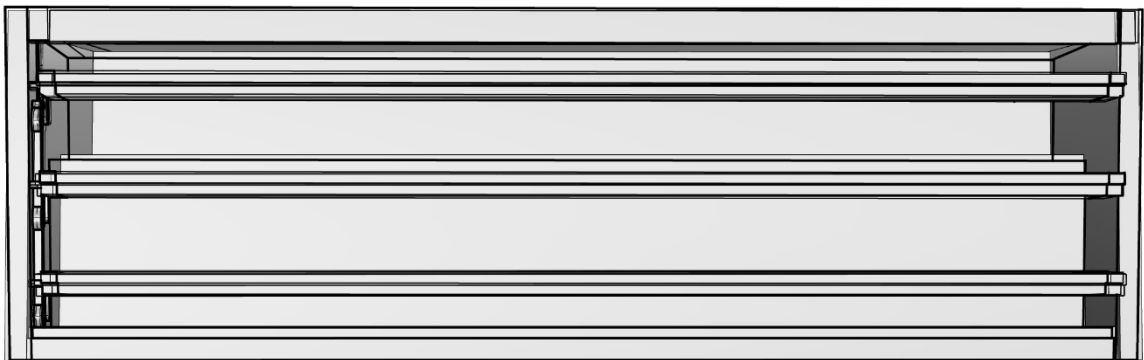


Figure 8.23
Front view of the SMA-driven adaptive ventilation component.

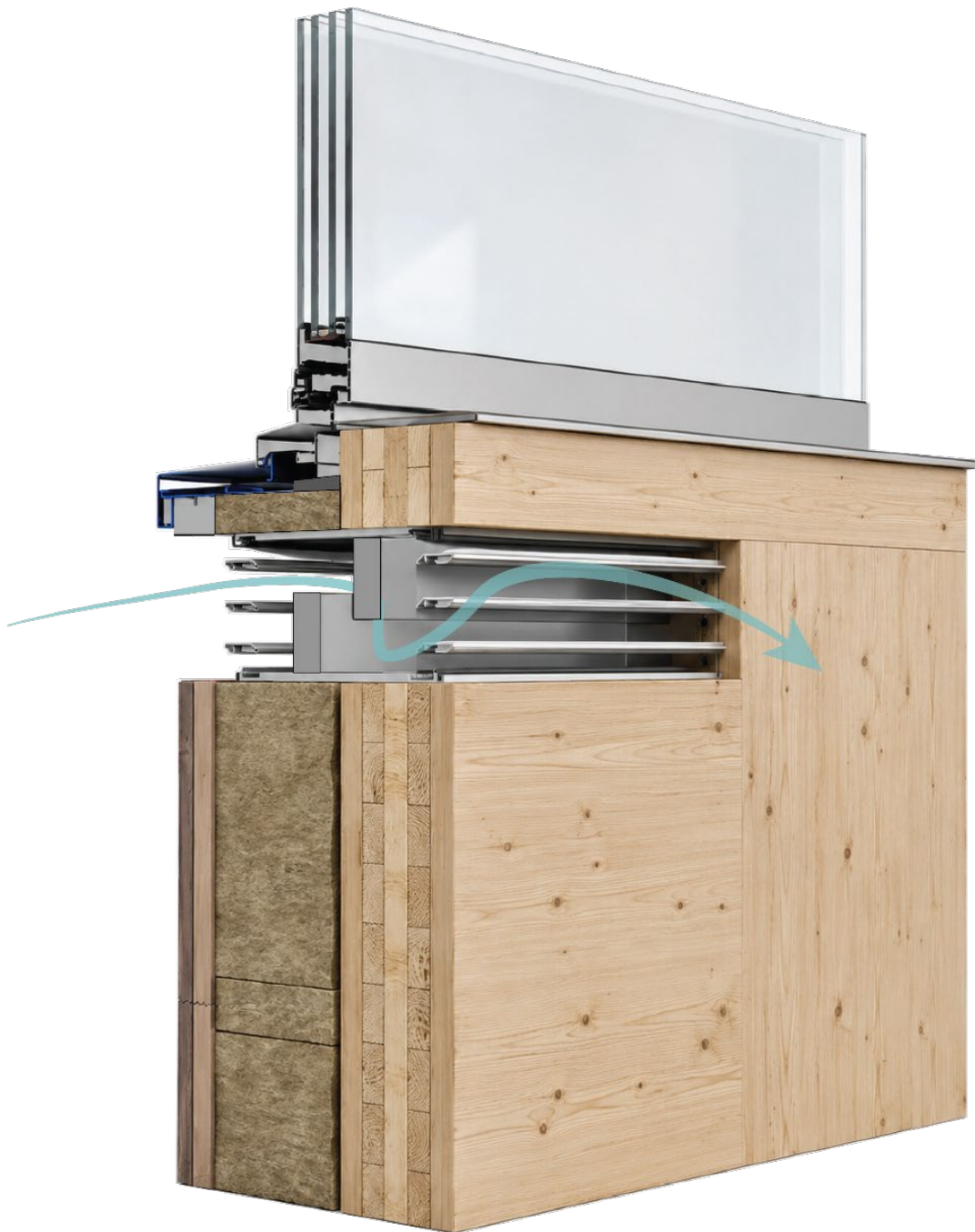


Figure 8.24
Adaptive ventilation component integrated in a CLT façade section.

8.7 Design Criteria Evaluation

This section evaluates the proposed adaptive ventilation system design according to the design criteria formulated in Section 7.3. The evaluation shows to what extent the adaptive ventilation component meets the initial requirements, and which aspects still require further development or testing. This is summarized in Table 8.7.

Table 8.7
Final evaluation of the product design based on the design criteria

Design criterion	Type	Evaluation	Explanation
Passive operation	Hard	++	The system operates through SMA activation and a return spring, without motors.
Temperature-responsive behaviour	Hard	+	The SMA responds to temperature changes, but practical tuning to 24°C remains important.
Reversible movement	Hard	+	The system can open and close but depends on the contra-force and spring return.
Limited SMA deformation	Hard	+	The SMA works mainly in linear contraction, but strain is close to the upper design limit.
Façade integration	Hard	+	The component is integrated into the façade section, including the actuation mechanism.
Ventilation capacity	Hard	+	The unit provides a modular opening; multiple units are needed for higher airflow.
Limited number of components	Soft	o	The mechanism is relatively simple, but still includes pins, yoke, spring and wire routing.
Stable movement	Soft	+	The yoke allows simultaneous and controlled movement of the ventilation elements.
Efficient force transmission	Soft	+	The Scotch yoke translates SMA contraction into rotation effectively.
Airtight closed state	Soft	o	The interlocking lamellas improve closure, but airtightness still requires physical testing.
Durability	Soft	o	Linear SMA movement supports durability, but long-term fatigue and friction need further testing.

Note. ++ = achieved, + = mostly achieved, o = partly achieved / needs further testing, - = not achieved.

This evaluation of the design criteria shows that the main hard criteria are mostly achieved. The design operates passively, responds to temperature changes, and can be integrated into the façade. However, several soft criteria still require further testing. Especially criteria such as, airtightness, durability, and long-term friction in the moving parts.

8.8 Conclusion

This chapter developed the adaptive ventilation component what is drive by shape memory alloys. This from the operating logic to the component geometry of the system. It's designed to passively open when cooling is favourable. Furthermore, it remains closed when ventilation could lead to overheating or unwanted heat losses.

For the physical mock-up the SMA wire was tested to determine its mechanical and thermal behaviour. The results showed that the wire can generate sufficient force when it's reaching its temperature threshold. Moreover, the contra force is required to deform the wire again during cooling. For the practical application, the system is based on target phase temperatures in which the SMA wire reaches its fully contracted state at approximately 24°C.

In addition, different actuation mechanisms were compared. The Scotch yoke mechanism was selected as the most suitable principle. This principle translates the linear contraction of the SMA wire into rotation of the lamellas. the final geometry includes three lamellas, crank arms with pins and the end, a sliding yoke, SMA wire, pulley, and a spring what functions as a contra-force.

The final adaptive ventilation system was evaluated by the design criteria. To conclude this, the hard criteria are achieved. The system operates passively, this in responds to temperature. Furthermore, the SMA wire is used in linear movement. And it can be integrated into a façade. Nevertheless, some aspects need further investigation, namely, the air tightness of the structure, its durability, and friction losses in its moving components. The next chapter will evaluate the effect of the designed adaptive ventilation component on the indoor climate. This based on building performance simulations.

9. Building Performance Simulations

In this chapter, performance assessment of the developed ventilation component is evaluated through building performance simulations. This to evaluate the design impact of the adaptive ventilation system. The building performance evaluation is carried out in two steps: first in a standard reference room and then in a case study from Arup. The performance simulations will include different simulation scenarios to compare the effect of the proposed adaptive façade system on thermal comfort, overheating, and natural ventilation. To will be done via design simulations using DesignBuilder. The chapter describes the simulation method, model setup, ventilation scenarios and performance indicators.

9.1 Aim and Scope of the Simulations

The aim of the performance simulations is to evaluate the effect of the proposed temperature driven ventilation system actuated with Shape Memory Alloys, on the indoor climate. This on aspects such as, on improving thermal comfort, avoiding overheating and increasing natural ventilation of room level.

Therefore, SMA properties such as phase transformation, contraction force, reaction time and fatigue behaviour are not modelled in DesignBuilder. Instead, the SMA opening principle will be simplified into a control logic for ventilation openings. It's assumed that the component is open when the indoor temperature threshold is reached. And when the outdoor temperature is below this threshold, when it is appropriate for passive ventilations.

Within the scope of the simulations, it includes an analysis of the influence of different ventilation configurations on the indoor environment. This for both the standard reference room and the case study.

9.2 Methodology

In this section the methodology of the simulations will be discussed. This section will mention the simulation software, climate and location, ventilation control logic, and the performance indicators for the building performance simulations. These performance indicators are used to compare the different scenarios for both the reference room and the case study.

9.2.1 Simulation Software

DesignBuilder will be used to run the simulations. This is a dynamic building performance analysis software that is based on the EnergyPlus calculation engine. The choice of this simulation software is because of its ability to model natural ventilation systems and evaluate façade integrated systems at room level. Thermal performance, ventilation, comfort, and energy-related variables can be examined over time. The biggest benefit offered by DesignBuilder is that it allows a comparison of various scenarios for ventilation while keeping same boundary conditions.

9.2.2 Climate and Location

The simulations were run using a Dutch climate file. In DesignBuilder the location was set to Amsterdam Airport Schiphol. The weather file is based on ASHRAE/IWEC climate data. The main climate file characteristics are presented in Table 9.1. With information regarding the outdoor weather conditions, including the temperature, radiation, humidity, and winds.

Table 9.1*Climate file information used for the building performance simulations*

Parameter	Value
Location name	Amsterdam AP Schiphol
Country	Netherlands
Climate data source	ASHRAE/IWEC
WMO station number	62400
ASHRAE climate zone	4A
Latitude	52.30°
Longitude	4.77°

Note. Climate file information retrieved from the DesignBuilder location template data report for Amsterdam AP Schiphol, based on ASHRAE/IWEC weather data.

9.2.3 General Ventilation and Control Logic

The ventilation strategy used in the simulations is based on a temperature driven natural ventilation system for passive cooling. This is controlled by a simple logic of on and off. If the indoor and outdoor passes the thresholds, then the system allows natural ventilation, this is summarized in Equation 9.1. When these setpoints are not met the ventilation openings will remain close. This improves night ventilation for passive cooling, when the outdoor temperatures are lower. Several different temperature thresholds will be tested. This to determine the most effective setpoint, to improve the indoor climate.

Equation 9.1

$$T_{indoor} > T_{threshold} \quad \text{and} \quad T_{outdoor} < T_{threshold}$$

To simulate natural ventilation behaviour, the calculated natural ventilation option was selected in the model options of DesignBuilder. Because this method takes into consideration the effect of pressure and temperature differences for the air flow. It gives more accurate results of natural ventilation than a simple scheduled air flow simulation. However, the calculated option only supports a setpoint for the indoor temperature. Therefore, Energy Management System (EMS) script was used. In this manner, an extra control operation logic could be implemented. This script regulates the operation of the ventilation openings. The full script is included in Appendix D.

The behaviour of the SMA can be modelled more realistically in DesignBuilder by gradually linking the free aperture of the ventilation to the setpoint temperatures with EMS scripting. Using multiple points within the hysteresis. This allows the component to open and close smoothly rather than suddenly at one setpoint for outdoor and indoor temperatures.

The hysteresis mainly affects the indoor SMA, which can stay open longer than 24 °C while the indoor temperature drops. The outdoor SMA, however, is fully contracted (A_f) at 24 °C and stays closed, so no warm outside air is brought in. Modelling the SMA with variable free aperture and hysteresis can influence the simulations in different ways. Positively, it can provide extra passive cooling during peak temperature moments, slightly lowering indoor temperatures below 24 °C and improving comfort. Negatively, the longer open period of the indoor SMA may cause over-ventilation when temperatures drop, potentially leading to slight overcooling or increased energy use during cooler weeks.

9.2.4 Performance Indicators

For evaluating the different scenarios, thermal comfort and ventilation performance indicators are used. These indicators are set to assess the implementation of the adaptive ventilation systems on the indoor climate. The focus is based on thermal comfort, overheating reduction, and natural ventilation.

The first performance indicator is the number of hours not comfortable. This indicator gives the number of hours when the thermal conditions of the indoor climate do not meet the selected comfort criteria. Furthermore, this indicator is used to determine the temperature setpoint for opening and closing of the ventilation system. This will be shown in the setpoint sensitivity analysis in the result chapter. The number of hours the indoor climate is not comfortable is based relative to the occupied time.

The second indicator is the indoor operative temperature. The operative temperature accounts for the effect of both air temperature and radiant temperature. In this way it makes it more representative of thermal comfort, compared to air temperature. The highest operative temperature and the temperature curve in warm periods will be analysed. This to see how the ventilation strategy is influencing the peak indoor temperatures.

Furthermore, the number of hours when the indoor temperature is exceeding the 24°C. this threshold corresponds to the control temperature of the adaptive ventilation system. This indicator is used to compare how often the indoor temperature exceeds this limit in different scenarios.

Moreover, the performance of the natural ventilation will be analysed based on the air change rate indicator. This indicator provides how much the air in the room is refreshed in one hour. This parameter can be used to analyse the amount of airflow provided by the natural ventilation strategy. Additionally, the timing when the ventilation system is active will be assessed. To explore whether the system mostly operates.

Finally, for the case study the indicator of cooling demand and cooling power will be analysed. The cooling demand is used to evaluate how much active cooling can be reduced. The cooling power is used to analyse the interaction between passive ventilation and active cooling.

Together, the indicators summarised in Table 9.2 provide insight into the thermal performance and ventilation performance of the adaptive system, while also showing the design impact of the proposed ventilation component on the indoor climate.

Table 9.2
Performance Indicators

Indicator	Unit	Use in analysis	Purpose
Time not comfortable	h	Setpoint sensitivity	Determine most suitable control threshold
Percentage not comfortable	%	Setpoint sensitivity	Compare discomfort relative to simulation time
Operative temperature	°C	Scenario comparison + summer analysis	Evaluate indoor thermal comfort
Maximum operative temperature	°C	Scenario comparison	Compare peak temperature reduction
Hours above 24°C	h	Scenario comparison	Evaluate exceedance of control threshold
Air changes per hour	ac/h	Scenario comparison + summer analysis	Evaluate ventilation performance

Indicator	Unit	Use in analysis	Purpose
Ventilation activation timing	time profile	Detailed summer analysis	Analyse when the adaptive system operates
Cooling demand	kWh	Case study comparison	Evaluate reduction in active cooling demand
Cooling power	kW	Detailed case study week	Analyse interaction between passive ventilation and active cooling

9.3 Reference Room

This section describes the setup of the standard reference room used for the first part of the building performance simulations. The reference room is used to evaluate the effect of the adaptive ventilation component under simplified conditions. The following sections define the model geometry, boundary conditions and simulation scenarios used for the comparison.

9.3.1 Model Geometry

The reference room is modelled as a single-zone space with a floor area of approximately 20 m². The reference room has a height of 3.0 m, a width of 3.6 m and a depth of 5.6 m, as illustrated in Figure 9.1. One side of the room is considered as the external façade with a window, which will be used for modelling the façade-integrated ventilation component. The window to wall ratio consists of 30%. What is resulting in a window of 2.0 m by 1.6 m, positioned at 0.9 m above the floor. During the simulations this window remains closed. This makes sure that the airflow is only related to the ventilation components. The window is used for the internal loads, such as solar gains.

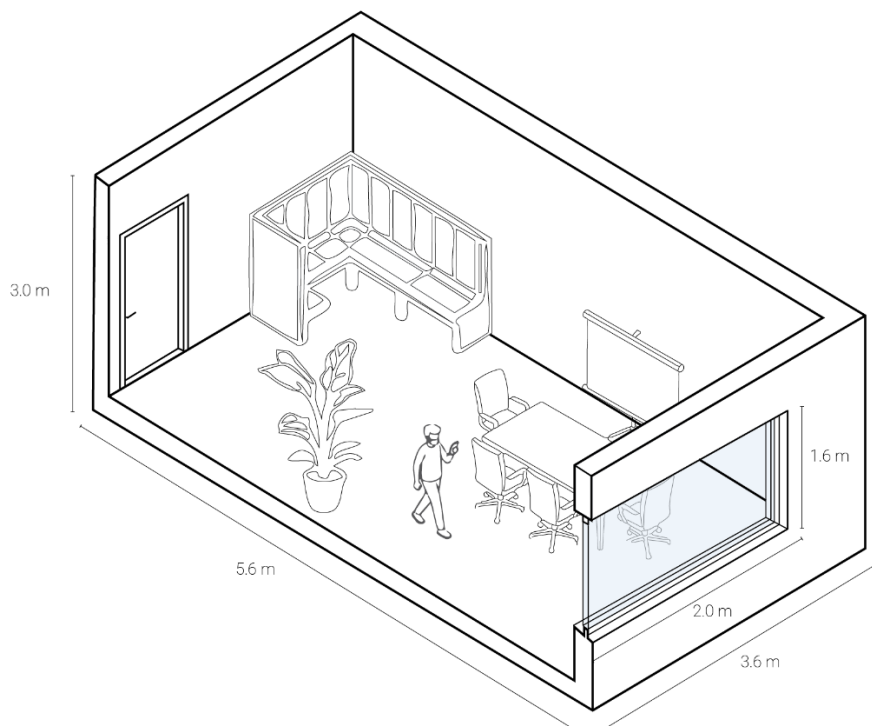


Figure 9.1
Standard Room Layout and Dimensions.

The ventilation component is based on the adaptive ventilation component, discussed in Chapter 8. The width of each individual component is 500 mm, and its height is 150 mm (see Figure 9.2).

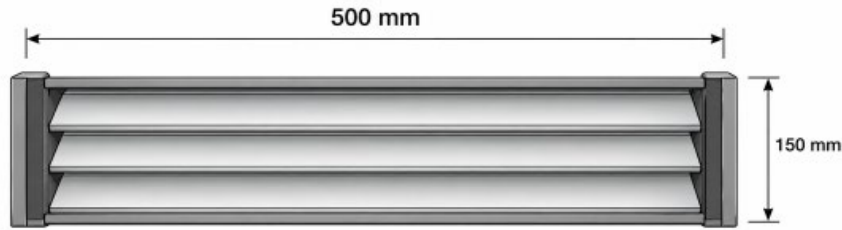


Figure 9.2
Dimensions for ventilation component in front view.

Furthermore, the ventilation system includes an acoustic ventilation box. The use of an acoustic box ensures reduction in noise transmission through the open ventilation system. Nevertheless, the full opening area cannot be considered as free airflow area. Therefore, the free aperture of each ventilation component was set to 70%. This value is used as a simplified design assumption for the reduced free area caused by the acoustic box. Furthermore, the gross opening area of one component is 0.075m^2 . With a free aperture of 70% this is reducing to a free opening area of 0.0525m^2 . To still achieve the required opening area of 0.30m^2 for two-sided ventilation (see Appendix B), six ventilation components must be implemented. Because $6 \times 0.0525 = 0.315\text{m}^2$. These findings are summarized in Table 9.3

Table 9.3
Free Opening Area with Acoustic Box

Parameter	Value
Gross opening area per component	0.075 m^2
Assumed free aperture	70%
Effective free area per component	0.0525 m^2
Number of components	6
Total effective free opening area	0.315 m^2
Required opening area for two-sided ventilation	0.30 m^2

9.3.2 Boundary Conditions

The reference room is modelled using the default DesignBuilder template for a typical office building. This template defines the construction properties, internal gains and occupancy conditions used in the simulation. U-values of external walls, roofs, and floors are determined by default values associated with the template. External glazing of the room will be "Project external glazing". The window will regulate daylight, thermal regulations. Furthermore, internal heat gains are determined by the conditions and equipment of the room. There are some occupant-based internal gains, like metabolic heat and lighting loads in addition to office equipment. This results in internal gains according to occupancy density. with a power density for office equipment set to 11.77 W/m^2 . And lighting power density is set at 5.0 W/m^2 . The radiant and convective fractions of internal gains are specified as 0.42 and 0.40. These are typical for office environments.

For the occupancy a density of 0.1110 people/m^2 is used. This is representing a standard office environment. The schedules used for occupancy and for equipment is predefined to activities schedule. This means that occupants are active during work times. Moreover, in this simulation infiltration is turned off. This is because to make sure that the only factor that affects the airflow is from natural ventilation from the adaptive ventilation components. Furthermore, there is no additional HVAC system, such as cooling, heating or mechanical ventilation in this model.

9.3.3 Simulation Scenarios

To evaluate the effectiveness on the indoor climate of this adaptive ventilation system three different scenarios are defined, see Figure 9.3 and Table 9.4. These different scenarios will be used to compare a room without natural ventilation, as reference case, with a façade with different natural ventilation configurations. These configurations show the differences between one-sided ventilation and two-sided ventilation, but with the same amount of ventilation components.

For all the scenarios, the same parameters including geometry, material properties, heating load, occupancy, schedule, and climate file are kept constant. This to isolate the effect of the ventilation system from the boundary conditions. So, the results rely on the changes in ventilation configurations, rather than the boundary conditions.

The first scenario, S0, represents the reference case. In this reference case the adaptive ventilation components do not operate. the purpose of this scenario is to evaluate the indoor climate without any additional ventilation via the façade elements. In this way it functions as a baseline. In this scenario there is no heating or cooling applied.

The second scenario, S1, represents one-sided ventilation. In this scenario there are six ventilation components placed in one side of the room. This allows to evaluate the effect on the indoor climate when ventilation is only applied through one side of the room.

The third scenario, S2, represents two-sided ventilation. Here there are placed six adaptive ventilation components on one side of the room. With on the opposite side of the room outlet grills. These outlet grills have approximately the same free aperture opening area as the adaptive components. So, on the other side there a placed four outlet grills of a total opening area of $0,3\text{m}^2$. This layout will enhance the airflow path through the room. Furthermore, the airflow can be supported by the buoyancy effect if the opposite grill is places higher in the wall. Here the differences between one-sided and two-sided ventilation can be analysed with still using the same amount of adaptive ventilation components.

The amount of ventilation components implemented in the façade is based on their effective free opening area. Because the ventilation components have an acoustic box, the full opening area reduces. To still meet the dimensions for two-sided ventilation the number of components is increased, as explained before.

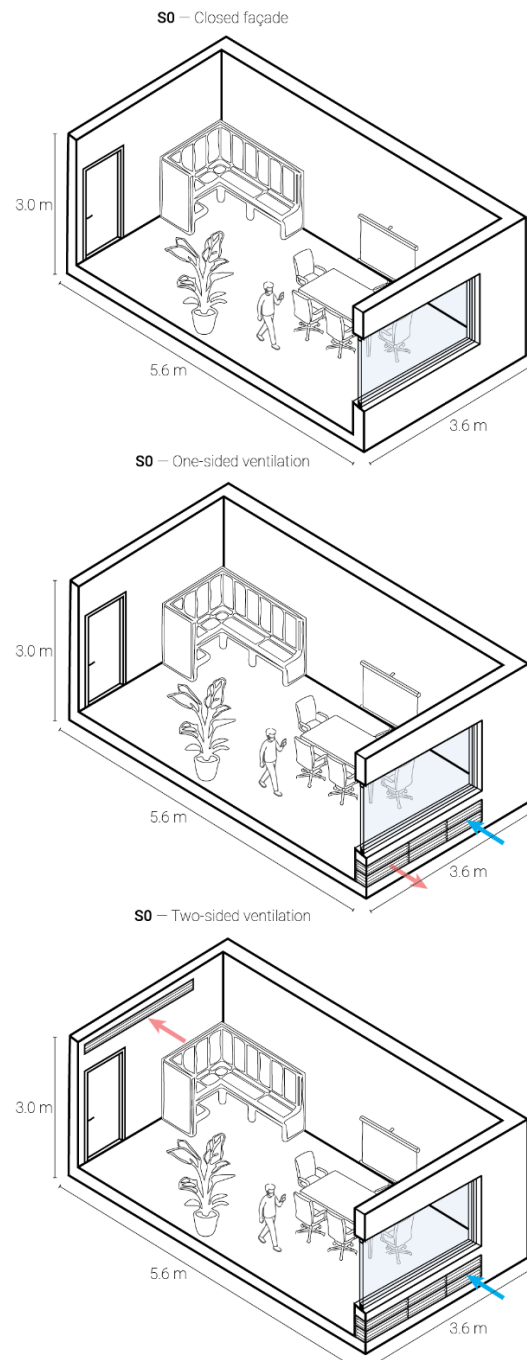


Figure 9.3
Reference room scenarios.

Table 9.4
Reference Room Simulation Scenarios

Scenario	Configuration	Components	Free aperture	Effective opening area	Purpose
S0	Closed façade	0	—	0 m ²	Reference case
S1	One-sided ventilation	6	70%	0.315 m ²	Evaluate single-sided ventilation
S2	Two-sided ventilation	6 + opposite openings	70%	0.315 m ²	Evaluate two-sided ventilation

9.4 Case Study Setup

This section describes the setup for the case study simulations. The adaptive ventilation system is applied to a residential building. The aim of the case study is to evaluate if this adaptive ventilation system can contribute to passive cooling as well as lower the cooling load. Based on this there will be a comparison between three different scenarios.

9.4.1 Case Study Description

In addition to the previous simulations of a reference room, the adaptive ventilation components will be tested on a real residential case study provided by Arup. The selected case study is a residential tower in Amsterdam, named Hartje Noord (see Figure 9.5). This project was used to evaluate how the adaptive ventilation systems work in realistic conditions rather than in the simplified model of the reference case.

The apartment MDH n.02 located on the 11th floor was chosen as the most critical apartment (see Figure 9.4). This apartment is south-oriented which results in high solar loads especially during the summer months. Moreover, the apartment includes a living room, a kitchen, a bathroom and two bedrooms. With an overall floor area of 59 m² for the apartment. The current ventilation system of the building is based on the VENTT principle. In the VENTT principle fresh air comes into the apartment through façade openings and then it is extracted through an exhaust box placed in the storage room. In addition, according to the project information provided by Arup, the CLT structure allows using the ventilation ducts only in the ceiling bulkheads.

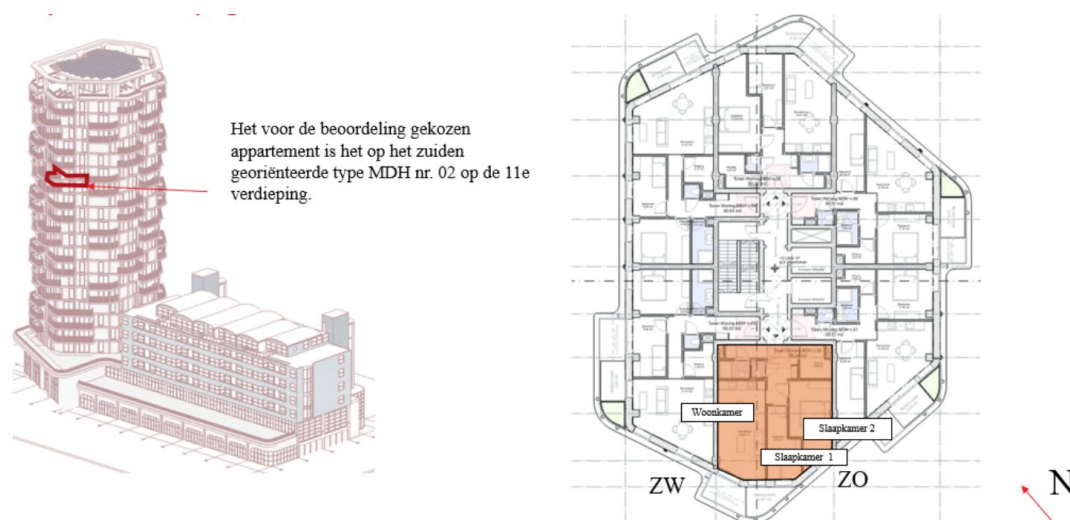


Figure 9.4
Critical apartment of Hartje Noord.



Figure 9.5
Residential tower Hartje Noord in Amsterdam.

9.4.2 Boundary Conditions

In this section the boundary conditions of the case study will be described. The climate and location conditions are described in Section 9.2.2. Furthermore, the ventilation control strategy for adaptive natural ventilation follows the same principle as mentioned in Section 9.2.3. Here there is only natural ventilation allowed when it is indoor above the thresholds of 24°C, while outdoor conditions must be below this threshold.

The simulation includes only the living room of MDH n.02 apartment. The living room is defined as a residential lounge with occupancy density equal to 0.0188 persons/m². Internal gains are set with the use of lightning and equipment loads. The lighting load is 5.0 W/m² and the equipment load is set to 3.9 W/m². Heating set point is set 21°C, cooling set point on 25°C. Construction of the apartment is the same as in project construction templates. Lastly, Infiltration is assumed to occur at 0.7 ac/h rate.

Nevertheless, there will be different case study scenarios, where the HVAC and ventilation settings differ. When there is mechanical ventilation, a zone-specific ventilation rate was set as 1.0 ac/h. This must represent the original mechanical ventilation principle, VENTT, for the apartment. Regarding adaptive natural ventilation, the calculated natural ventilation approach was used as it enables the

airflow to be driven by differential pressures, winds, and temperature differences. To conclude, overall boundary conditions remained similar to the extent that was possible, while ventilation systems were different in each scenario. The different scenarios for the case study will be discussed after the adaptive ventilation configuration in the next section.

9.4.3 Adaptive Ventilation Configuration

The developed adaptive ventilation components will be implemented in the southwest façade of the living room. Three adaptive ventilation elements will be applied into the façade. This to improve the airflow. These ventilation elements have all the same measurements as in the reference room simulations. Which include a width of 500 mm and height of 150 mm. Consequently, the gross opening area will be 0.225 m². For the free aperture of 70%, the resulting opening area will be 0.1575 m² for all three components together. Furthermore, the adaptive ventilation components follow the same control logic as discussed in Section 9.2.3.

Furthermore, an outlet grille was included towards the hallway, this to support two-sided ventilation. The position of this inner grille is relatively high in the wall, this to take advantage of buoyancy driven airflow and the stack effect. The location of this grill follows the layout of the case study. Because in the layout of this case study the ventilation routes are place in the CLT structure and are integrated through the local ceiling bulkhead.

9.4.4 Simulation Scenarios

For analysing the effect of the adaptive ventilation system on the case study, three different simulation scenarios were designed, what is summarized in Table 9.5. These scenarios compare the existing mechanical ventilation and cooling system to the proposed adaptive ventilation system and a hybrid configuration. The geometries, constructions, internal gains, occupancy, climate file, and temperature setpoints remain the same for all cases. Only ventilation and cooling strategies will be changing in the scenarios.

The first scenario, CS0, refers to the reference scenario that is based on the original VENTT principle of the apartment. This scenario has mechanical ventilation and an active cooling system. This scenario is used to represent the original case study and will be used later in comparing with the existing Vabi results to verify the model.

The second scenario, CS1, refers to the passive adaptive ventilation scenario. Here the active ventilation and cooling are turned off. Only the adaptive components will be used. Thus, the purpose of CS1 scenario is to explore whether the adaptive ventilation can reduce indoor temperature enough to minimize the overheating hours.

The third scenario, CS2, refers to a hybrid system. Here the adaptive natural ventilation system is combined with the active cooling. Therefore, this scenario is used to explore if the adaptive ventilation system can reduce the cooling demand to the reference case CS0. Figure 9.6 provides a schematic overview of the three case study scenarios, showing the difference between the reference, adaptive ventilation and hybrid configuration.

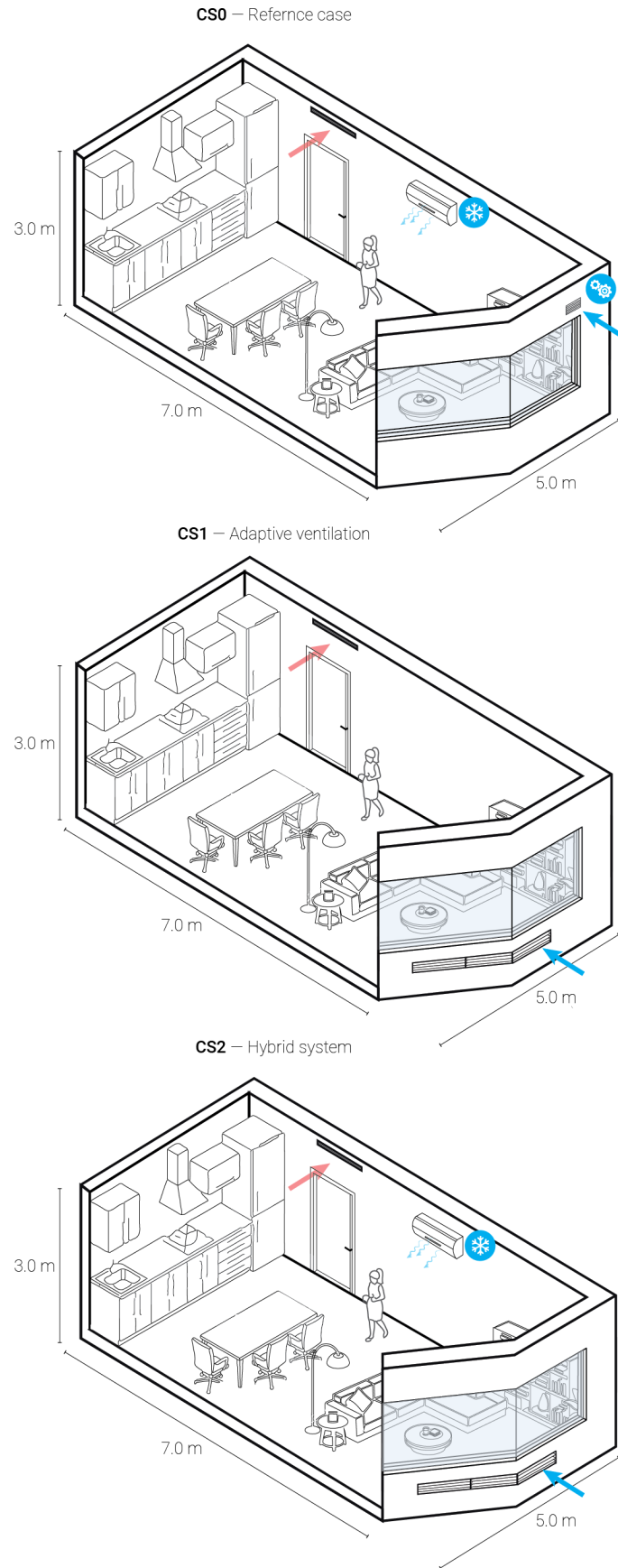


Figure 9.6
Schematic overview of the case study simulation scenarios.

Table 9.5*Case Study Simulation Scenarios*

Scenario	Natural ventilation	Active cooling	Purpose
CS0	No	Yes	Reference case based on original VENTT principle
CS1	Yes	No	Evaluate passive ventilation without active cooling
CS2	Yes	Yes	Evaluate cooling demand reduction in hybrid configuration

Performance indicators for these scenarios are in line with the performance indicators in Section 9.2.4. So, the performance indicators used for the case study are operative temperature, hours above 24°C, cooling demand, and ventilation rate.

9.5 Conclusion

This chapter defined the simulation approach what is used to evaluate the design impact of the adaptive ventilation component. The SMA-driven ventilation system was simplified into a temperature-based control logic for natural ventilation in DesignBuilder.

The evaluation was structured in two steps: first through a reference room and then through the Hartje Noord case study. For both models, different scenarios were defined to compare the influence of the adaptive ventilation strategy on operative temperature, ventilation performance and cooling demand. The simulation setup presented in this chapter forms the basis for the performance results discussed in Chapter 10.

10. Simulation Results

This chapter shows the results of the performance simulations. The aim of this chapter is to present and compare the outputs of the simulations. First, the setpoint sensitivity analysis is presented to determine the temperature threshold used in the simulations. After this, the results of the reference room are discussed, including the scenario comparison, detailed summer week and winter period check. Finally, the results of the Hartje Noord case study are presented, focusing on indoor temperature, ventilation performance and cooling demand.

10.1 Setpoint Sensitivity Analysis

In this section, the results of setpoint analysis will be presented. The analysis was performed to investigate the impact of using different temperature setpoints for the control logic of the adaptive ventilation system. The setpoint was for both the indoor temperature as outside temperature conditions. This means that ventilation is allowed when the indoor is above this setpoint and when the outdoor temperature is below this same threshold. Otherwise, the system remains closed.

The setpoint sensitivity analysis was performed for the two-sided ventilation configuration. The simulations period was selected from 1 April till 30 September. Which results in 4392 hours of the total simulation time. The performance indicator for comparing the results of the simulations is the number of hours that are not comfortable. This according to the Simple ASHRAE 55-2004 comfort model. To allow comparison of various thresholds, percentage of not comfortable hours was calculated with Equation 10.1.

Equation 10.1

$$\% \text{ not comfortable} = \frac{\text{time not comfortable}}{\text{hours simulated}} \times 100$$

Five different temperature setpoints were tested. Namely, 21°C, 22°C, 23°C, 24°C and 25°C. The results are presented in Table 10.1 and visualised in Figure 10.1.

Table 10.1
Setpoint Sensitivity Results

Temperature threshold	Time not comfortable	Hours simulated	Not comfortable
21°C	350 h	4392 h	8.0%
22°C	326 h	4392 h	7.4%
23°C	317.5 h	4392 h	7.2%
24°C	312.5 h	4392 h	7.1%
25°C	512 h	4392 h	11.7%

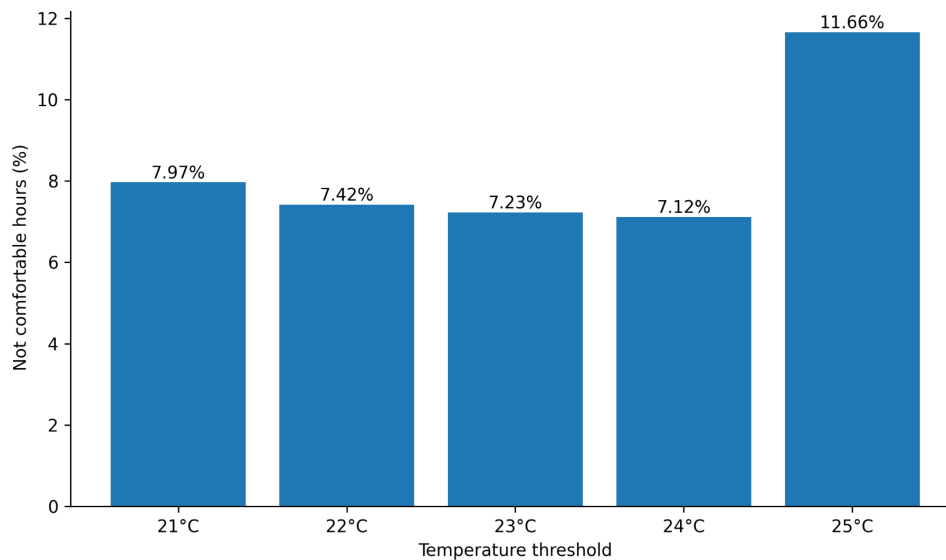


Figure 10.1
Percentage of not comfortable hours for different temperature thresholds.

Within the testes range of 21 till 25 degrees, the 24 degrees threshold gives the lowest not comfortable hours. The threshold with 24 degrees has 313 hours of not comfortable. Which is equal to 7.1% of the entire simulation period from 1 April till 30 September. Therefore, this value will be used for the simulations of the reference room and the case study.

10.2 Reference Room

This section presents the simulation results for the standard reference room. The results compare the closed façade scenario with the one-sided and two-sided adaptive ventilation configurations. The comparison is used to evaluate the effect of the proposed ventilation component on operative temperature, hours above 24°C and air change rate during the summer period. A detailed summer week and a winter period check are included to further analyse the operating behaviour of the system.

10.2.1 Scenario Comparison

This section provides simulation results of the three different scenarios, S0, S1, and S2. The selected threshold is based on the setpoint sensitivity analyse in the previous section. Resulting that the system operates with the threshold of 24 degrees. All the scenarios are simulated for the full summer, ranging from 1 April to 30 September. Which is equal to 4392 simulated hours. Results will be compared according to the operative temperature, the number of hours above 24 degrees, and air change rate.

Overall Summer Performance

The different scenarios, as described in the methodology, are compared over the full summer. This provides an overall indication on the influence of the adaptive natural ventilation system on the indoor thermal conditions. Table 10.2 shows the main performance indicators for the three scenarios. Including, the main operative temperature, maximum operative temperature, total hours exceeding 24°C, average air change rate, and maximum air change rate.

Table 10.2
Simulation Results for The Full Summer Period

Scenario	Mean operative temp [°C]	Max operative temp [°C]	Hours > 24°C [h]	Mean ACH [ac/h]	Max ACH [ac/h]
S0 (Closed façade)	27.7	40.4	3458	0.0	0.00
S1 (one-side ventilation)	24.0	36.9	1841	1.0	4.2
S2 (two-sided ventilation)	21.8	33.8	422	3.2	27.9

First, scenario S0, has the highest mean operative temperature of 27.7 °C with 3458 hours above 24°C. This compared to the other scenarios, S1 and S2. This result that in the absence of ventilation the room temperature exceeds the set temperature threshold for most of the summer period. The highest operative temperature recorded is 40.4 °C, showing that indoor peaks are high in the reference case.

Secondly, scenario S1, here there is one-sided ventilation. Where the operative temperature reduces to 24.0°C. Whereas the hours above 24 °C reduce to 1841 hours. This indicates that the one-sided ventilation strategy lowers the overall indoor temperature, compared to S0. However, there is still a considerable number of hours the temperature is above the temperature threshold. Therefore, one-sided ventilation does not fully prevent high indoor temperatures during the summer.

Lastly, scenario S2, with two-sided ventilation. What demonstrates the lowest mean operative temperature off all three scenarios. With an average main operative temperature of 21.8 °C. The number of hours when the temperature exceeds 24°C is decreased up to 422 hours. Furthermore, the maximum operative temperature reduces to 33.8°C. It can be suggested that the effect of two-sided ventilation on the indoor air climate has a stronger influence, compared to the S0 and S1 configurations. An increase in the mean air change rate from 1.0 ac/h in S1 to 3.2 ac/h in S2 corresponds with this decrease in the operative temperature and the number of hours exceeding the threshold of 24°C.

The lower performance of S1 does not mean that one-sided ventilation is unsuitable. However, with the same number of adaptive ventilation components, the one-sided configuration provides lower air change rates than the two-sided configuration. To achieve a comparable cooling effect, one-sided ventilation would require a larger effective opening area and therefore more façade-integrated components, as indicated by the opening area estimation in Appendix B.

The maximum air change rate in S2 is 27.9 ac/h. This value is significantly higher compared to the maximum air change rate in S1. It indicates that there are short intervals with high airflow rates with two-sided ventilation. These intervals could be caused by certain outdoor conditions or by night ventilation. The timing of these peaks will be analysed in more detail in Section 10.2.2.

Daily Operative Temperature

For further analysis of the development of the temperature over the entire summer period, a comparison is made of daily average operative temperatures for all three cases. Figure 10.2 shows the daily mean operative temperature from 1 April to 30 September for scenarios, S0, S1, and S2.

There is a clear difference in the daily mean operative temperature between the three scenarios. The S0 scenario has a higher daily mean operative temperature than the other two throughout the summer period.

This implies that the two methods of ventilation decrease the indoor temperature in comparison to the closed façade. Scenario S2 shows the greatest reduction in daily mean operative temperature then that of the scenarios S0 and S1 for most of the time simulated. This is consistent with the higher mean air change rate showed by Scenario 2 in Table 10.2. The difference is clearly noticeable during the warmest days. Because the daily mean operative temperature in S0 increases more heavily.

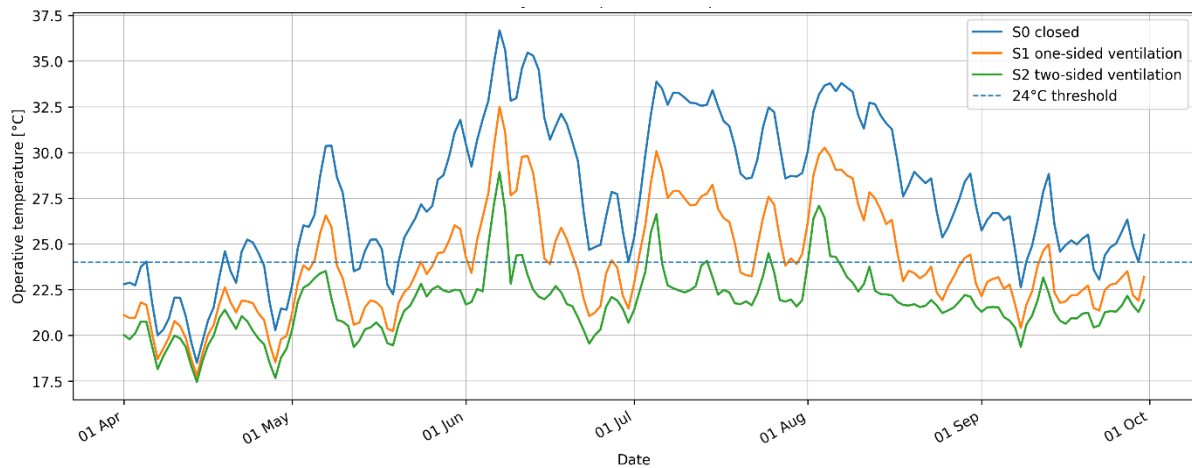


Figure 10.2
Daily mean operative temperature for S0, S1, and S2 during the full summer period.

In addition to the daily mean operative temperature, the daily maximum operative temperature is presented in Figure 10.3 This figure provides an overview of the maximum operative temperature achieved every day and how effective the implemented ventilation techniques are in reducing the indoor temperature and its peaks.

The daily maximum operative temperature has a very similar behaviour pattern to the daily average operative temperature. In the case of S0, maximum daily temperatures are higher, compared to S1 and S2. The reduction in temperature peak is the greatest for S2. Here the maximum operative temperatures are on average lower at warm periods. Nevertheless, maximum temperatures remain high regardless of the scenario. It indicates that natural ventilation can decrease the indoor temperature but cannot fully avoid maximum indoor temperature peaks even at the hottest summer days.

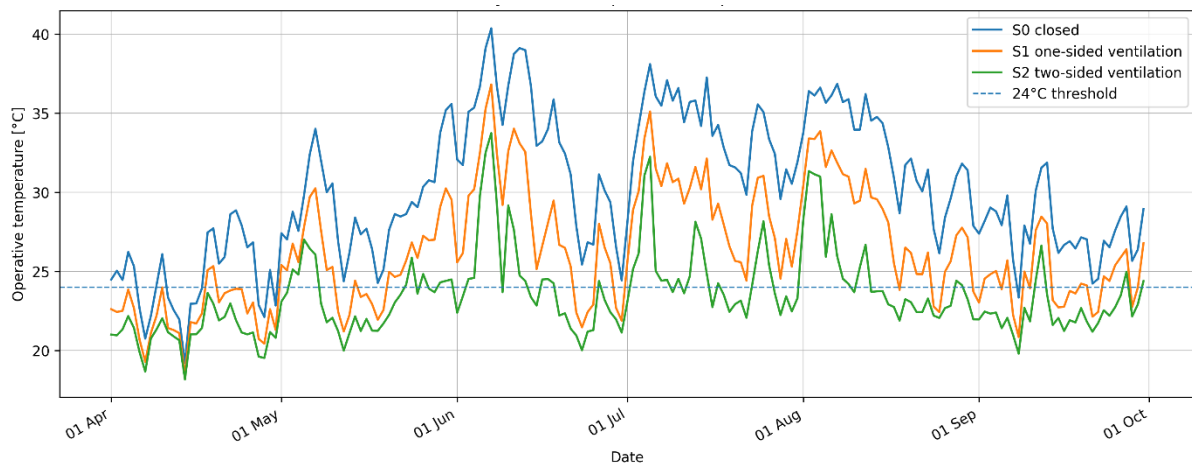


Figure 10.3
Daily maximum operative temperature for S0, S1, and S2 during the full summer period.

Daily Hours Above 24 °C

The daily hours above 24°C is presented in Figure 10.4. The parameter is used to indicate the frequency and duration of exceeding the indoor temperature relative to the control threshold of 24°C in summertime. There is a considerable increase in the daily number of hours above 24 °C in S0 compared to S1 and S2. In S0, the operative temperature often rises above 24 °C for much of the day. This coincides with the high total number of exceedance hours as seen in Table 10.2. The daily number of hours above 24 °C in S1 is less compared to S0, but excesses still happen quite often during the whole summer season. The lowest exceedance hours are in S2, meaning that two-sided ventilation is more successful in reducing indoor temperatures above the chosen threshold.

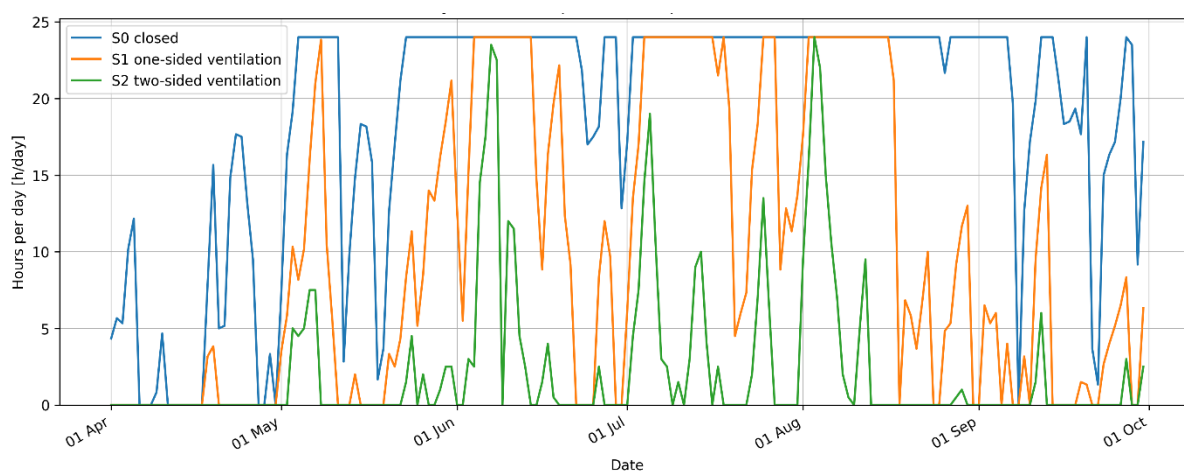


Figure 10.4

Daily hours above 24 °C for S0, S1, and S2 during the full summer period.

Daily Air Change Rate

Daily mean air change rate is illustrated in Figure 10.5. As mentioned before, since S0 has no adaptive ventilation openings, the air change rate will be zero for this case. Thus, the graph only illustrates the air change rates in S1 and S2.

In general, daily mean air change rate is higher in S2 than in S1 throughout most of the simulation time period. This follows from the fact that two-sided ventilation has higher airflow rates than one-sided ventilation due to openings on both sides of the room. Increased air change rates in S2 correlate with decreased operative temperature and less hours above 24 °C presented in previous sections. In the S2 scenario there are some days with a high increase in ventilation rates. These peaks can cause discomfort what will be analysed in more detail in section 10.2.2.

In general, based on the analysis of the summer season, both one-sided and two-sided ventilation has a decrease in the operative temperature and hours above 24°C when compared to the closed façade case. The most efficient reduction in terms of operative temperature and hours exceeding is seen in S2. Where two-sided ventilation gives the lowest average operative temperature and exceedance hours. Furthermore, the daily average air change rate for S2 gives higher ventilation rates compared to S1. Nevertheless, the maximum air change rate is frequently higher than the average value of S2. This indicates that there are short periods with a very high airflow. Therefore, these peaks will be analysed in the next section.

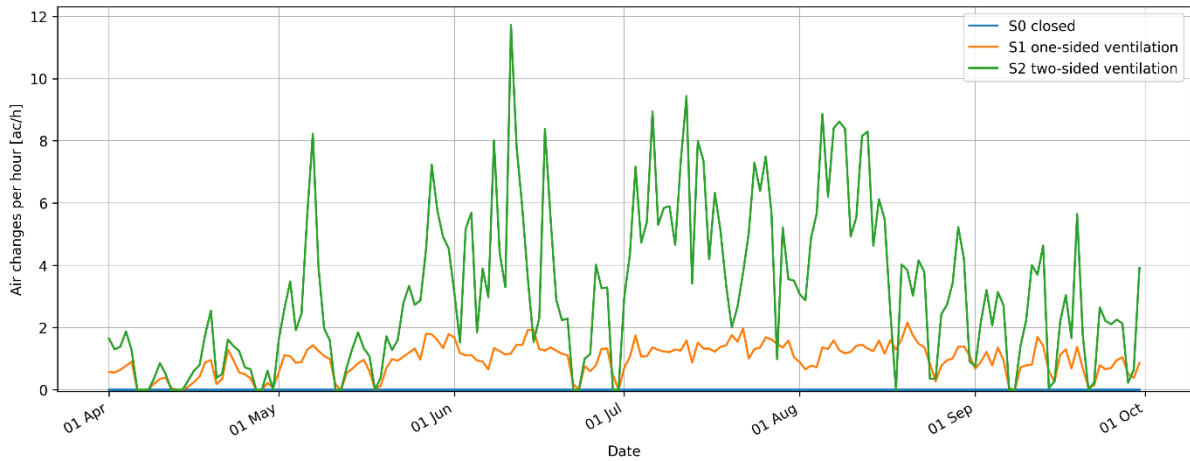


Figure 10.5
Daily mean air change rate for S1 and S2 during the full summer period.

10.2.2 High Air Change Rates Peaks

The results from the full summer season indicate that S2 achieves a peak air change rate of 27.9 ac/h. These high airflow peaks are likely related to short moments with stronger pressure differences across the openings. Since the calculated natural ventilation model is driven by wind pressure and temperature differences. Periods with higher wind speeds can result in temporary high air change rates. As this is much higher than the peak air change rate in S1, the occurrence of high air change rates is further analysed. This to see whether such peaks occur during the night, when they can play a role in night cooling. Or during the occupied periods when they would affect occupant comfort. Figure 10.6 shows the occupied and unoccupied periods according to the DesignBuilder occupancy schedule for an office building. Timesteps that had the occupancy great than zero were considered as occupied. While timesteps having an occupancy equal to zero were considered unoccupied. According to this schedule the office room will be occupied from approximately 05:00 till 19:00.

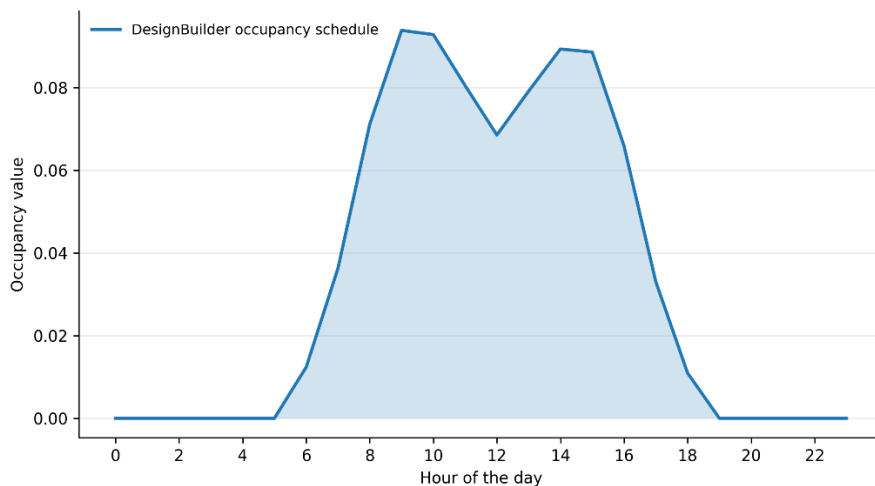


Figure 10.6
DesignBuilder occupancy schedule for an office.

Figure 10.7 shows the air exchange rate in S2 during the summer. To detect periods where the airflow rates are abnormally high, a percentile-based threshold was applied. So, the 95th percentile of the air change rate in the S2 simulations during the entire summer period was determined, see the dashed line

in Figure 10.7. This implies that 95% of all air change rate values fall below the threshold. While in the meanwhile the remaining 5% fall above it. The value of the 95th percentile of the air change rate in S2 is 11.8 ac/h. This threshold is not a comfort indicator but to identify the extreme high peaks of airflow events in de time simulated.

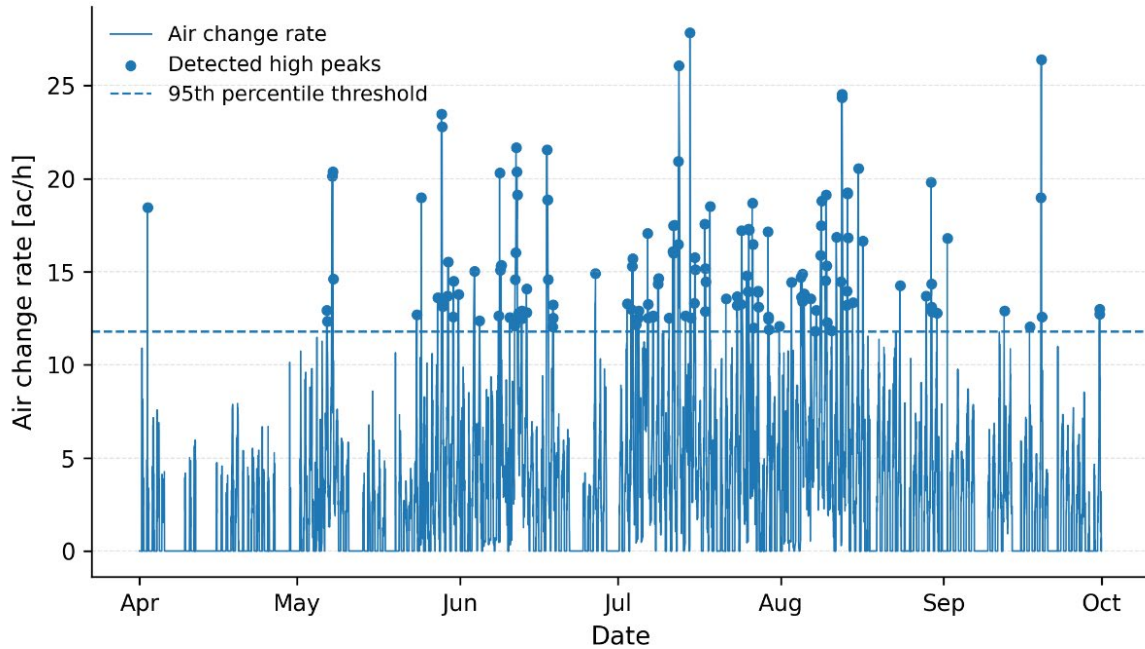


Figure 10.7

Air change rate in S2 during the full summer period with detected high peaks.

This analysis has been done by comparing the occurrence of these peaks with the occupancy schedule. Table 10.3 summarises the detected high air rates peaks in S2 and illustrates how these peaks behave between occupied and unoccupied periods. According to Table 10.3, there were 144 peaks where the air change rate was high. This according to the 5% highest peaks during the full summer period. Of all these peaks, 109 were during occupied periods while 35 during unoccupied time. This implies that 75.7% of the air changes per hour peaks were recorded during occupied time. Figure 10.8 shows the distribution of air changes per hour peaks between occupied and unoccupied time. So, the higher percentage of air changes per hour peaks occurs during occupied time. In case the maximum rates of airflow happened during nighttime or unoccupied hours, they would mainly contribute to night cooling without influencing the occupant's comfort. However, since most of the peaks happen during occupied hours, it can cause discomfort through draughts. This must be considered as a comfort limitation in the further design development of the ventilation system.

After investigating the total summer performance and the occurrence of high air change rate peaks, the next section is an analysis during a week of the warmest part of the summer. The goal is to examine the interaction between outdoor temperature and operative temperature. Furthermore, to get a detailed analysis of the ventilation behaviour during the peak temperatures in the summer.

Table 10.3
Summary of Detected High Air Change Rate Peaks in S2

Indicator	Value
Peak detection threshold	11.8 ac/h
Total detected high ACH peaks	144
Peaks during occupied periods	109
Peaks during unoccupied periods	35
Share during occupied periods	75.7%
Maximum ACH	27.9 ac/h

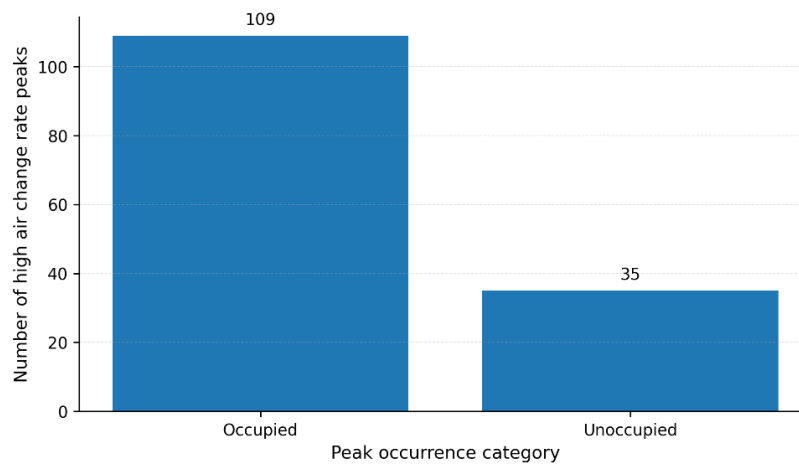


Figure 10.8
Occurrence of high air change rate peaks in S2 during occupied and unoccupied periods.

10.2.3 Detailed Summer Week

In this section a detailed analysis of a selected warm summer week during the summer period is provided. In this section an analysis of the hourly behaviour of the indoor operative temperature and air change rate is presented. The objective of this analysis is to gain a deeper insight into the performance of the ventilation strategies under warm outdoor weather and the response of the ventilation system to daily temperature variations.

Selection of Warmest Summer Week

In case of the detailed summer period, there must be a selection when this warmest summer week occurs. Based on the data retrieved from DesignBuilder, in the summer period from 1 April till 30 September, the warmest 7-day period in the simulation is from 1 till 7 August (see Figure 10.9). This period was selected on the outdoor dry-bulb temperature. As it represents the warmest 7-day period according to the highest average outdoor temperature for seven continuous days during the full summer simulation. With a mean outdoor temperature of 21.2 °C. While the maximum outdoor temperature is 30.5 °C.

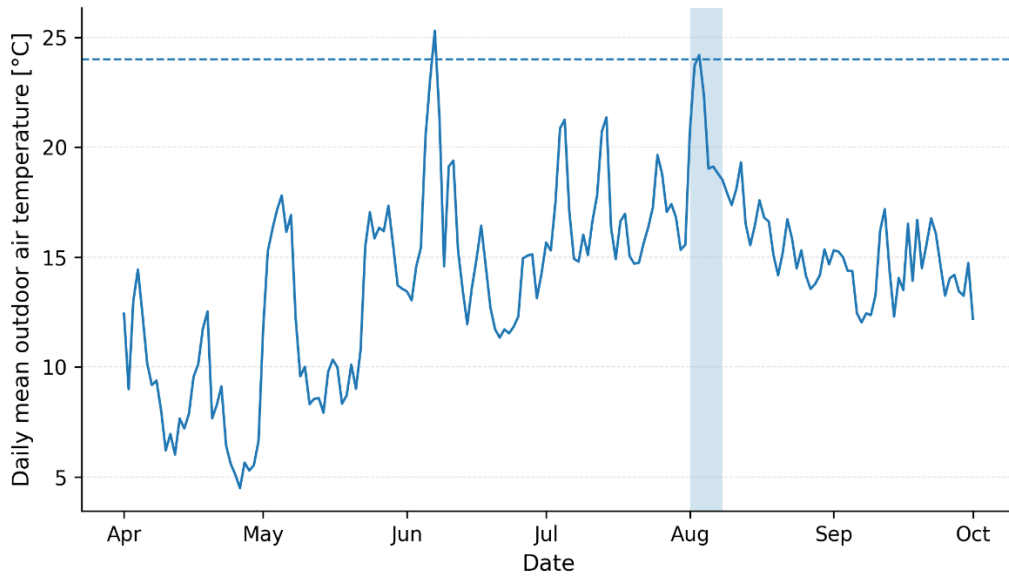


Figure 10.9

Daily mean outdoor air temperature during the full summer period, with the selected warm period highlighted.

How the temperature is fluctuating during this week, from 1 till 7 August is shown in Figure 10.10. With a mean outdoor temperature of 21.2 °C. While the maximum outdoor temperature is reaching its peak at 30.5 °C. During the night, considered from 20:00 till 06:00, the outdoor air temperature drops to a mean temperature of 18.7°C. What makes it sufficient for night cooling through natural ventilation.

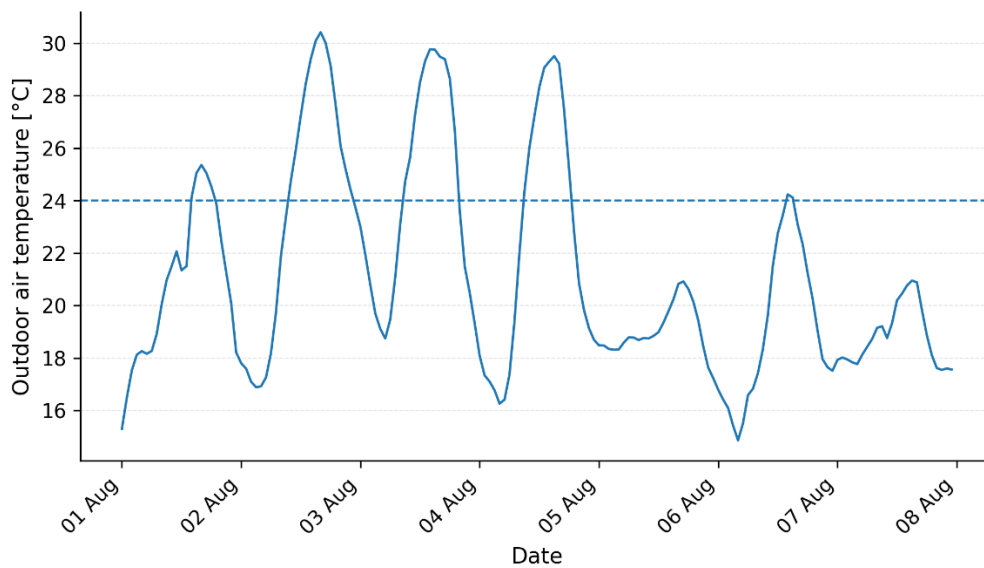


Figure 10.10

Hourly outdoor temperature for selected warmest summer week (1 to 7 August).

Performance During the Selected Summer Week

Table 10.4 shows the main performance indicators for the selected summer week for the three scenarios, S0, S1, and S2. From the table it becomes clear that S0 has the highest mean operative temperature during the selected week, with 32.9 °C. This is reasonable because there is no passive or active cooling. Furthermore, scenario S0 has 168 hours exceeding the threshold of 24°C.

In the S1 scenario, the mean operative temperature is reduced compared to S0, reaching 29.0°C. nevertheless, the numbers of hours above 24°C remains high, with 162 hours. Therefore, one-sided ventilation lowers indoor temperature level. But does not help to significantly decrease time when the temperature is exceeding.

Scenario S2 shows the lowest operative temperature among all the other scenarios. With a mean operative temperature of 25.2 °C. The hours with an air temperature above 24°C is decreased to 104 hours. The air change rate of S2 is 5.7 ac/h, while that in S1 was 1.0 ac/h. This corresponds with the lower operative temperatures observed in the S2 scenario.

Table 10.4
Simulation Results for the Selected Summer Week

Scenario	Mean operative temp [°C]	Max operative temp [°C]	Hours > 24°C [h]	Mean ACH [ac/h]	Max ACH [ac/h]
S0	32.9	36.8	168	0.0	0.0
S1	29.0	33.8	162	1.0	2.1
S2	25.2	31.3	104	5.7	14.9

Hourly Operative Temperature

The hourly operative temperature during the selected summer week for the scenarios S0, S1, S2 is presented in Figure 10.11. The sensitivity setpoint of 24°C is used as limit to identify where the operative temperature is exceeding the threshold.

The hourly temperature development indicates that S0 is always above the threshold limit of 24 °C in the selected week. While comparing S1 with S0, the operative temperature is below that of S0. Nevertheless, it is still above the 24 °C. S2 experiences the highest reduction in operative temperature during the week. This occurs mostly when the ventilation system is active. However, the operative temperature in the S2 scenario also remains most of the time above the threshold. What is negatively for the occupant’s comfort.

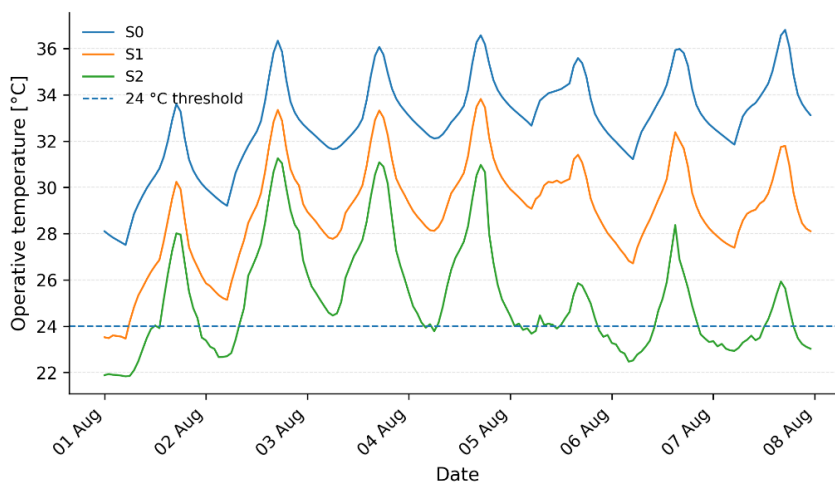


Figure 10.11
Hourly operative temperature for S0, S1, and S2 during the selected summer week.

Hourly Air Change Rate

The hourly air change rate of S1 and S2 is presented in Figure 10.12 for the selected summer week. Since the S0 scenario is a closed façade there is not an air change rate, and therefore not plotted in Figure 10.12. The figure shows when the ventilation system is active and what the air change rate per hour is, this compared for one-sided ventilation, S1, and two-sided ventilation, S2. The figure makes clear that the hourly air change rate is extremely higher in Scenario S2 compared to S1. This is related to the two-sided ventilation configuration. Where opposite openings in the façade increase the airflow. In the S1 scenario, the air change rate is relatively low. Which related to the higher operative temperatures, which is discussed in the previous section.

In the S2 scenario, there is more variation in the hourly air change rate. These high air change rates occurred during particular periods of time. These high air flow rates are in relation with the stronger reduction in operative temperature compared to S0, and S1. The time these high peaks occur must be investigated as they can cause discomfort during occupant hours. This is discussed in the next section.

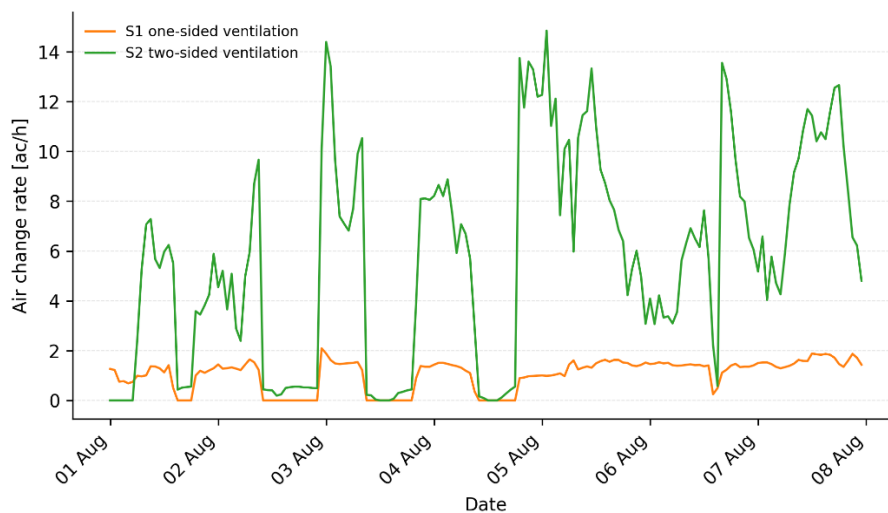


Figure 10.12
Hourly air change rate for S1 and S2 during the selected summer week.

Interactions Between Outdoor Temperature, Ventilation and Night Cooling

In order to analyse the cooling capability of natural ventilation during the warmest summer week, the operative temperature of S2 is plotted against the outdoor air temperature. This section considers only scenario S2. Which show the interactions between the outdoor temperature, ventilation and night cooling during the selected summer. For this detailed analysis is only S2 used. Because S2 has a stronger decrease in operative temperature and a higher air changes rate then S0 and S1. Furthermore, S0 has no adaptive ventilation, while in S1 the airflow rates are relatively low. Therefore, S2 is the most appropriate scenario for analysing the performance of ventilation depending on outdoor temperature.

Figure 10.13 presents the S2 operative temperature, outdoor air temperature and air change rate during the selected summer week. The grey shaded sections in the figure correspond to night-time periods from 20:00 to 06:00. The aim of this Figure is to analyse whether the ventilation system operates at night-time and whether this helps to achieve night cooling.

The grey intervals in Figure 10.13 corresponds with the night. This indicate that the outdoor air temperature decreases during the evening and night periods. This provides an opportunity of night cooling. As cooler outdoor air could be used to reduce the indoor operative temperature. In some of these intervals the air change rate in scenario S2 increases. This is noticeable because the operative

temperature decreases or is more stable. So, night ventilation is sufficient in reducing the heat build-up during the day of the warm summer weeks. Furthermore, during the day the outdoor temperature reaches sometimes values higher than 24°C. Its cooling capacity is then not sufficient anymore to cool the indoor climate. This also explains why the operative temperature can remain above the thresholds during this warm summer week. This even during the S2 scenario with relatively high air change rates.

High ventilation rates take place during intervals and are followed by a decrease or stabilization of the operative temperature. When there is no ventilation, the operative temperature rises. Thus, it can be indicated that the impact of the ventilation strategy is not only dependent on the airflow rate but also on the outdoor temperature levels. Moreover, ventilation occurs not only during nighttime but also during daytime, when the temperature outside is higher, and thus cooling opportunity is lower. Still, this is only allowed when the outdoor temperature is below the threshold of 24 degrees. But is less efficient for cooling. This shows that the system allows night cooling but does not work only at night. Hence, additional control can be required to increase occupant’s comfort. Or an additional active cooling system, to cover the hours when the ventilation system is closed.

In summary, the analysis of the summer period shows that the effectiveness of two-sided ventilation is the most visible during the warmest week of the summer season. In addition, the efficiency of natural ventilation for cooling is highly dependent on the timing of efficient outdoor climate conditions. In particular, night ventilation plays an important role. This because due to low outdoor temperatures. Nevertheless, considering that ventilation not only occur at night, but also during the day, some additional regulation is necessary. Additional figures are provided in Appendix E. Showing the separate relationship between S2 operative temperature, outdoor temperature, air change rate, and occupancy.

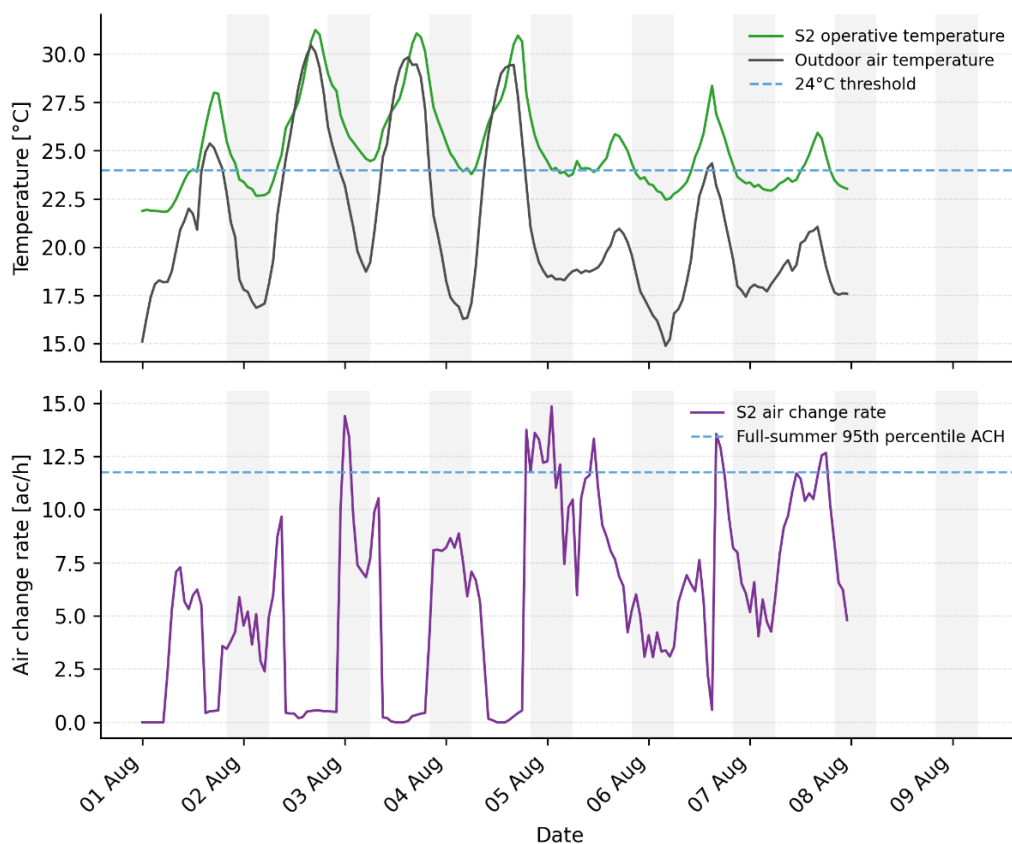


Figure 10.13

S2 operative temperature, outdoor air temperature, and air change rate during the selected summer week.

Note. Grey shaded areas indicate night-time periods, defined as 20:00 to 06:00.

10.2.4 Winter Period Check

The winter period check is simulated to determine whether the adaptive ventilation system remains closed during colder outdoor conditions in the winter. Because the control logic of the adaptive ventilation system only allows natural ventilation when the indoor operative temperature is above 24 °C and the outdoor temperature below this threshold is. Therefore, ventilation should only occur when the indoor temperature is exceeding the control threshold. Furthermore, in this simulation there is no active heating or cooling included. Therefore, the results of the indoor temperature should not be interpreted as a prediction of the indoor climate. Instead, the winter check is used to evaluate if the ventilation control logic keeps the adaptive system closed during the colder months. The winter simulation is ranging from 1 October to 31 March.

Figure 10.14 shows the daily operative temperature for the scenarios S1 and S2 for the winter season. The threshold of 24°C when the ventilation system must open or close is also plotted. The figure shows that the operative temperature does not exceed the 24°C during the winter season. This indicates that the indoor conditions are not warm enough to activate the ventilation system, based on the daily average basis.

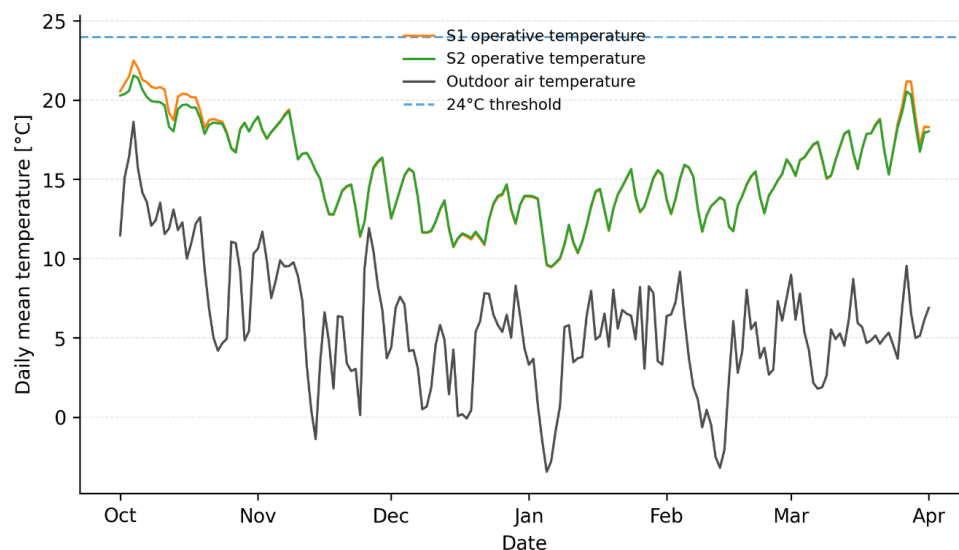


Figure 10.14

Daily mean operative temperature for S1 and S2 and daily mean outdoor air temperature during the winter period.

Furthermore, Figure 10.15 illustrates the daily maximum air change rate during the whole winter for S1 and S2. The figure shows that ventilation takes place only during the transition periods at the start and at the end of the winter simulation. The rest of the time, there is no air change rate. It means that the ventilation system operates in the closed mode in the middle of the winter season, when the operative temperature cannot activate the system.

The winter period check shows that the adaptive ventilation system remains closed the main part of the winter period. The daily mean operative temperature is below the 24 °C limit. While the air change rate remains almost at zero throughout the winter period. In this way the control strategy of the system helps avoid unnecessary natural ventilation in cold weather.

Nevertheless, some ventilation happens during the transition periods at both ends of the winter period. Thus, a winter override or the locked-closed state can be considered when designing the system. In this way, the system will stay completely closed during the winter when the heating system is on in the building. This override or locked-closed state will help reduce unnecessary air infiltration in winter and

improve the energy efficiency of the façade. Furthermore, since there was no active heating or cooling system used during the simulations, these results should mainly be interpreted as an indication of the control behaviour of the ventilation system. Rather than as a prediction of the winter indoor temperature.

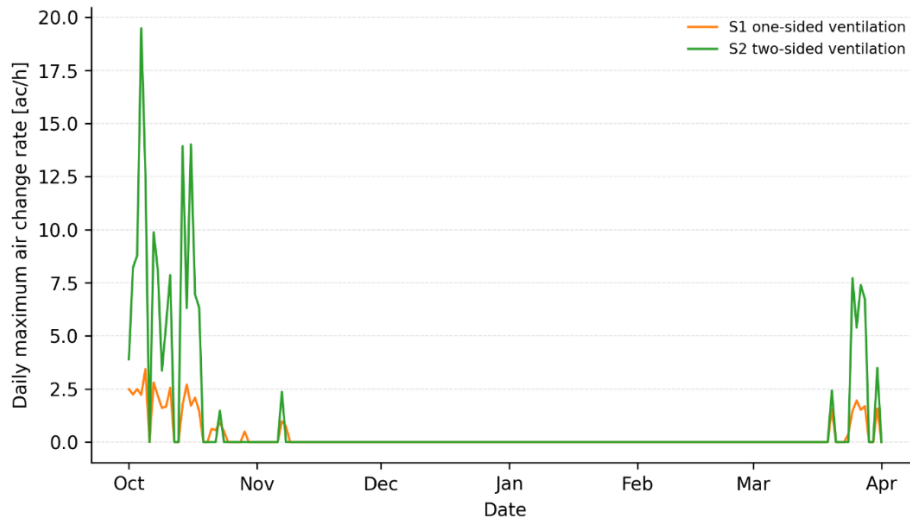


Figure 10.15
Daily maximum air change rate for S1 and S2 during the winter period.

10.3 Case Study

This section presents the results of the simulation of the case study of Hartje Noord. Firstly, the reference model will be verified by comparing the reference model results with the Vabi results. Then, the three different case study scenarios, CS0, CS1, and CS2, will be compared for the entire duration of the summer. This is done based on operative temperature, ventilation rate, and high-airflow occurrence. From there the cooling demand reduction will be determined. Finally, there will be a detailed summer week provided. To analyse when the adaptive ventilation system operates.

10.3.1 Model Verification with Vabi Results

To validate the model made in DesignBuilder, the CS0 scenario, was compared to the Vabi simulation results of a full year. With the goals to verify whether the reference model gives an adequate representation of the apartment in its original conditions. Since only the living room is modelled in DesignBuilder, the comparison is also only applied on the living room data available.

The scenario CS0 is the most representative to the original VENTT principle, as it includes mechanical ventilation and air conditioning. According to the Vabi model, the cooling load for the living room is 659 kWh. The scenario CS0 resulted in a cooling demand of approximately 716 kWh over the whole year for the living room. That means that the design builder's estimate is 8.7% higher than the Vabi simulation. Furthermore, the maximum temperature during CS0 is a little bit higher than the comfort temperature in the Vabi results, while the total cooling demand is within acceptable levels. The comparison between the Vabi results and the simulations in DesignBuilder for the CS0 scenario are summarised in Table 10.5.

Table 10.5*Model verification between Vabi and CS0 DesignBuilder results of a Full Year*

Indicator	Vabi result	CS0 DesignBuilder result	Difference
Cooling demand	659 kWh	716 kWh	+8.7%
Maximum comfort / operative temperature	27.6°C	28.9°C	+1.3°C
Mechanical ventilation rate	48 m ³ /h \approx 1.0 ac/h	1.0 ac/h	Similar

The comparison illustrates that the CS0 scenario is not perfectly the same as the Vabi model. But for the purpose of the research, the difference in cooling demand is sufficient close enough. Therefore, CS0 will be used as the baseline scenario when evaluating the impact of the adaptive ventilation system. This model verification is mainly used to check the reliability for the comparison between the scenarios CS0, CS1, and CS2. Rather than fully calibrate the DesignBuilder model to the Vabi results. In the next section the different scenarios will be compared.

10.3.2 Scenario Comparison

This section compares the overall summer performance of the three case study scenarios. All scenarios are simulated for the full summer period, from 1 April to 30 September, which equals 4392 simulated hours. The comparison focuses on operative temperature, hours above 24°C and air change rate. In this way, the effect of passive adaptive ventilation and the hybrid ventilation strategy can be evaluated against the reference scenario with mechanical ventilation and active cooling.

Daily Operative Temperature

Table 10.6 shows the main results temperature-related of the three scenarios of the case study. The mean operative temperature in CS0 is equal to 24.0°C while the maximum operative temperature is 28.9°C. In CS1, the mean operative temperature is slightly increased to 24.2°C while the maximum operative temperature is highly increased up to 39.8°C. Consequently, it can be said that the adaptive natural ventilation system is unable to avoid overheating in hot periods. As there is no active cooling available.

The average operative temperature for CS2 is 24.0°C. Nevertheless, the maximum operative temperature is still greater than the corresponding value in CS0. This with a maximum value for the operative temperature of 34.7°C. While scenario CS1 experiences fewer hours when the temperature exceeds the 24°C compared to the CS2 scenario, the maximum operative temperature of CS1 is much higher. Therefore, the number of hours above 24°C alone does not fully represent the overheating in buildings. Furthermore, the hybrid system is able to decrease the period when the temperature is above 24°C. but cannot completely prevent high temperature peaks.

Table 10.6*Case Study Scenario Comparison for the Full Summer Period*

Scenario	Mean operative temperature [°C]	Max operative temperature [°C]	Hours > 24°C
CS0	24.0	28.9	2544
CS1	24.2	39.8	1948
CS2	24.0	34.7	2007

Figure 10.16 shows the average daily operative temperature throughout the full summer period. The differences between the scenarios are the most visible during the warmer periods. Furthermore, as could be expected, CS1 provides the highest temperature because there is no active cooling. The temperature peaks are decreased in CS2, where there is a hybrid system, compared to CS1.

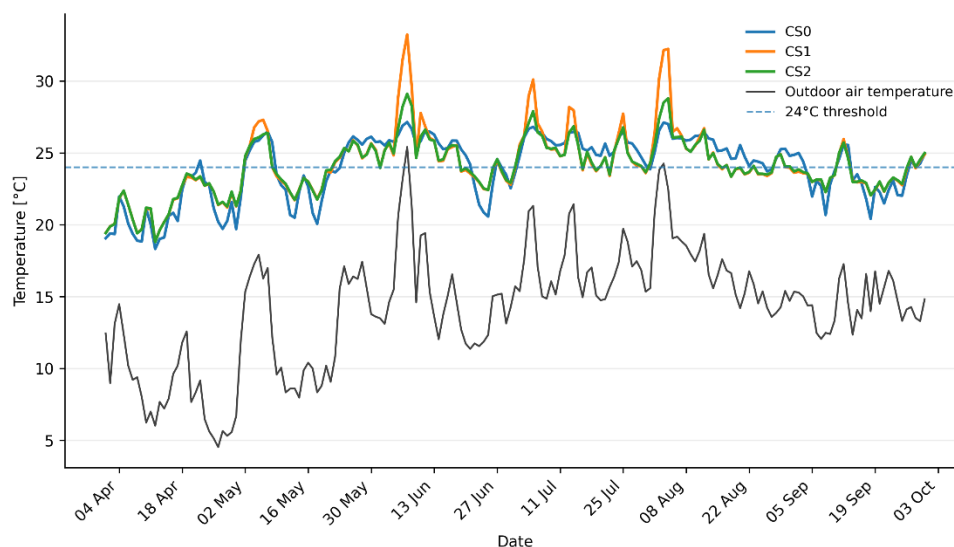


Figure 10.16
Daily mean operative temperature during the summer period.

Daily Air Change Rate

This section will discuss the daily mean air change rate during the full summer period, illustrated in Figure 10.17. This figure shows the main air change rate for both cases CS1 and CS2. The dashed line in blue illustrates the mechanical ventilation setpoint of 1.0 ac/h in CS0.

The figure shows that both adaptive ventilation scenarios CS1 and CS2 have higher levels of air change rates in comparison to the reference case, CS0, with mechanical ventilation. Moreover, there is a significant variation in airflow rates through the whole summer period. This behaviour is expected, since the adaptive ventilation system depends on climate parameters, indoor operative temperature, and pressure differences. Therefore, the air change rate varies with time. Furthermore, there are similar patterns in airflow for both CS1 and CS2. However, CS1 reaches a little higher air change rate in comparison to CS2.

While Figure 10.17 provides an overview over the whole summer performance of the adaptive ventilation system. The daily average data of the air change rate hide any possible short-term variations in the airflow. Therefore, a more detailed analyses on the warmest week during the summer periods must be provide. This can better illustrate the opening and closing behaviour of the adaptive ventilation system.

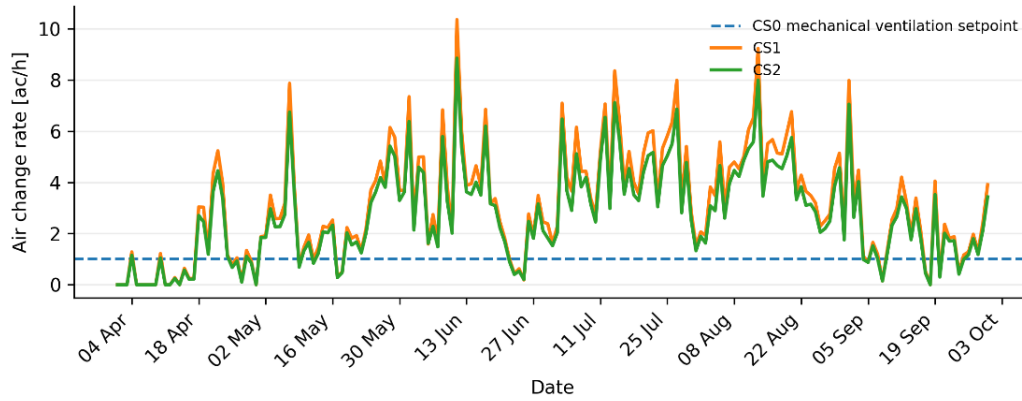


Figure 10.17
Daily mean air change rate during the summer period.

10.3.3 High Air Change Rate Peaks in CS2

This section will focus on the occurrence of high peaks of air change rates in CS2 for the full summer. The CS2 scenario was selected for this analysis because it presents the most relevant scenario of the adaptive ventilation system. Furthermore, it is relevant to investigate whether the high air change rates happen during occupied hours or unoccupied hours. When these peaks occur during unoccupied hours this do not affect comfort and contribute to passive cooling. However, in case these peaks happen during occupied periods of time, it might cause some discomfort due to air movements inside the room or even draught.

The occupied and unoccupied periods were divided according to the DesignBuilder occupancy schedule for a living room. Timesteps that had the occupancy great than zero were considered as occupied. While timesteps having an occupancy equal to zero were considered unoccupied. According to this schedule, the living room is mostly occupied in the afternoon and in the evening. This is approximately between 15:00 and 22:00, as summarized in Figure 10.18.

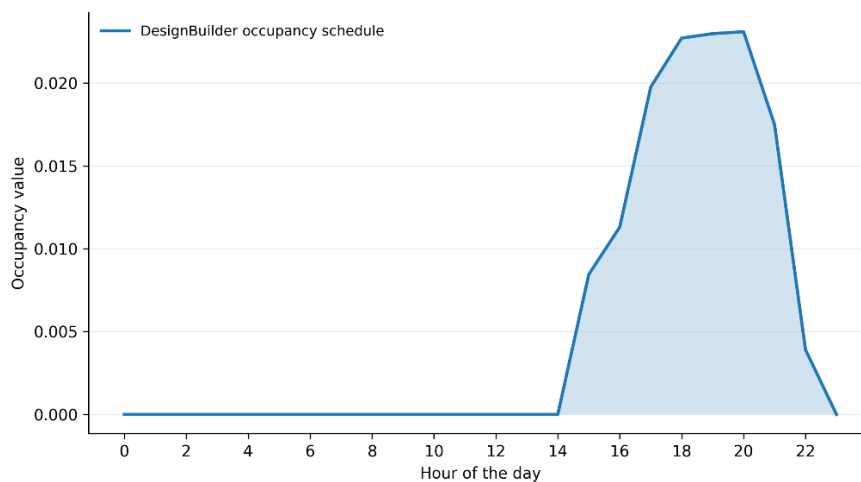


Figure 10.18
DesignBuilder occupancy schedule for a living room.

To identify when high airflow periods occur a percentile threshold was used. So, 95th percentile of the air change rate was determined for the full summer season. This indicates the top 5% air change rate values were considered as high peaks. This is similar as section 10.2.2, where also the high air change rates were discussed for the standard room. For CS2, the 95th percentile threshold is 14.6 ac/h. The air

change rate reaches its maximum at 39.5 ac/h. Figure 10.19 demonstrates the air change rate for the entire summer period with high peaks that are exceeding the threshold of 95th percentile.

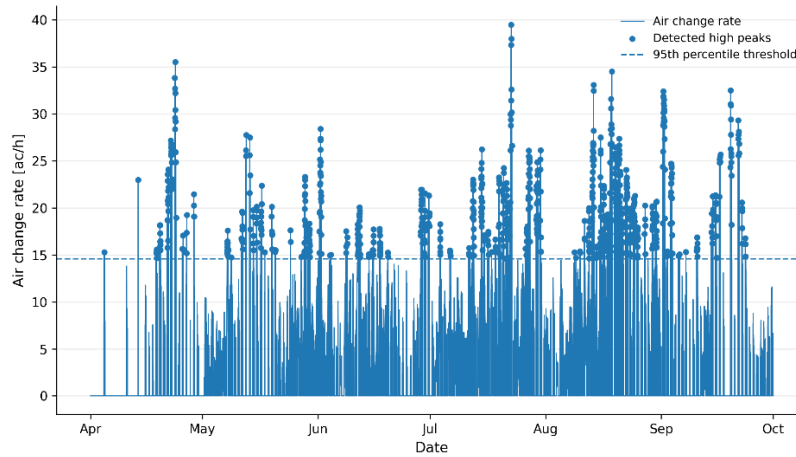


Figure 10.19
Detected high ACH peaks in CS2.

Table 10.7 provides an overview of high air change rate peaks found in scenario CS2. The results show 870 detected high ACH peaks. Out of these 870 peaks, 467 peaks were recorded during occupied periods and 403 peaks during unoccupied periods. Therefore, the percentage of high air change rate peaks during occupied periods is 53.7% of all the high peaks.

Table 10.7
Summary of Detected High Air Change Rate Peaks in CS2

Indicator	Value
95th percentile threshold	14.6 ac/h
Total detected high ACH peaks	870
Peaks during occupied hours	467
Peaks during unoccupied hours	403
Share during occupied hours	53.7%
Share during unoccupied hours	46.3%
Maximum ACH	39.5 ac/h

Figure 10.20 illustrates the distribution of the high air change rate peaks during occupied and unoccupied periods. The Figure indicates that the presence of the high peak is not only during unoccupied periods. A slightly higher frequency was found during occupied hours. These high air flow rates could possibly influence occupant's comfort.

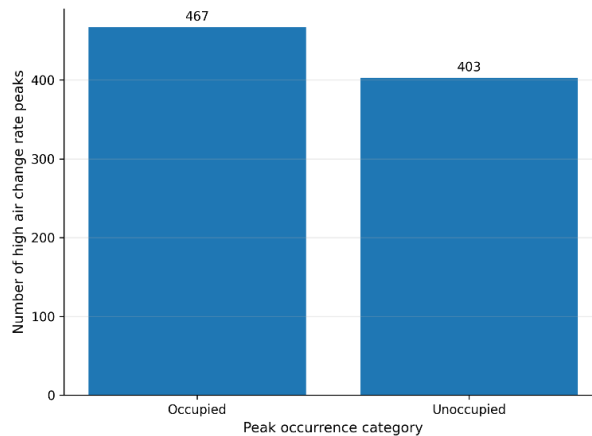


Figure 10.20
CS2 occupied vs unoccupied high ACH peaks.

Compared to the reference room, the case study shows higher air change rate peaks. Nevertheless, S1 had fewer adaptive ventilation components integrated in the façade compared to CS2. In S2, six components resulted in a maximum air change rate of 27.9 ac/h, while in CS2, three components resulted in a maximum air change rate of 39.5 ac/h. This indicates that the airflow is not only determined by the number of components or the opening area, but also by the building context. The apartment is located on the 11th floor, where higher wind speeds and wind-induced pressure differences can occur. This likely contributes to the higher airflow rates through the adaptive ventilation openings.

A self-regulating grille could be added at the outside inlet, before the SMA-driven lamellas. The lamellas would still control opening and closing based on temperature, while the grille would limit the effective free aperture during high wind pressure. This could reduce excessive airflow and draught risk while keeping the system passive.

To summarize, the results of the high air change rate peaks shows that the passive adaptive ventilation system can create strong airflow events in scenario CS2. Since more than half of these peaks occur during occupied time, careful design development must take into account the possibilities of draught.

10.3.4 Cooling Demand

This section provides an evaluation of the decrease in cooling demand resulting from the hybrid adaptive ventilation comparison. Since CS1 does not have active cooling, this scenario is excluded in the evaluation of the cooling demand. So, the comparison of the cooling demand will only be made between the CS0 and CS2 scenarios. Where scenario CS0 is represented as a reference case with mechanical ventilation and active cooling. While scenario CS2 is a hybrid system where it combines adaptive natural ventilation under certain thresholds and active cooling.

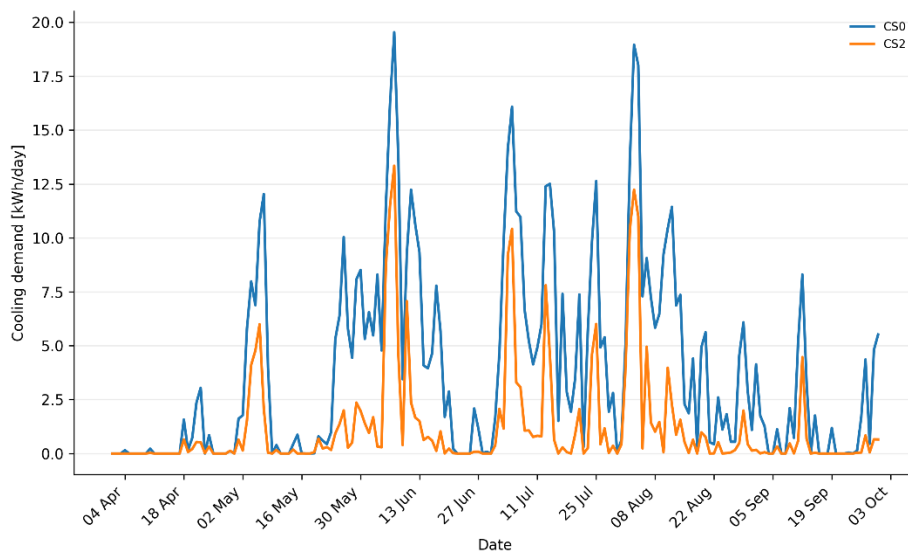
Table 10.8 shows the total cooling demand of the reference case, CS0, reaches 709 kWh for the entire duration of the summer season. On the other hand, scenario CS2 shows a total cooling demand of 227 kWh. Thus, the proposed hybrid system leads to approximately 68% decrease in the cooling demand.

This significant reduction in cooling demand indicates that the adaptive natural ventilation system can effectively lower the dependency on active cooling. When there are favourable outdoor conditions, the adaptive ventilation components provide extra passive cooling. Therefore, less mechanical cooling is needed in the CS2 scenario.

Table 10.8*Cooling Demand Comparison between CS0 and CS2 for the Full Summer Period*

Scenario	Cooling demand [kWh]	Reduction compared to CS0
CS0	709	–
CS2	227	68.0%

Figure 10.21 shows the daily cooling load for both scenarios, CS0 and CS2, within the summer period. It can be noted that the cooling load in CS2 is consistently lower than the CS0 scenario for most of the summer period. Especially during the warmer periods of the summer, this difference becomes clearer. This suggests that the adaptive ventilation systems are most effective during periods with high cooling loads. Only when there is passive cooling potential available, when the conditions are favourable.

**Figure 10.21***Daily cooling load during the summer period.*

10.3.5 Detailed Summer Week

This section provides an analysis of the simulation for all the different scenarios, CS0, CS1, and CS2, for the warmest week of the full summer period. This warmest week is the same as selected in Section 10.2.3. So, the week used for the warmest summer week is ranging from 1 August to 7 August. The main objective of this analysis is to see how the adaptive ventilation system performs during the most critical conditions of the year. Wherein the first part of the results was focused on day averages. This part presents an evaluation of the hourly behaviours of the systems during more extreme outdoor conditions.

Performance During the Selected Warmest Week

The main findings of the analysis of the warmest week are summarised in Table 10.9. It shows that even though CS1 has the highest air change rate, it also has the highest mean and maximum operative temperature. This indicates that only an adaptive natural ventilation system is inefficient during peak

summer periods. Furthermore, CS2 has a lower maximum operative temperature compared to CS1. However, scenario CS1 is not able to decrease the temperature level as effectively as CS0. So, active cooling is required during extremely hot conditions during the summer.

Overall, according to the results out of Table 10.9, it shows that higher ventilation rates do not automatically result in effective temperature control. How effective the adaptable passive ventilation system depends on whether the outdoor temperature is cool enough to remove excessive indoor heat from the room. Consequently, the adaptive ventilation system can be used as an additional strategy within a hybrid system. Rather than fully replace an active cooling system.

Table 10.9
Simulation Results of the Case Study for the Selected Summer Week

Scenario	Mean operative temp [°C]	Max operative temp [°C]	Hours > 24°C [h]	Mean ACH [ac/h]	Max ACH [ac/h]
CS0	26.3	28.9	159	1.0*	1.0
CS1	28.6	39.7	157	3.5	17.0
CS2	26.9	34.3	158	3.0	14.4

Note. *The setpoint used in DesignBuilder.

Hourly Operative Temperature

The hourly operative temperature for all the scenarios of the case study, CS0, CS1, and CS2 in the warmest week of the summer period is shown in Figure 10.22. The shaded areas represent the night, from 20:00 till 06:00. Figure 10.22 gives a more detailed comparison than the weekly statistic presented in Table 10.9.

Scenario CS1 shows the greatest differences in temperature peaks during the whole week. The operative temperature rises significantly at daytime and drops during the night. During the night natural ventilation becomes more efficient. Nevertheless, during the day there are still high operative temperature peaks. Especially during the warmest days of the selected summer week.

Scenario CS2 is similar to CS1 in terms of pattern. However, the temperature peaks are smaller. This because of the presence of an active cooling system. Scenario CS0 provided the most stable temperatures since the active cooling is always provided. Furthermore, here ventilation does not depend on outdoor and indoor temperatures. Moreover, the hourly results show that the greater differences are shown during the day, when outdoor temperatures are relatively high. During the night these differences become smaller.

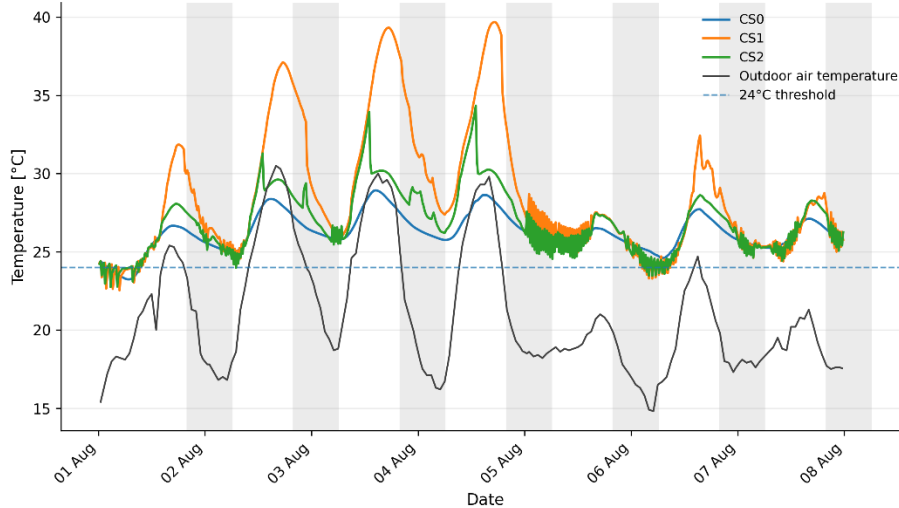


Figure 10.22
Hourly operative temperature for CS0, CS1, and CS2 during the selected summer week.

10.3.6 Ventilation and System Operation

This section provides an overview of when the adaptive ventilation system is active and what the air change rate is during the week. Figure 10.23 illustrates the hourly air change rate for the selected summer week of scenarios CS0, CS1, and CS2. The dashed blue line is the set point for CS0 and has the value of 1.0 ac/h.

The figure shows that CS1 and CS2 have highly fluctuating values throughout the week. It demonstrates that the adaptive ventilation system opens and close based on indoor and outdoor temperatures. The highest air change rate values are reached within the evening, night, and early mornings. During these times the outdoor temperatures overall lower, this is also illustrated in Figure 10.23. These lower outdoor temperatures increase the potential for passive cooling. During the day the air change rate it either relatively low or even absent. This is expected, because the outside air is at some part exceeding the temperature threshold of 24°C. The adaptive ventilation system is only efficient when the outdoor air is cool enough to remove heat from the living room.

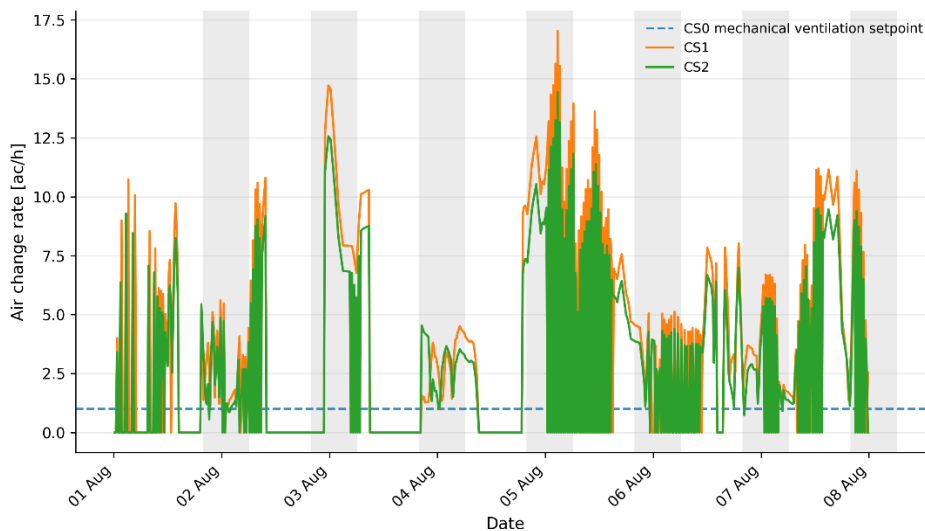


Figure 10.23
Hourly air change rate for selected summer week of scenarios CS0, CS1, and CS2.

Moreover, out of the results it becomes clear that scenario CS2 represents the most realistic applications of the adaptive ventilation system. The previous results showed that passive ventilation alone is not enough to cool the indoor climate during peak temperatures. Therefore, CS2 was used to evaluate whether the adaptive ventilation system can reduce the cooling load, when it is used in a combination with an active cooling system. Therefore, Figure 10.24 combines the air change rate and the cooling energy used for the CS2 scenario.

Figure 10.24 shows the interaction between the adaptable ventilation system and the active cooling system. As mentioned in the previous section natural ventilation is only active when the outdoor conditions are favourable. Hereby reducing the cooling demand of the building. Furthermore, when the system is closed during the peak temperature moments of the day, where the outdoor temperatures are exceeding the 24°C threshold. Then the active cooling is more active during the moments when the ventilation system is closed.

To summarize, CS2 shows the most relevant application of the adaptive ventilation system. This hybrid strategy where passive ventilation and active cooling work together to lower the energy demand in buildings.

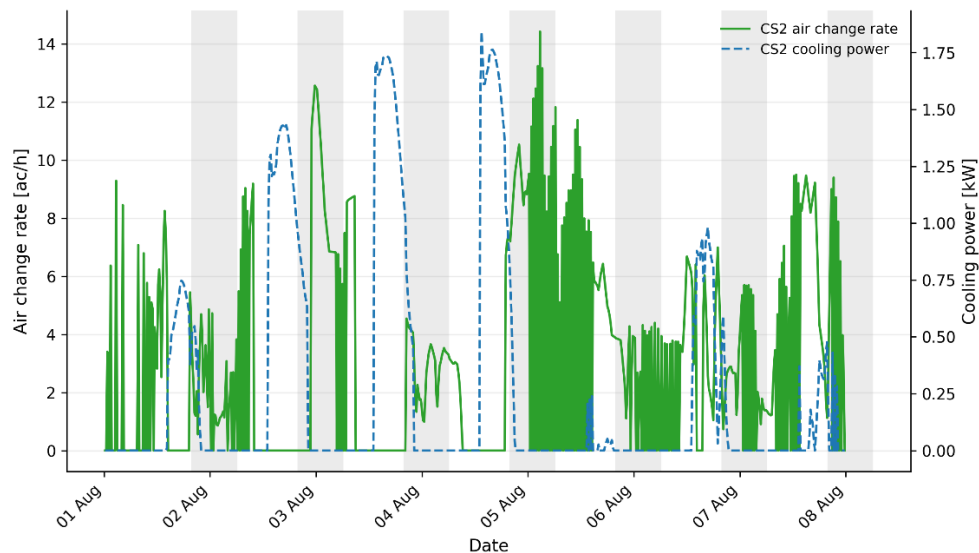


Figure 10.24
CS2 air change rate plus cooling power for the selected summer week.

10.3.7 Case Study Summary

In summary, the results from the case study analyses indicates that the adaptive ventilation system is not effective enough as a complete substitute for active cooling systems. Scenario CS1 shows that during peak summer conditions high operative temperatures occur. However, scenario CS2 indicates that an adaptive ventilation system combined with active cooling can significantly reduce the summer cooling demand in a building. When the CS2 scenario is compared to the reference scenario, CS0, the cooling demand can be reduced by approximately 68%.

The detailed analysis of the warmest summer week shows that the cooling capacity of the adaptive ventilation is mostly beneficial during the night, evenings, and early mornings. This when the outdoor temperature is relatively lower. However, during the warmest moments of the day, active cooling is still necessary.

Therefore, the case study validates that the adaptive ventilation system is the most appropriate with the use of a hybrid cooling.

10.4 Conclusion

To conclude the results of the simulations, it proves that adaptive natural ventilation can contribute to reducing overheating risks, provided under specific indoor and outdoor conditions. The systems show optimal performance when the cooler outdoor air is available. Particularly during the evening, nights, and morning hours. These findings suggest that the designed ventilation components should mainly be understood as a passive night ventilation strategy, rather than an independent cooling system.

Furthermore, the results from the case study demonstrate that passive ventilation alone was not sufficient to endure thermal comfort during peak summer conditions. Nevertheless, the hybrid scenario where adaptive ventilation is combined with active cooling, can substantially reduce the cooling demand. This indicates that the main value of adaptive ventilation actuated by SMAs relies in minimizing the reliance on active cooling systems. While still requiring mechanical support during critical warm periods.

Overall, the simulations support the potential of the proposed adaptive façade component as part of a hybrid climate strategy.

11. Discussion

This research examined the feasibility of Shape Memory Alloys (SMA) as a key building block of an adaptive façade. In particular, the objective was to design a passive ventilation component actuated by SMA wires and triggered by change in temperature. The study encompassed a literature study of smart materials, development of a prototype, experimental testing, and building performance simulations. The results suggest that adaptive ventilation based on SMAs could lead to improved indoor climate together with reduced cooling demands. However, there are some limitations and uncertainties that must be acknowledged when interpreting the results.

Simulation Simplifications

The first limitation concerns the translation from the SMA behaviour into building performance. This study effectively demonstrated that the SMA wire generates enough force and contraction to activate the developed ventilation system. In addition, the proposed design of the Scotch yoke appeared to be suitable for converting the linear contraction of the SMA wire in rotation of the lamellas. However, the simulations did not directly simulate the physical component itself. Instead, the adaptive ventilation strategy was simplified to an opening logic with temperature setpoints in DesignBuilder. Therefore, the results of the simulations show the effectiveness of the ventilation strategy rather than the exact performance of the designed ventilation component. Hence, the decrease in operative temperature and cooling demands show the theoretical potential of the strategy, rather than a predicted outcome of the final product performance.

Airflow and Draught

A further limitation concerns the high air change rates observed in the simulations. These high air change rates have a positive impact in terms of passive cooling. However, such high rates may also result in draught discomfort. The highest value for the air change rate was 39.50 ac/h, in scenario CS2, and more than half of these peaks occur during occupied hours. As occupant comfort was not assessed through local air speed air draught criteria, the practical implications of these airflow peaks remain unexplored. Therefore, the cooling benefits of the adaptive ventilation strategy should be interpreted together with the potential impact on occupant comfort.

The case study results also suggest that building height and façade exposure can strongly influence the resulting airflow rates. Since the apartment is located on the 11th floor, higher wind speeds may have contributed to the high ACH peaks observed in CS2. Therefore, the system should not only be evaluated by its ability to provide airflow. But also, by its ability to control extreme airflow events. In high-rise applications, this may require an additional pressure-responsive element, such as a passive flow limiter or self-regulating grille. While the SMA-driven lamellas remain responsible for the temperature-controlled opening and closing of the system.

SMA Hysteresis

Besides this, another limitation concerns the thermal behaviour of the SMA. During the experimental tests of the SMA wire, it confirmed the hysteresis during heating and cooling. Hysteresis is a characteristic behaviour of SMAs. It directly affects how the ventilation component opens and closes. Furthermore, it results in a difference between the activation and deactivation temperature. So, the system does not open and close at only specific temperature threshold. While this might help avoid rapid oscillation at one specific temperature setpoint, it will increase the uncertainty of the operating temperature of the system. This hysteresis behaviour was not modelled in the simulations but simplified to a setpoint opening logic.

Environmental Exposure

Additionally, this research did not consider the effect of the interaction between airflow through the component and the SMA behaviour. When the ventilation system is open, cool outdoor air flows through the component. This cool air could initiate the reverse phase transformation from austenite to martensite, where the SMA wire is reducing its force. This could result in decrease of the opening duration of the system.

This issue was considered during the component design through the routing of the SMA wire. In the current design the wire was embedded to reduce direct exposure to the main airflow, wind and solar radiation. Furthermore, different strategies were explored, of which the separated compartment was considered the most suitable option. This because it allows the SMA wire to respond to indoor and outdoor temperatures while reducing direct environmental disturbance. However, this solution was only developed conceptually. It was not validated through physical testing or detailed airflow simulations. Therefore, the actual influence of local airflow, solar radiation and temperature gradients on the SMA response remains uncertain.

Durability and Integration

Furthermore, durability and long-term performance must also be considered. The proposed ventilation system is designed to operate with 4% strain in order to minimize metal fatigue and increase the lifespan of the SMA wire. While this value falls into the range of acceptable values, no long-term cycle tests were done. The prototype was examined only through short-term experiments. In actual façade applications the SMA wire will experience thousands of thermal cycles. In addition to metal fatigue, the friction between the moving parts, such as, pins, crank arms, and the yoke, may influence the performance of the system. Therefore, the long-term reliability of the SMA wire and the complete mechanism cannot be determined.

Moreover, the design of the adaptive ventilation component was developed with a strong focus on adaptive behaviour and thermal performance. However, there are several other properties that stayed outside the scope of this research. For instance, airtightness of the component was achieved by using interlocking lamellas. When airtightness is not secured, unwanted air leakage could lead to heat losses during the colder periods of the year, when the system should remain closed. Although passive and active override options were explored to keep the system closed when ventilation is not desired, their practical performance was not tested. Therefore, the actual airtightness and closed-state reliability of the component remain uncertain.

Similarly, even though the implementation of an acoustic box in the ventilation component, this to minimize the noise pollution, the impact of such an element on the airflow was not analysed with tests. Both airtightness and acoustic performance are critical requirements for façade integration. Although the free opening area was reduced during the simulations because of the presence of the acoustic elements, the actual ventilation rates may therefore differ than the results from the simulations. Consequently, the real-world performance may also differ.

Climate and Context Dependency

It is also important to consider the specific climate and case study context when interpreting the results of the research. The proposed adaptive ventilation system was developed for the temperature of the oceanic climate zone of the Netherlands. This climate produces a trend towards overheating, which is associated with extremely well insulated buildings. The effectiveness of night ventilation relies mostly on the availability of sufficient cool temperatures during the evening, night, and early mornings. If under future climate scenarios these temperatures also increases, this can decrease the effectiveness of the passive cooling system.

In addition to climate, the performance of natural ventilation also depends on the position of the components and the façade orientation. Single-sided and two-sided ventilation are influenced by wind direction and façade exposure. Stack-effect ventilation is less dependent on façade orientation but still depends on the height difference and position of the inlet and outlet openings. Since the proposed ventilation component is modular, multiple components could be implemented in different configurations depending on the building design. This is especially relevant for one-sided ventilation. Although one-sided ventilation could still be applied, it would require a larger number of components to achieve sufficient airflow and cooling capacity. This may affect the architectural expression and aesthetic quality of the façade. However, this research did not aim to optimise the number or position of the components. Therefore, the simulation results should be interpreted in relation to the specific component placement and case study configuration, rather than as a universally applicable performance outcome.

Proof-of-Concept

Despite these limitations, the research shows the potential of using smart materials as a passive alternative to conventional motorized adaptive façade systems. Most adaptive façades require the use of sensors, motors, and other control systems. This results in increased complexity, maintenance, and a higher energy demand. The proposed adaptive ventilation system, driven by temperature, represents an alternative approach to adaptation whereby the material is used as a machine that does not need an external control system.

Overall, this research should be considered as a proof-of-concept. It shows the possibility of translating the behaviour of SMAs into an adaptive ventilation system. The findings indicate a significant improvement in the indoor climate due to the passive adaptive ventilation system. However, several uncertainties remain, including simulation simplifications, airflow and draught risk, SMA hysteresis, environmental exposure, durability, façade integration, and climate and context dependency. These considerations indicate that the current design should be interpreted as a proof-of-concept rather than a market-ready façade product.

12. Conclusion

The findings of this research demonstrate that the integration of smart materials into building façades offers a suitable strategy for improving indoor climate performance while reducing energy demand. The literature study showed that adaptive façades can improve the interaction between indoor and outdoor conditions. By allowing the façade to respond to changing environmental conditions. Smart materials are relevant in this context because they can passively respond to environmental changes, instead of relying on mechanical adaptation.

The evaluation of smart materials showed that not all smart materials are suitable for façade integration. Materials with a direct influence on the indoor climate, a passive and reversible response, and sufficient but not fully mature technological development were considered most relevant. Based on these criteria, Shape Memory Alloys, thermo-bimetals, and hygro-morphic materials were selected as the most promising. SMAs were selected for further development because they offer the most suitable balance between temperature-responsive behaviour, reversible actuation, actuation force and design flexibility.

The design study illustrated the translation of SMA behaviour into an adaptive natural ventilation component. The linear SMA contraction is converted, by the Scotch yoke mechanism, into rotation of the lamellas. This shows that material behaviour can be implemented into a façade when the material properties are working together with system requirements. Such as, actuation thresholds, force transmissions, displacement and mechanical constraints. Thus, the research objective was obtained by creating an adaptive ventilation component driven by SMAs and explore its design impact through building performance simulations.

According to the simulation results, the adaptive natural ventilation strategy can improve indoor thermal comfort if the outdoor temperature is cool enough to reduce the indoor temperature. Mostly, in the evenings, night, and early mornings. The greatest impact was observed with two-sided ventilation in the reference room, with the strongest reduction in overheating. One-sided ventilation can also contribute to passive cooling but would require more adaptable ventilation components to achieve comparable airflow rates. This may therefore affect the architectural expression of the façade. Furthermore, the case study demonstrated that the passive ventilation strategy alone is not sufficient to guarantee thermal comfort during the peak hours of the day in summer. The most efficient approach involves a hybrid strategy, using adaptive ventilation where possible but combined with active cooling. Under the simulated case study conditions, this scenario shows that the adaptive ventilation system can reduce the summer cooling demand with approximately 68% compared to the reference case.

To answer the main research question: smart materials can be integrated into adaptive building façades. This by translating their intrinsic response behaviour into a façade component that directly influences the indoor climate. In this thesis, an SMA actuator was embedded into a passive ventilation component. This system can reduce overheating risks and lower the cooling demand in buildings. The system should not be understood as a complete replacement for active cooling, but as a supportive strategy within a hybrid concept.

Overall, this thesis demonstrates that SMA-driven adaptive ventilation can contribute to lower-energy building performance as part of a hybrid climate strategy. At the same time, the proposed component should be interpreted as a proof-of-concept. Further development is needed to address airflow control, draught risk, durability, airtightness, acoustic performance and real-world façade integration before practical application can be considered.

Recommendations

Several recommendations can be made for further development of the SMA driven adaptive ventilation component.

First, the behaviour of the prototype could be verified by doing additional test under more realistic boundary conditions. This includes testing the component with actual airflow, outdoor temperature changes, solar radiation, and multiple cycles of opening and closing. In addition, CFD simulations could be used to analyse the airflow patterns through and around the ventilation component, including the possible cooling effect of incoming air on the SMA wire. This gives a better understanding of the responds of the SMA wire when it is integrated into a façade component, rather than tested separately.

Secondly, the durability of the system should be investigated. Further research should assess the fatigue behaviour of the SMA wires, the reliability of the return spring, and the effect of friction and wear in the moving parts.

Third, the comfort impact of the proposed ventilation system should be evaluated in more detail. The simulations showed a high air change rate during occupied hours. Further research should therefore include local air speed, draught risk and occupant comfort criteria. The potential integration of a passive flow limiter or self-regulating grille should also be explored to reduce excessive airflow during high wind pressure.

Fourthly, the façade integration of the component should be further developed. Essential requirements for practical façade applications, are airtightness, acoustic performance, water resistance, and maintenance accessibility. These aspects were outside the scope of this research. Nevertheless, they are necessary to determine whether the component can function reliably in a real building envelope. In addition, future design studies should investigate the optimal number and position of ventilation components, especially for one-sided ventilation where more components may be required. This should include both airflow performance and the architectural impact on the façade.

13. Reflection

This graduation project was positioned at the intersection of façade and climate design with smart materials. Looking back, the main challenge was to translate the behaviour of Shape Memory Alloys into a façade component that could have a measurable effect on the indoor climate. This made the process highly iterative, moving between literature research, material understanding, mechanical design, prototyping and simulations.

Scope

At the start of the research, the topic felt broad and difficult to frame. Smart materials can respond to many different environmental stimuli and can be linked to several façade functions. This created many possible design directions. The literature study helped to structure this complexity. By defining selection criteria, I was able to move from a broad exploration of smart materials towards a more focused design study with Shape Memory Alloys. This taught me the importance of narrowing down a research topic and making clear design choices based on the objective of the project.

Design

During the design process, the behaviour of the SMA wire became one of the main drivers for the component geometry and operating logic. The SMA wire could not simply be treated as a standard actuator. Its limited contraction, hysteresis, force development and sensitivity to temperature all influenced the geometry and operating logic of the component. The choice for the Scotch yoke mechanism was therefore not only a mechanical design decision. But also, a response to the limitations of the SMA wire.

The physical prototype was valuable because it made the behaviour of the SMA wire tangible. Testing showed that the wire could generate sufficient force and contraction to actuate the mechanism. At the same time, the prototype revealed that a working principle in theory does not automatically result in a reliable façade product. Issues such as friction, wire routing, and return forces became more visible during the development of the mock-up.

Simulations

The building performance simulations added another scale to the project. They made it possible to test the design impact of the adaptive ventilation strategy at room level. Learning to work with new software tools as, DesignBuilder and EnergyPlus, was a valuable part of the process. However, the physical SMA-driven component was not modelled directly. Instead, its behaviour was simplified into a temperature-based opening logic in DesignBuilder. This distinction became important in interpreting the results critically.

One important insight from the simulations was that adaptive natural ventilation can contribute to passive cooling, but that its effectiveness depends strongly on the ventilation configuration and building context. This creates a direct link between performance and architectural expression. In Building Technology, this is important because technical solutions are never isolated from the façade as an architectural element.

Comfort and Control

Another important lesson concerns occupant comfort. High air change rates can be beneficial for cooling, but they may also create draught discomfort. This showed that improving thermal performance alone is not sufficient. A façade component must also maintain comfort.

The project also raised considerations about user control. A fully passive system can reduce energy use and complexity. But it should not remove the possibility for occupants to overrule the system when ventilation is unwanted. This is why the manual override became a part of the design.

Overall, this project changed the way I look at innovation in façade technology. I learned that a technical principle only becomes valuable when it can be translated into a reliable and meaningful part of a building. For me, one of the most important insights was that technical solutions are never isolated from the façade as an architectural element. A ventilation component can reduce cooling demand, but it also affects the appearance of the façade, occupant comfort, construction complexity and long-term reliability. This project helped me move between different scales: from material behaviour and mechanical movement to indoor climate performance and façade integration. In that sense, the main value of the research for me lies in understanding how material intelligence can become a critically evaluated Building Technology application.

References

- Addington, M., & Schodek, D. (2005). *Smart materials and technologies for the architecture and design professions*. Architectural Press.
- Akhras, G. (2024, December 4). *Work smarter, not harder: What are smart materials?* University of the Built Environment. <https://www.ube.ac.uk/whats-happening/articles/smart-materials/>
- Alvarez Gutiérrez, R., Audenaert, A., & Verbeke, S. (2025). Passive phase change materials integration in office buildings: Review on impact of HVAC operation controls on thermal performance. *Journal of Building Engineering*, Advance online publication. <https://doi.org/10.1016/j.jobe.2025.115026>
- Architizer. (n.d.). *8 impossibly dynamic façades that were actually built*. Retrieved February 6, 2026, from <https://architizer.com/blog/inspiration/collections/8-impossibly-dynamic-facades-that-were-actually-built/>
- Balcerak-Woźniak, A., Dzwonkowska-Zarzycka, M., & Kabatc-Borcz, J. (2024). *A comprehensive review of stimuli-responsive smart polymer materials—Recent advances and future perspectives*. *Polymers*, 16(3), Article 401. <https://doi.org/10.3390/polym16030401>
- Baylis, C., & Cruickshank, C. A. (2023). *Review of bio-based phase change materials as passive thermal storage in buildings*. *Renewable and Sustainable Energy Reviews*, 186, 113690.
- Barbhuiya, S., Das, B. B., Adak, D., & Rajput, A. S. (2025). *Next-generation building envelopes: Smart materials, energy efficiency and environmental impact*. *Next Materials*, 9, 101226. <https://doi.org/10.1016/j.nxmte.2025.101226>
- Bengisu, M., & Ferrara, M. (2018). *Materials that move: Smart materials, intelligent design*. Cham: Springer International Publishing. <https://doi.org/10.1007/978-3-319-76889-2>
- Bilow, M. (2012). *International façades – CROFT: Climate related optimized façade technologies* (Doctoral dissertation). Delft University of Technology, Delft, The Netherlands.
- Boostani, H., & Modirrousta, S. (2016). *Review of nanocoatings for building application*. *Procedia Engineering*, 145, 1541–1548. <https://doi.org/10.1016/j.proeng.2016.04.194>
- Chen, J., Qiu, Q., Han, Y., & Lau, D. (2019). *Piezoelectric materials for sustainable building structures: Fundamentals and applications*. *Renewable and Sustainable Energy Reviews*, 101, 14–25.
- Costa, C. M., Pereira, N., & Lanceros-Méndez, S. (2025). Smart materials: Definition and main physical-chemical principles. In C. Costa & S. Lanceros-Méndez (Eds.), *Advanced smart and multifunctional materials volume 1: Fundamentals and types* (ACS Symposium Series). American Chemical Society.
- Fathi, S., & Fakhraeimanesh, S. (2025). Smart materials in building façades: A systematic review of applications. *Energy Reports*, 14, 2123–2140. <https://doi.org/10.1016/j.egy.2025.08.042>
- Fedorik, F., Zach, J., Lehto, M., Kymäläinen, H.-R., Kuisma, R., Jallinoja, M., Illikainen, K., & Alitalo, S. (2021). *Hygrothermal properties of advanced bio-based insulation materials*. *Energy and Buildings*, 253, 111528. <https://doi.org/10.1016/j.enbuild.2021.111528>
- Formentini, M., & Lenci, S. (2018). An innovative building envelope (kinetic façade) with Shape Memory Alloys used as actuators and sensors. *Automation in Construction*, 85, 220–231. <https://doi.org/10.1016/j.autcon.2017.10.006%20with%20Shape%20Memory%20Alloys.pdf> [An innovat...ory Alloys | PDF]

- García, A., Tubío, C. R., Seoane-Rivero, R., Rubio-Peña, L., & Lanceros-Méndez, S. (2023). *Magnetoactive and electroactive biobased and biopolymer composites*. *Progress in Polymer Science*, 137, 101640. <https://doi.org/10.1016/j.progpolymsci.2022.101640>
- Gosztonyi, S. (2022). *Biomimetics for adaptive façades: Function-oriented design strategies for thermal adaptation in energy-efficient building skins (A+BE | Architecture and the Built Environment, Issue 2022/04)*. Delft University of Technology. <https://doi.org/10.7480/abe.2022.04>
- Halawa, E., Ghaffarianhoseini, A., Ghaffarianhoseini, A., Trombley, J., Hassan, N., Baig, M., Yusmah Yusoff, S., & Ismail, M. A. (2018). A review on energy conscious designs of building façades in hot and humid climates. *Renewable and Sustainable Energy Reviews*, 82, 2147–2161. <https://doi.org/10.1016/j.rser.2017.08.061>
- Hameury, S. (2005). *Moisture buffering capacity of heavy timber structures exposed to an indoor climate*. *Building and Environment*, 40, 1400–1412.
- Holstov, A., Bridgens, B., & Farmer, G. (2015). Hygromorphic materials for sustainable responsive architecture. *Construction and Building Materials*, 98, 570–582.
- Holstov, A., Farmer, G., & Bridgens, B. (2017). *Sustainable materialisation of responsive architecture*. *Sustainability*, 9(3), 435. <https://doi.org/10.3390/su9030435>
- Homedit. (n.d.). *Buildings with dynamic façades*. Retrieved February 6, 2026, from <https://www.homedit.com/building-with-dynamic-facades/>
- inspire AG. (n.d.). *Shape memory alloys*. Retrieved May 11, 2026, from <https://www.inspire.ch/en/research-for-the-industry/manufacturing-processes-quality/additive-manufacturing-3d-print-design-for-am/postprocessing-quality-6/>
- Jali, V. M. (2025). *Smart materials: A comprehensive review of fundamentals, types and applications*. *The Spring Chronicle*, 1(4), 40–58. <https://www.springchronicle.org/home/article/smart-materials-a-comprehensive-review-of-fundamentals-types-and-applications>
- Kamalisarvestani, M., Saidur, R., Mekhilef, S., & Javadi, F. S. (2013). Performance, materials, and coating technologies of thermochromic thin films on smart windows. *Renewable and Sustainable Energy Reviews*, 26, 353–364. <https://doi.org/10.1016/j.rser.2013.05.038>
- Khdair, A. I., Aburumman, G. A., Tahmasbi, F., Tahmasebi, M., Kalbasi, R., & Afrand, M. (2026). *Advancing natural ventilation in sustainable architecture: Mechanisms, innovations, and climate-responsive design for energy-efficient buildings*. *Renewable and Sustainable Energy Reviews*, 226, 116314. <https://doi.org/10.1016/j.rser.2026.116314>
- Khdair, A. I., Kalbasi, R., Dara, R. N., & Afrand, M. (2025). *Phase change materials in buildings: A comprehensive review of applications, climate strategies, and 3E performance*. *Journal of Energy Storage*, 132, 117675. <https://doi.org/10.1016/j.est.2025.117675>
- KNMI. (n.d.). *Summer*. Retrieved February 26, 2026, from <https://www.knmi.nl/kennis-en-datacentrum/uitleg/zomer>
- KNMI. (2022). *Zomer 2022*. <https://www.knmi.nl/nederland-nu/klimatologie/maand-en-seizoensoverzichten/2022/zomer>
- KNMI. (2023, 13 juli). *Groter natuurbrandgevaar door dalende luchtvochtigheid*. Koninklijk Nederlands Meteorologisch Instituut. <https://www.knmi.nl/over-het-knmi/nieuws/groter-natuurbrandgevaar-door-dalende-luchtvochtigheid>

- Lelieveld, C. M. J. L. (2013). *Smart materials for the realization of an adaptive building component* (Doctoral dissertation, Delft University of Technology). Delft University of Technology. ISBN: 978-94-6186-114-6.
- Li, C., Pei, Z., Lin, Y., Xie, W., Ukrainczyk, N., Koenders, E. A. B., & Cai, J. (2026). Thermoelectric brick with solid–solid phase change materials for building-integrated energy harvesting: Design, simulation, and global evaluation. *Applied Thermal Engineering*, 282, 128844. <https://doi.org/10.1016/j.applthermaleng.2025.128844>
- Li, S., Sha, Y., Wu, Y., Gao, Y., He, M., Wang, X., Yang, L., & Mai, X. (2025). *Experimental investigation of indoor lighting/thermal characteristics of highly sensitive mechano-chromic energy-saving windows*. *Energy*, 322, 135659.
- Liu, B., Yang, Y., Huang, D., et al. (2025). *An innovative MXene modified melamine foam shape-stabilized hydrated salt-based composite PCM for indoor thermal comfort and energy saving in buildings*. *Construction and Building Materials*, 466, 140289.
- Loonen, R. C. G. M., Trčka, M., Cóstola, D., & Hensen, J. L. M. (2013). Climate adaptive building shells: State-of-the-art and future challenges. *Renewable and Sustainable Energy Reviews*, 25, 483–493. <https://doi.org/10.1016/j.rser.2013.04.016>
- Mu, Y., Xin, L., Meng, T., & Li, X. (2024). Reversible thermochromic $K_2O \cdot nSiO_2$ -based anti-fire glass with bidirectional response and memory function. *Ceramics International*, 50, 37147–37166. <https://doi.org/10.1016/j.ceramint.2024.07.106>
- OliKrom. (n.d.). *Chemochromic materials: pigments, inks, paints*. Retrieved May 17, 2026, from <https://www.olikrom.com/en/chemochromic-materials/>
- Ou, K. et al. (2024). *Phase-change composite elastomers for efficient thermal management at contact interface*. *Composites Communications*, 52, 102149.
- Pérez-Lombard, L., Ortiz, J., & Pout, C. (2008). *A review on buildings energy consumption information*. *Energy and Buildings*, 40(3), 394–398. <https://doi.org/10.1016/j.enbuild.2007.03.007>
- Persiani, S. G. L., Molter, P. L., Aresta, C., & Klein, T. (2016). *Mapping of environmental interaction and adaptive materials for the autoreactive potential of building skins*. In *41st IAHS World Congress: Sustainability and Innovation for the Future* (pp. 1–10). Albufeira, Algarve, Portugal.
- Pitsika, E., & Stathatos, E. (2026). *Optical and photonic performance of one-step synthesized boron carbon oxynitride-phosphor as promising luminescent solar concentrator*. *Materials Chemistry and Physics*, 349, 131825.
- Riganti, M., Li Castri, G., Serra, V., Manca, M., & Favoino, F. (2025). *Energy saving potential of advanced dual-band electrochromic smart windows for office integration*. *Energy & Buildings*, 327, 115084. <https://doi.org/10.1016/j.enbuild.2024.115084>
- Roostaei Firouzabad, M., & Razi Astaraei, F. (2024). *Energetical effect of electrochromic glazing on the double-skin façade of the building in different climates*. *Energy & Buildings*, 316, 114344.
- Scirè Mammano, G., & Dragoni, E. (2014). *Functional fatigue of Ni–Ti shape memory wires under various loading conditions*. *International Journal of Fatigue*, 69, 71–83. <https://doi.org/10.1016/j.ijfatigue.2012.03.004>
- Scrucca, F., Ingrao, C., Barberio, G., Matarazzo, A., & Lagioia, G. (2023). On the role of sustainable buildings in achieving the 2030 UN Sustainable Development Goals. *Environmental Impact Assessment Review*, 100, 107069. <https://doi.org/10.1016/j.eiar.2023.107069>

- Singh, H. D., Kapur, A., & Singh, M. P. (2024). *Thermo-bimetals: A step forward in innovative materials*. *Goya Journal*, 17(4), 18-23. <https://doi.org/12.163022.Gj.2024.v17.04.003>
- Singh, J., & Nayak, P. (2023). *pH-responsive polymers for drug delivery: Trends and opportunities*. *Journal of Polymer Science*, 61(22), 2828–2850. <https://doi.org/10.1002/pol.20230403>
- Su, M., & Song, Y. (2021). Smart materials and devices: Strategies and applications. *Chemical Reviews*, 122(5), 3214-3262. <https://doi.org/10.1021/acs.chemrev.0c00972>
- Sung, D. K. (2011). *Skin Deep: Making Building Skins Breathe With Smart Thermobimetals*. *Architectural Design*, 81(6), 145–152.
- Szolomicki, J., & Golasz-Szolomicka, H. (2019). Technological advances and trends in modern high-rise buildings. *Buildings*, 9(9), 193. <https://doi.org/10.3390/buildings9090193>
- Teixeira, H., Rodrigues Moret, A., Aelenei, D., & Gomes, M. G. (2025). Literature review of solar control smart building glazing: Technologies, performance, and research insights. *Building and Environment*, 274, 112784. <https://doi.org/10.1016/j.buildenv.2025.112784>
- Vailati, C., Bachtiar, E., Hass, P., Burgert, I., & Rüggeberg, M. (2018). *An autonomous shading system based on coupled wood bilayer elements*. *Energy and Buildings*, 158, 1013–1022. <https://doi.org/10.1016/j.enbuild.2017.10.042>
- W/E adviseurs. (2018, April 30). *Temperatuuroverschrijding in nieuwe woningen in relatie tot voorgenomen BENG-eisen (W/E 9604)*.
- WindHarvest. (n.d.). *What are Technology Readiness Levels and where is Wind Harvest in the process?* WindHarvest. Retrieved May 11, 2026, from <https://windharvest.com/blog/faq-items/what-are-technology-readiness-levels-and-where-is-wind-harvest-in-the-process/>
- World Health Organization. (2009). *Moisture control and ventilation (Indoor Air Quality Guidelines)*. In WHO Guidelines for Indoor Air Quality. <https://www.ncbi.nlm.nih.gov/books/NBK143947/>
- Yang, M., Wang, S.-Q., Liu, Z., Chen, Y., Zaworotko, M. J., Cheng, P., Ma, J.-G., & Zhang, Z. (2021). *Fabrication of moisture-responsive crystalline smart materials for water harvesting and electricity transduction*. *Journal of the American Chemical Society*, 143, 7732–7739.
- Zhang, J., Fang, Y., Tang, M., Wu, X., Yu, X., & Ou, R. (2025). *Switchable and highly selective Hg(II) capture enabled by a thermo-responsive MOF–polymer nanohybrid*. *Chemical Engineering Journal*, 521, 166826. <https://doi.org/10.1016/j.cej.2025.166826>

Appendix A

This appendix contains of an overview of the Technology Readiness Levels (TRLs) of smart materials. Table A.1 was used to compare the maturity of each material in the material selection phase.

Table A.1
Technology Readiness Levels (TRL) of Smart Materials

Material	TRL Range	Description
Thermochromic Materials	8-9	VO ₂ coatings for glazing systems.
Thermoelectric Materials	3-4	Power harvesting devices, experimental phase.
Phase Change Materials (PCMs)	8-9	Used in temperature regulation, thermal storage.
Thermo-Responsive Polymers	4-6	Shape memory polymers for temperature-driven applications.
Shape Memory Alloys (SMAs)	3	Still in proof-of-concept stage for façade integration.
Thermo-Bimetals	4-5	Widely used in thermostats but still prototype for façade use.
Photochromic Materials	9	Commercially available, used in switchable glass.
Luminescent Solar Concentrator (LSC) Materials	4-6	Transparent photovoltaics with emerging application.
Photocatalytic Materials	5-7	Used for self-cleaning and air purification in façades.
Hygro-Morphic Materials	1-7	Early-stage materials, potential for adaptive façades.
Moisture-Responsive Crystalline Materials	3-5	Self-sustained wireless sensing, early-stage development.
Hygroscopic Bio-based Insulation Materials	7-8	Stable indoor climate regulation, used in construction.
Electrochromic Materials	8-9	Dynamic glazing for solar radiation control, widely used.
Magnetoactive Polymer Composites	5-6	Self-sensing functions, experimental in smart infrastructure.
Mechano-Chromic Materials	4-7	Prototype stage, used for optical adaptation in façades.
Piezoelectric Materials	4-7	Energy harvesting and structural monitoring, lab validation.
Chemo-Chromic Materials	3-5	Emerging for visual chemical detection in façades.
PH-Responsive Polymers	3-6	Still developing, used for corrosion protection.

Appendix B

This appendix provides a simplified estimation of the required ventilation opening area for the standard room used in this research. The calculation is used to compare the required opening area for one-sided and two-sided natural ventilation.

The required ventilation capacity depends on the floor area that needs to be ventilated. In this estimation, a ventilation flow rate of 6 L/s per m² is used. The required airflow can be calculated using Equation B.1.

Equation B.1

$$Q_{Vent} = Q_{Flow\ rate} \times A$$

Where Q_{vent} is the airflow rate, $Q_{flow\ rate}$ is 6 L/s/m², and A_{floor} is the floor area.

For this research, a standard room is considered with dimensions of 3.0 m height, 3.6 m width and 5.6 m depth. This results in a floor area of approximately 20 m². A standard window is applied with a window-to-wall ratio of 30%, resulting in a window of 2.0 m by 1.6 m, positioned at 0.9 m above the floor, illustrated in Figure B.1. This standard room is used later in the simulations to evaluate the influence of the adaptive ventilation system on the indoor climate.

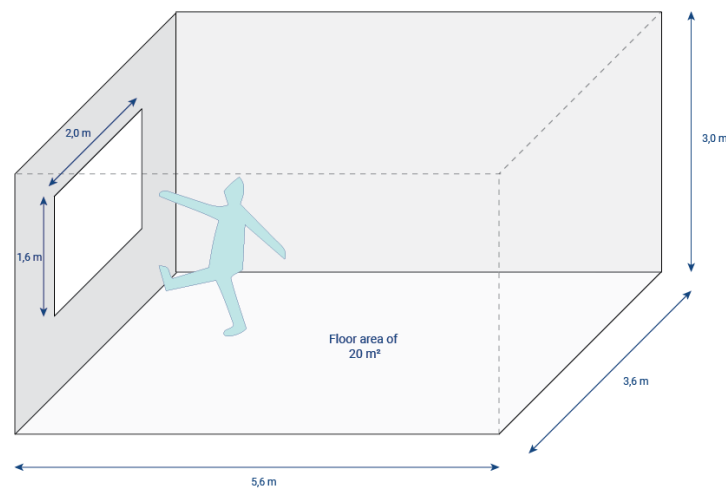


Figure B.1
Standard Room Layout and Dimensions.

The required opening area is calculated using Equation B.2, where A is the opening area (m²) and v is the air velocity (m/s). For one-sided ventilation, an air velocity of 0.1 m/s is assumed. While for two-sided ventilation, 0.4 m/s is used.

Equation B.2

$$A = \frac{Q_{Vent}}{v}$$

This results in different required ventilation opening areas, as shown in Table B.1.

Table B.1
Required ventilation opening area for different ventilation types

Ventilation type	Assumed air velocity (m/s)	Required ventilation opening area (m ²)
One-sided ventilation	0.1	1.2
Two-sided ventilation	0.4	0.3

To achieve the required ventilation opening area, different design approaches are possible. One large ventilation opening can be used, or multiple smaller openings can be distributed across the façade. This choice depends on the façade layout, aesthetic preferences and the shape and functionality of the opening and closing mechanism.

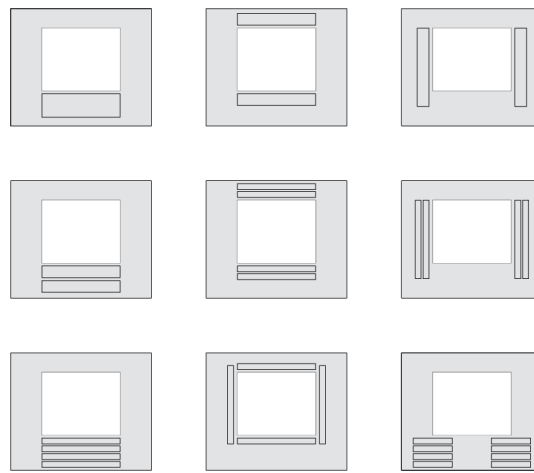


Figure B.2
 Design options for one-sided ventilation in front view.



Figure B.3
 Design options for two-sided ventilation in front view.

The design options shown in Figures B.2 and B.3 were used as a step to understand how the required opening area could be divided across the façade. These options show that the ventilation demand could be met through one large opening or through several smaller openings. However, these dimensions were not directly used for the final component design. Instead, a specific modular component size was selected in Chapter 8. Therefore, this calculation should be interpreted as a reference for estimating the total required ventilation area, rather than as the final dimensioning of the adaptive ventilation component.

Appendix D

This appendix contains of the Energy Management System (EMS) script. This script is used to add an outdoor temperature setpoint in the calculated natural ventilation model in DesignBuilder. Because of this script, the ventilation openings are only allowed to operate when the outdoor temperature is below the selected threshold, and the indoor temperature is above the same threshold.

```
EnergyManagementSystem:Sensor,  
  Site_Outdoor_Air_Drybulb_Temperature,  
  Environment,  
  Site Outdoor Air Drybulb Temperature;
```

```
EnergyManagementSystem:Actuator,  
  Venting_Opening_Factor_BLOCK1_ZONE1_Wall_4_0_0_0_0_6_Win,  
  BLOCK1:ZONE1_Wall_4_0_0_0_0_6_Win,  
  AirFlow Network Window/Door Opening,  
  Venting Opening Factor;
```

```
EnergyManagementSystem:Actuator,  
  Venting_Opening_Factor_BLOCK1_ZONE1_Wall_4_0_0_1_0_5_Win,  
  BLOCK1:ZONE1_Wall_4_0_0_1_0_5_Win,  
  AirFlow Network Window/Door Opening,  
  Venting Opening Factor;
```

```
EnergyManagementSystem:Actuator,  
  Venting_Opening_Factor_BLOCK1_ZONE1_Wall_4_0_0_2_0_4_Win,  
  BLOCK1:ZONE1_Wall_4_0_0_2_0_4_Win,  
  AirFlow Network Window/Door Opening,  
  Venting Opening Factor;
```

```
EnergyManagementSystem:Actuator,  
  Venting_Opening_Factor_BLOCK1_ZONE1_Wall_4_0_0_3_0_3_Win,  
  BLOCK1:ZONE1_Wall_4_0_0_3_0_3_Win,  
  AirFlow Network Window/Door Opening,  
  Venting Opening Factor;
```

```
EnergyManagementSystem:Actuator,  
  Venting_Opening_Factor_BLOCK1_ZONE1_Wall_4_0_0_4_0_2_Win,  
  BLOCK1:ZONE1_WALL_4_0_0_4_0_2_WIN,  
  AirFlow Network Window/Door Opening,  
  Venting Opening Factor;
```

```
EnergyManagementSystem:Actuator,  
  Venting_Opening_Factor_BLOCK1_ZONE1_Wall_4_0_0_5_0_1_Win,  
  BLOCK1:ZONE1_WALL_4_0_0_5_0_1_WIN,  
  AirFlow Network Window/Door Opening,  
  Venting Opening Factor;
```

```
EnergyManagementSystem:ProgramCallingManager,  
  Outdoor_Temperature_Natural_Vent_Control,
```

```
BeginTimestepBeforePredictor,  
Control_Natural_Vent_By_Outdoor_Temp;
```

```
EnergyManagementSystem:Program,  
Control_Natural_Vent_By_Outdoor_Temp,  
IF Site_Outdoor_Air_Drybulb_Temperature >= 24,  
  SET Venting_Opening_Factor_BLOCK1_ZONE1_Wall_4_0_0_0_0_6_Win = 0.0,  
  SET Venting_Opening_Factor_BLOCK1_ZONE1_Wall_4_0_0_1_0_5_Win = 0.0,  
  SET Venting_Opening_Factor_BLOCK1_ZONE1_Wall_4_0_0_2_0_4_Win = 0.0,  
  SET Venting_Opening_Factor_BLOCK1_ZONE1_Wall_4_0_0_3_0_3_Win = 0.0,  
  SET Venting_Opening_Factor_BLOCK1_ZONE1_Wall_4_0_0_4_0_2_Win = 0.0,  
  SET Venting_Opening_Factor_BLOCK1_ZONE1_Wall_4_0_0_5_0_1_Win = 0.0,  
ELSE,  
  SET Venting_Opening_Factor_BLOCK1_ZONE1_Wall_4_0_0_0_0_6_Win = Null,  
  SET Venting_Opening_Factor_BLOCK1_ZONE1_Wall_4_0_0_1_0_5_Win = Null,  
  SET Venting_Opening_Factor_BLOCK1_ZONE1_Wall_4_0_0_2_0_4_Win = Null,  
  SET Venting_Opening_Factor_BLOCK1_ZONE1_Wall_4_0_0_3_0_3_Win = Null,  
  SET Venting_Opening_Factor_BLOCK1_ZONE1_Wall_4_0_0_4_0_2_Win = Null,  
  SET Venting_Opening_Factor_BLOCK1_ZONE1_Wall_4_0_0_5_0_1_Win = Null,  
ENDIF;
```

Note. The value of $T_{threshold}$ was changed manually for each setpoint sensitivity simulation, while the control logic remained the same.

Appendix E

Appendix E contains of other relevant figures that are associated with the detailed analysis of the warmest week during the summer period of the reference case. These figures give more information about the relationship between operative temperature, outdoor temperature, air change rate, nighttime and occupancy.

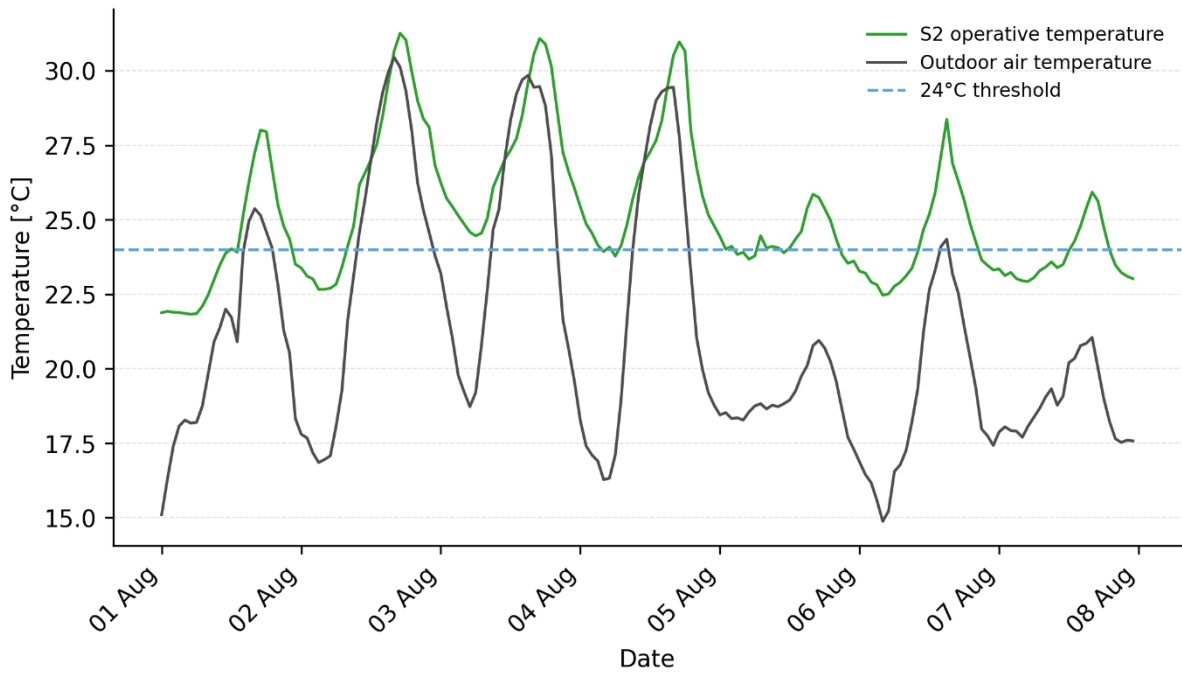


Figure E.1
S2 operative temperature and outdoor air temperature during the selected summer week.

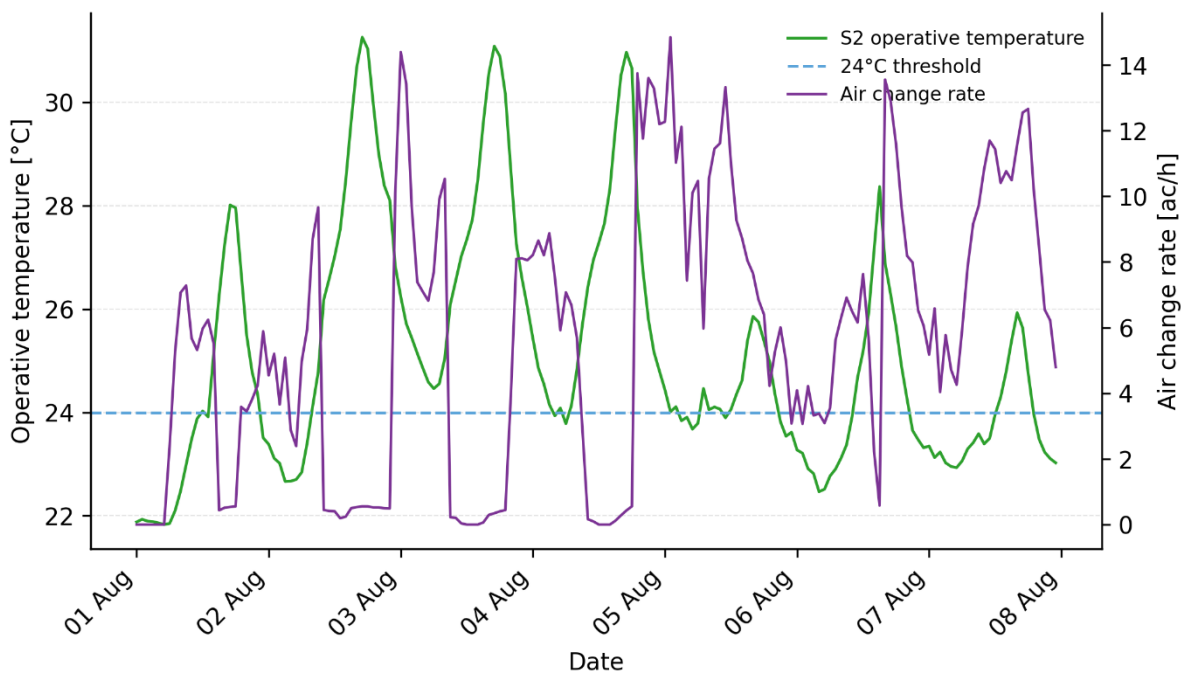


Figure E.2
S2 operative temperature and air change rate during the selected summer week.

Note. Shows the relation between ventilation activity and the operative temperature in S2.

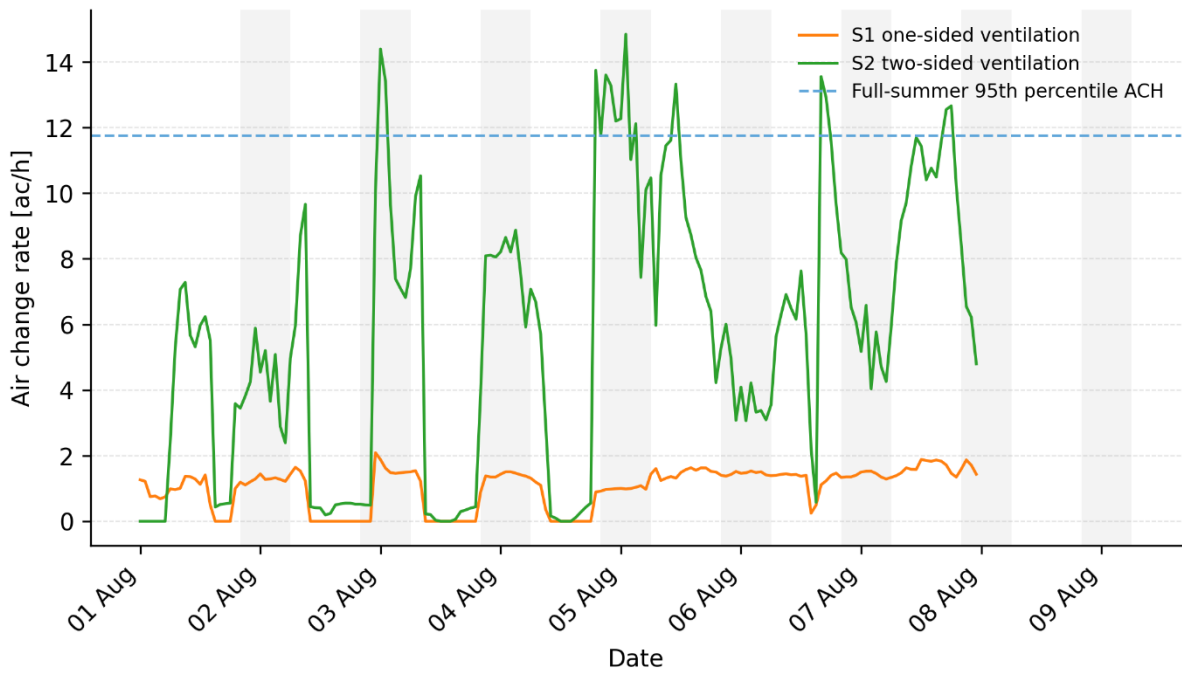


Figure E.3
Hourly air change rate for S1 and S2 during the selected summer week with night-time periods indicated.

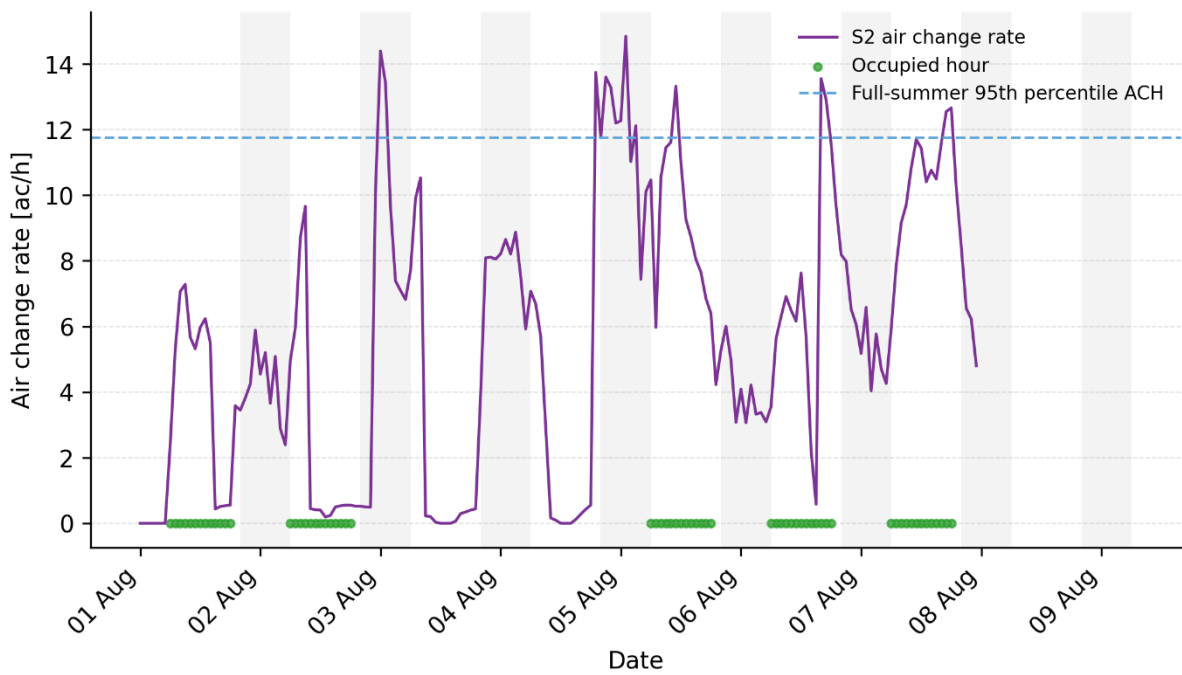


Figure E.4
S2 air change rate with night-time periods and occupied hours during the selected summer week.
Note. Green bullets on the x-axis indicate occupied hours according to the simulation schedule.